DOCTORAL THESIS

Glass Transitions in 1-Propanol and Isocyanocyclohexane Studied by a Polaro-calorimeter

by

Isao KISHIMOTO

Department of Chemistry
Faculty of Science
Osaka University

1992

Acknowledgements

I would like to express my sincere gratitude to Professor Hiroshi Suga for his valuable instruction and kind encouragement throughout the course of this work. I am also deeply indebted to Associate professor Takasuke Matsuo for his helpful suggestions, valuable discussions, continuing collaboration and assistance in refining the expression in this thesis. I wish to express my great thanks to Dr. Jean-Jacques Pinvidic, collaborator on the study of isocyanocyclohexane, for introducing the interesting substance to me, his cooperation and discussions. I am also grateful to Dr. Osamu Yamamuro for his useful advice and discussions. I also would like acknowledge Professor Michio Sorai for his fruitful discussions.

I gratefully acknowledge warm support and encouragement from fellows of the Suga's Laboratory and the Microcalorimetry Research Center.

ABSTRACT

Glass transitions in 1-propanol and isocyanocylohexane were studied by the use of a polaro-calorimeter newly developed. The relaxational behavior of the configurational enthalpy and the electric polarization was observed simultaneously using the apparatus combining a dielctric polarization meter and an adiabatic calorimeter. The apparatus is essentially an adiabatic calorimeter with built-in electrodes in the sample cell. An electric field of up to 55 kV m^{-1} can be applied to the sample. The electric current released by the polarization decay is measured with an electrometer to a precision of about 10 fA. The temperature range of the apparatus is from 5 to 300 K.

The relaxation in 1-propanol around the glass transition temperature was studied. The results of the measurement showed the non-exponential nature for the enthalpy and the polarization relaxations. The non-exponential relaxations in the enthalpy and the polarization were separated into two components which have different relaxational rates. The long-time component was described well by an exponential function. The long-time component for the polarization relaxation had a relaxation time 5 to 12 times longer than that for the corresponding component of enthalpy relaxation. The short-time component was described approximately as an exponential function. The relaxation time for the short-time relaxation was roughly the same for the enthalpy and the polarization. The long-time and short-time relaxations of the polarization

proved to correspond to the Debye and non-Debye type relaxations which have been found by previous dielectric measurement.

Two glass transitions of isocyanocyclohexane crystal were observed around 160 K (T_{g1}) and 130 K (T_{g2}). The relaxation nature was studied by the simultaneous measurement of the enthalpy and polarization. The enthalpy relaxation around T_{g1} was described well as the Debye relaxation. This relaxation is associated with the interconversion between the axial and equatorial conformers of the internally flexible molecule. The barrier height between two confomers was determined as 53.6 kJ mol^{-1} from an Arrhenius plot of the relaxation time.

Non-exponential relaxation was observed around T_{g2} in the exothermic-depolarizing experiment. The relaxational behavior was analyzed in terms of Kohlrausch-Williams-Watts (KWW) function. The relaxation time τ and the non-exponential parameter β in the KWW function were determined for the enthalpy and the polarization. The relaxation time for the enthalpy was longer than that for the polarization and the value β for the enthalpy was larger than that for the polarization.

A phase transition between plastically crystalline and ordered low-temperature crystalline phases was found at 192.6 K. Thermodynamic quantities associated with the phase transition were determined. The residual entropy of glassy state was determined as 6.3 J $K^{-1}mol^{-1}$. The low temperature phase did not show any relaxational behavior in the polarization and enthalpy. This indicates that the low temperature phase is fully ordered with respect to position and orientation of the constituent molecules.

CONTENTS

Chapter 1 INTRODUCTION

1-1 General Introduction

Glass transition is regarded as a kind of kinetic boundary between equilibrium and non-equilibrium states in any disordered systems such as liquids and orientationally-disordered crystals. When a glassy substance is heated from a low temperature where the position and/or orientation of the constituent molecules are frozen, the molecules become mobile progressively to recover the equilibrium configuration as the temperature increases across a certain region, the glass transition region. Various physical quantities, such as enthalpy, volume and electric polarization, exhibit relaxational behavior around the glass transition. Enthalpy relaxation is observed straightforwardly by calorimetry. Electric polarization relaxation is observed conventionally by TSDC method which is described below.

In calorimetry, one usually finds spontaneous warming of the sample under an adiabatic condition as the glass transition temperature is approached from below. At the same time, an increase in the heat capacity is observed over a narrow temperature range. The glassy state has generally smaller heat capacity than the equilibrium supercooled phase because the frozen molecular configuration does not contribute to the heat capacity below the temperature region. Calorimetry[1)] has been recognized as a powerful experimental method for studying the glass transitions

because the heat capacity change and thermal relaxation are important indications of the glass transition. It also enables us to quantify the molecular disorder frozen in a glassy state by determination of the residual entropy. Historically, the residual entropy and the glass transition were observed in glycerol for the first time by an adiabatic calorimeter.

Dielectric measurement is a useful experimental method for studying relaxational phenomena from another point of view. Its characteristic time is usually 10^{-1} to 10^{-6} s. On the other hand, the characteristic time of the adiabatic calorimetry is much longer, 10^{2} to 10^{5} s. A technique known as thermally stimulated depolarization current (TSDC)[2] method has a characteristic time comparable to that of the calorimetry. This technique is applicable to relaxation involving motion of polar molecules or polar segments of molecules as the dielectric measurement is. In this technique, a sample polarized by an external field is heated in the absence of the field. If the molecular dipole becomes mobile as the substance undergoes glass transition, the TSDC curve shows a peak in the corresponding temperature region.

In order to investigate glass transition in more details, a new apparatus called a polaro-calorimeter was constructed. By this apparatus the enthalpy and electric polarization of a relaxing material can be measured simultaneously. The simultaneous measurement of the two properties is essential for the clarification of the nature of glass transition. A comparative study based on two separate experiments often does not lead to a significant conclusion because properties of a glassy state strongly depend on the

sample prehistory. It is extremely difficult to realize the same non-equilibrium state of a material in different apparatuses. The simultaneous measurement of the relaxing enthalpy and polarization does not suffer from this difficulty. The apparatus enables us to make a direct comparison between the enthalpy and polarization relaxations.

Relaxation time is an important parameter characterizing a large variety of rate processes. In the simplest model of a glass-forming substance, its relaxation behavior is described by an exponential function or Debye type relaxation function, $X(t) = X(0)\exp[-t/\tau(T)]$, where a physical quantity X relaxes as time t progresses. Furthermore the relaxation time follows the Arrhenius law, $\tau(T) = \tau_0\exp(E_a/RT)$, in the simplest model. But almost all the glassy substances are not described accurately by the Debye-Arrhenius expression. Instead of the Debye equation, stretched exponential functions are often used, for example, in Cole-Davidson[4] and Kohlrausch-Williams-Watts[5] formulations. Instead of the Arrhenius law, the Vogel-Tammann-Fulcher[6] (VTF) formula, $\tau(T) = \tau_0\exp[A/R(T-T_0)]$, is often used to describe the temperature dependence of the relaxation time. The non-Debye, non-Arrhenius behavior has not been understood microscopically, although the stretched exponential and VTF equations are known to represent many experimental observations better than the ordinary exponential and Arrhenius equation, respectively. It is ever not clear whether these equations have anything more than the increased number of adjustable parameters to recommend themselves as a better representation of the experimental facts. The

comparison between enthalpy and polarization with the polarocalorimeter is expected to deepen the understanding of relaxation kinetics of actual substances.

1-2 1-Propanol

Although many glassy substance show departure from the Debye type relaxation, some aliphatic mono-alcohols[7] are known to obey the Debye law. Davidson and Cole[4] measured the complex dielectric permittivity of 1-propanol in 1951 and described the dielectric constant by the Debye equation. Lyon and Litovitz[8] compared the dielectric relaxation time and the ultrasonic relaxation time. They determined the ratio of the dielectric relaxation time τ_D and the volume relaxation time τ_V as τ_D/τ_V ~19 at 143 K. This ratio is lower than that for other associated liquids (polyalcohols) and van der Waals liquids[9] ($2<\tau_D/\tau_V<6$) which exhibit non-Debye dielectric relaxation. In the present work, a quantitative relation between the polarization and enthalpy relaxation was studied by the long-term experiments.

1-3 Isocyanocyclohexane

By infrared and Raman spectroscopies, Woldbaek *et al.*[10] found that both of the plastically crystalline phases of isocyanocyclohexane ($C_6H_{11}NC$) and cyanocyclohexane ($C_6H_{11}CN$) are easily

supercooled, and that axial and equatorial conformers coexist in their glassy crystalline, plastically crystalline and liquid phases, respectively. Gonthier-Vassal *et al.*[11] performed differential scanning calorimetry and observed glass transitions at 129 K and 170 K in isocyanocyclohexane, and at 135 K and 170 K in cyanocyclohexane, respectively. J. -J. Pinvidic[12] measured the heat capacity of cyanocyclohexane with an adiabatic calorimeter and observed three glass transitions at 55 K, 133.5 K and 156 K and a phase transition at 215 K. Multiple glass transitions are not usual in a simple substance, if not unprecedented[13]. In view of the polarity of the molecule (see below) simultaneous calorimetric and electric measurements on isocyanocyclohexane were carried out by using a polaro-calorimeter.

The plastically crystalline phase of isocyanocyclohexane supercools readily even with a slow cooling rate. This is a useful property for the relaxation measurement because one can study the metastable phase for a long time without being intervened by the phase transformation into a low-temperature ordered phase. This favorable situation, however, brings about a difficulty in producing the low temperature phase and hence in determining the equilibrium temperature of the transition into the plastically crystalline phase. In fact, the stable low temperature phase of isocyanocyclohexane had been reported to be realizable only in a high pressure experiment[10]. In the present experiment, the substance could be transformed completely into the low temperature modification at normal pressure by a long annealing experiment at an appropriate temperature range, and thus the tempera-

ture, enthalpy and entropy of the transition have been determined accurately. These data are necessary to calculate the residual entropy of the glassy crystalline phase.

The dipole moment of isocyanocyclohexane is not known experimentally. However, cyanocyclohexane has been reported to have a dipole moment of 3.79 D = 1.26×10^{-29} C m[14]. In view of the general similarity of the two molecules, this will give a measure of the polarity of isocyanocyclohexane. The large polarity is another favorable factor for the polaro-calorimetric experiment as noted above.

References

1. H. Suga and T. Matsuo, *Pure & Appl. Chem.*, 61(6), 1123 (1989).

2. J. Vanderschueren and J. Gasiot, *Thermally Stimulated Relaxation in Solids, Topics in Applied Physics 37.*, ed. by P. Bräunlich, Springer-Verlag: Berlin. (1979) .

4. D. W. Davidson, R. H. Cole, *J. Chem.Phys.* ,19,1484 (1951)

5. R. Kohlrausch, *Ann. Phys. (Leipzig),* 12,393 (1847). G. Williams and D. C. Watts, *Trans. Faraday Soc.,* 66, 80 (1970).

6. H. Vogel, *Phys. Z.*, 22, 645 (1922). G. S. Fulcher, *J. Am. Ceram. Soc.*, 8, 339 (1925). G. Tammann and G. Hesse, *Z. Anorg. Allg. Chem.*, 156, 245 (1926).

7. C. J. F. Böttcher and P. Bordewijk, *Theory of electric polarization*, Vol. 2, p.106, Amsterdam (1978).

8. L. Lyon and T. A. Litovitz, *J. Appl. Phys.*, 27, 129 (1956).

9. T. A. Litovitz and G. E. McDuffie, Jr., *J. Chem. Phys.*, 39, 729 (1963).

10. T. Woldbaek, A. Berkessel, A. ,A. Horn and P. Klaeboe, *Acta Chem.Scand.*, A36(9), 719. (1982)

11. A. Gonthier-Vassal, and H. Szwarc, *Chem. Phys. Lett.*, 129(1), 5 (1986).

12. J. -J. Pinvidic, Ph.D. Thesis., Universite de Paris Sud (1988).

13. H. Suga and S. Seki, *J. Non-Crystalline Solids*, 16, 171 (1974).

14. C. W. N. Cumper, S. K. Dev, and S. R. Landor, *J. Chem. Soc., Perkin Trans.*, 2(5), 537 (1973).

Chapter 2 POLARO-CALORIMETER

2-1 Principle of the Polaro-calorimetric Experiment

The polaro-calorimetric experiment is concerned with determining the enthalpy and electric polarization which respond to two controlled variables, the electric field and temperature.

The principle of enthalpy measurement is described first. The heat capacity of a substance at constant pressure is defined by

$$C_p \equiv \left(\frac{\partial H}{\partial T}\right)_p . \tag{2.1}$$

This quantity is determined experimentally according to the following relation.

$$\left(\frac{\partial H}{\partial T}\right)_p = \lim_{Q \to 0} \frac{Q}{\Delta T} , \tag{2.2}$$

In adiabatic calorimetry, the heat Q is supplied by Joule heating and ΔT determined as the difference between the temperatures before and after the heating. The infinitesimal quantities defining the differential heat capacity are approximated with finite increments in an actual experiment. Q is given by

$$Q = E_h - \Delta T \cdot C_{ves} - q, \tag{2.3}$$

where E_h is the electric energy for the heating, C_{ves} the heat

capacity of the sample vessel, and q the heat leakage from the sample vessel to the surroundings. The final term would not appear in an ideal *adiabatic* calorimeter. Slight heat leakage occurs inevitably in a real adiabatic calorimeter and is corrected as described later. Description for the measurements of the energy and temperature is given in section 2-3.

In the study of glasses we are interested in the configurational enthalpy as well as the total enthalpy. Strictly speaking, the configurational and vibrational degrees of freedom of a glassy substance are not independent of each other. Intermolecular vibrations, for instance, could have different frequencies in the same substance in different configurational states. Different vibrational frequencies, of course, mean different vibrational heat capacities. However, we ignore this possibility. This simplification is justified because it has been experimentally observed that a glassy substance has, within the experimental error, the same vibrational heat capacity even when it is in different configurational states as a result of quenching and long annealing. The measurement of the configurational enthalpy is formulated as follows. We consider a system consisting of the sample and vessel. The enthalpy of the system can be divided into two parts, the configurational enthalpy H_C and the vibrational enthalpy H_{vib},

$$H = H_C + H_{vib} \ . \qquad (2.4)$$

H_C is written as,

$$H_C = n\, H_{C,m}, \qquad (2.5)$$

where n is the sample amount and $H_{c,m}$ molar configurational enthalpy. The sample vessel contributes only to the fast responding vibrational enthalpy. The vibrational term H_{vib} is thus the sum of the vibrational enthalpy of the sample and enthalpy of the vessel,

$$H_{vib} = n\, H_{vib,m} + H_{ves}, \tag{2.6}$$

where $H_{vib,m}$ is the molar vibrational enthalpy. An infinitesimal change in enthalpy of the system dH is defined by heat flux per unit time J to the system.

$$dH = J(t)dt. \tag{2.7}$$

Eqs. (2.4) and (2.7) are combined to give the following equation.

$$dH_c + dH_{vib} = J(t)dt. \tag{2.8}$$

By introducing the vibrational heat capacity C_{vib} ($= dH_{vib}/dT$), Eq. (2.8) is reformed as

$$dHc + C_{vib}\, dT = J(t)dt. \tag{2.9}$$

Similarly to Eq. (2.6), the vibrational heat capacity is written as

$$C_{vib} = n\, C_{vib,m} + C_{ves}, \tag{2.10}$$

where C_{ves} is the heat capacity of the sample vessel and $C_{vib,m}$ the vibrational molar heat capacity of the sample. Since the

configurational heat capacity does not contribute to the measured heat capacity at temperatures lower than glass transition region, $C_{vib,m}$ can be measured directly for a glassy state. At temperatures higher than T_g, it can be estimated from the low temperature heat capacity without introducing a significant error by the use of an appropriate extrapolation function. Integration of Eq. (2.9) with respect to time gives the difference in the configurational enthalpy between time t_i and t_f,

$$H_c(t_f) - H_c(t_i) = \int_{t_i}^{t_f} dH_c$$

$$= \int_{t_i}^{t_f} J(t)\, dt$$

$$- \int_{T(t_i)}^{T(t_f)} C_{vib}\, dT. \qquad (2.11)$$

Departure from the equilibrium state is defined by the actual configurational enthalpy H_c and the equilibrium configurational enthalpy $H_{c,eq}$,

$$\Delta H_c \equiv H_c - H_{c,eq}. \qquad (2.12)$$

$H_{c,eq}$ is a unique function of the temperature, while H_c can vary with time and depends on the sample prehistory. Using the quantity ΔH_c, Eq. (2.8) is rewritten as

$$d\Delta H_c + dH_{c,eq} + dH_{vib} = J(t)\, dt. \qquad (2.13)$$

By introducing the configurational heat capacity $C_{c,eq}$ (= $dH_{c,eq}/dT$), Eq. (2.13) is further rewritten as follows:

$$d\Delta H_c + C_{c,eq}\, dT + C_{vib}\, dT = J(t)\, dt, \qquad (2.14)$$

$$C_{c,eq} = n\, C_{c,eq,m}. \qquad (2.15)$$

Here, $C_{c,eq,m}$ is the molar configurational heat capacity. This quantity is determined at temperatures higher than T_g by subtracting the molar vibrational enthalpy $C_{vib,m}$ from the whole molar heat capacity. Below T_g, it is estimated by the extrapolation. Integration of Eq. (2.14) with respect to time gives

$$\Delta H_c(t_f) - \Delta H_c(t_i) = \int_{t_i}^{t_f} J(t)\, dt - \int_{T(t_i)}^{T(t_f)} \{C_{vib}+C_{c,eq}\} dT. \qquad (2.16)$$

If the system is in equilibrium at time t_f, then $\Delta H_c(t_f)$ is equal to zero. ΔH_c at any other times t_i can be determined by this equation.

If the configurational enthalpy exhibits a Debye type relaxation, its behavior is represented by a linear differential equation as

$$\frac{dH_c}{dt} = -\frac{\Delta H_c}{\tau_H(T)}. \qquad (2.17)$$

This equation means that the configurational enthalpy is governed by two quantities. One is the magnitude of the departure from the equilibrium and the other the relaxation time. The relaxation time is a function of only temperature in the Debye type relaxation. If Eq. (2.17) is valid, H_c observed in isothermal relaxation is described by a simple exponential function. However, non-exponential relaxation behavior is observed frequently in many substances undergoing a glass transition. For such systems we introduce an apparent (time dependent) relaxation time $\tau_{H,ap}(t)$ which is obtained by

$$\tau_{H,ap}(t) = -\frac{\Delta H_c}{dH_c/dt}. \qquad (2.18)$$

The quantity dH_c/dt in the right hand side is determined by the following equation.

$$\frac{dH_c}{dt} = J(t) - C_{vib}\frac{dT}{dt}. \qquad (2.19)$$

This equation is derived from Eq. (2.9). Substitution Eqs. (2.11) and (2.19) into Eq. (2.18) gives

$$\tau_{H,ap}(t) = \frac{\int_{t}^{t_f} J(t)\,dt - \int_{T(t)}^{T(t_f)} \{C_{vib} + C_{c,eq}\}\,dT - \Delta H_c(t_f)}{J(t) - C_{vib}\,(dT/dt)} . \tag{2.20}$$

Experiments described in section 2-4 employ several different temperature control programs such as continuous heating and intermittent heating. Equation (2.20) is applicable to any such experiment because it is a general expression.

For the polarization measurement, the sample is placed in an electric field E provided by electrodes connected to a voltage source. The electric field polarizes the sample. The electric polarization of the sample is given by

$$P(t) = D(t) - \varepsilon_0 E(t), \tag{2.21}$$

where ε_0 is the permittivity of vacuum and D is the electric displacement which is related to the amount of charge $Q(t)$ on electrodes,

$$D(t) = A\,Q(t), \tag{2.22}$$

where A is a constant dependent on the geometrical arrangement of the electrodes. If the electrodes are a pair of parallel plates, the inverse of A is the area of the plate. Substituting Eq. (2.21) into Eq. (2.22), one obtains

$$P(t) = A\,Q(t) - \varepsilon_0 E(t). \tag{2.23}$$

For a constant electric field, the polarization change is determined by time dependence of the charge,

$$P(t_f) - P(t_i) = A \{Q(t_f) - Q(t_i)\}. \qquad (2.24)$$

By an electrometer connected between the voltage source and electrodes, the change in the amount of the charge can be determined by the current $I(t)$,

$$I(t) = dQ(t)/dt. \qquad (2.25)$$

Combining Eqs. (2.25) and (2.24), one obtains the following equation.

$$P(t_f) - P(t_i) = A \int_{t_i}^{t_f} I(s)\, ds. \qquad (2.26)$$

Response of the polarization to the electric field is determined by the integration of the current. The current is proportional to the rate of change in the polarization,

$$\frac{dP}{dt} = A\, I(t). \qquad (2.27)$$

Supposed that the polarization approaches the equilibrium value by a Debye type relaxation, then it follows the differential equation,

$$\frac{dP}{dt} = -\frac{\Delta P}{\tau_P(T)}. \tag{2.28}$$

In this equation, ΔP is defined by

$$\Delta P \equiv P - P_{eq}(E, T), \tag{2.29}$$

where $P_{eq}(E,T)$ is the equilibrium polarization as a function of temperature and field strength. For a non-Debye relaxation, an apparent relaxation time for the polarization is defined by

$$\tau_{P,ap}(t) = -\frac{\Delta P}{dP/dt}. \tag{2.30}$$

Since P_{eq} is equal to 0 with E=0 in the paraelectric state, ΔP is determined experimentally by integration of the current with respect to (Eq. (2.26)). dP/dt is obtained by combining Eqs. (2.27) and (2.25).

$$\tau_{P,ap}(t) = \frac{\int_t^{t_f} I(s)ds - \{P(t_f) - P_{eq}(E, T(t))\}/A}{I(t)}. \tag{2.31}$$

Therefore apparent relaxation time is determined from the measurement of the current that flows in the circuit containing a polarized paraelectric substance as the substance loses the polarization by relaxation.

Equation (2.19) defines the apparent relaxation time for the enthalpy and Eq. (2.30) for the polarization. The measurement of the two quantities can be performed simultaneously. In the

simultaneous measurements the influence of electric field to the enthalpy has to be considered. It is estimated by the comparison of the electrostatic energy and configurational enthalpy involved in the experiment. The electrostatic energy is given by $\frac{1}{2} C Q^2$ (C is the capacitance of the cell with the sample in it). The magnitude of configurational enthalpy is measured in an adiabatic relaxation experiment. As shown later in the section of experimental results, the electrostatic energy is very small compared with the magnitude of the enthalpy. It is therefore reasonable to assume that the enthalpy is carried solely by short range molecular interaction and that macroscopic electrostatic energy contributes a negligibly small amount to the enthalpy.

In the discussion above, the polarization of the sample was assumed to be configurational. In actual substances, electronic polarization contributes to the total polarization. This gives rise to a fast response of the sample to applied field. The response is so fast that its effect in the experimental record is simply limited by the response function of the electrometer. Much slower configurational response was easily separated from the electronic polarization effect. Also the magnitude of the electronic effect was much smaller than the configuration polarization.

2-2 Structure of the Polaro-calorimeter

A schematic diagram of the cryostat is shown in Fig. 2-1. The function of this assembly is to maintain the sample cell under

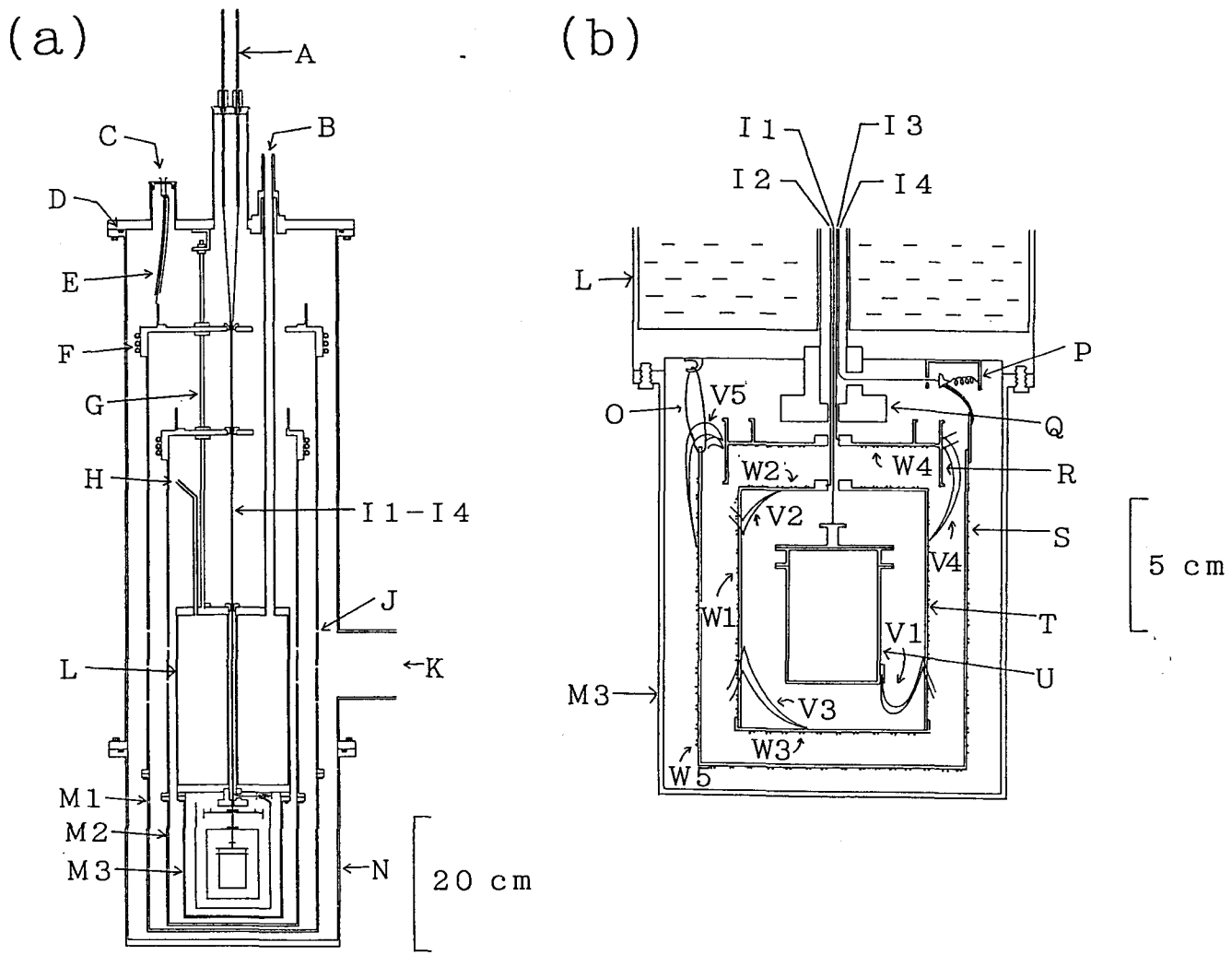
(a)
A
B
C
D
E
F
G
H
I1－I4
J
K
L
M1
M2
M3
N
20 cm
(b)
I1
I2
I3
I4
L
P
O
V5
Q
W2
W4
R
V2
S
V4
W1
T
V1
U
M3
V3
W3
W5
5 cm

Fig. 2-1. Schematic diagram of the cryostat, (a) a whole view and (b) an expanded view around the sample cell. A: hoists of the thermal switches, B: refrigerant inlet, C: vacuum feedthrough of the leads for the polarization measurement, D: rubber O-ring gasket, E: cables with high resistance insulation for the polarization measurement, F: heat exchange spiral for boiled-off refrigerant vapor, G: suspension, H: refrigerant exit tube, I1-I4: Nylon threads suspending the cell and adiabatic shields, J: perforation in the shields for efficient evacuation, K: outlet to vacuum line, L: refrigerant tank, M1-M3: radiation shields, N: vacuum jacket, O: Nylon loop suspending the outer shield and thermal anchoring disc, P: thermal switch of the outer shield. Q: thermal contact block, R: thermal anchoring disc, S: outer adiabatic shield, T: inner adiabatic shield, U: sample cell, V1-V5: thermocouples, W1-W5: heater wires.

adiabatic condition at any desired temperatures between 4 and 300 K. Precise adiabaticity is very important for long-time relaxation experiment. The spaces within the jacket (N) are evacuated to 6×10^{-4} Pa by an oil diffusion pump, so that thermal conduction by gas is almost eliminated. Three radiation shields (M1-M3) set up zones of uniform and progressively lower temperatures inwards to the refrigerant tank (L). Inside the radiation shield an outer shield (S), an inner shield (T) and a thermal anchoring disc (R) form an adiabatic environment around the sample cell (U). The temperatures of the adiabatic shields are controlled separately in five parts: the top, side and bottom of the inner shield, the outer shield and the thermal anchoring disc. Each part has a Manganin heater wire (W1-W5). Chromel-Constantan thermocouples (V1-V5) detect the temperature differences and compensatory heating energies are supplied to the five parts of the shields to equalize the temperatures to $\pm 0.1\ \mu$V in terms of the thermocouple EMF. In normal operation of the adiabatic control the maximum heat leakage due to the imperfection of the adiabatic controls was 0.18 mW at 300 K.

The refrigerant tank (L) accepts liquid nitrogen, liquid hydrogen or liquid helium, depending on the temperature of the experiment. Cold vapor that boils out of the tank passes through two copper tubings (F) in good thermal contact with the radiation shields, whereby it exchanges heat with the shields to economize the refrigerant consumption.

The sample cell and adiabatic shields are cooled as follows. The thermal anchoring disc, the inner shield and the sample cell

are held up into thermal contact with each other and with the contact block (Q) by pulling up the hoists (A). The thermal contact piece of the thermal switch (P) is also pulled to the contact plate, by which the outer shield is cooled. When all the components of the adiabatic shields have been cooled to a starting temperature, the thermal switches are released to thermally isolate the sample and shields from the refrigerant bath and from each other.

The sample cell is shown in Fig. 2-2. A thermometer, heater wire and electrodes are attached to the sample cell. The thermometer is fixed on the thermometer unit that can be detached from the main body of the cell by loosening the two pairs of screws (D1).

The thermometer unit is made of copper. The thermometer (3.2 mm in diameter, 20 mm long) is wrapt in gold leaf and put into the tubing (B) tightly. The gold leaf ensures good thermal contact between the thermometer and the tubing. The thermal equilibrium of the sample cell and thermometer was achieved within four minutes after heating the sample cell at all the temperatures between 4 and 300 K.

The calorimeter vessel consists of the following four parts: the lid, main body, heater wire (K) and outer shell (I). The lid, main body and outer shell are made of copper and gold-plated. The lid and main body are sealed together by eight pairs of screws (D2) with an indium gasket between them.

Electrodes are special features of the present cell that distinguishes it from other calorimetric cells. They are used to

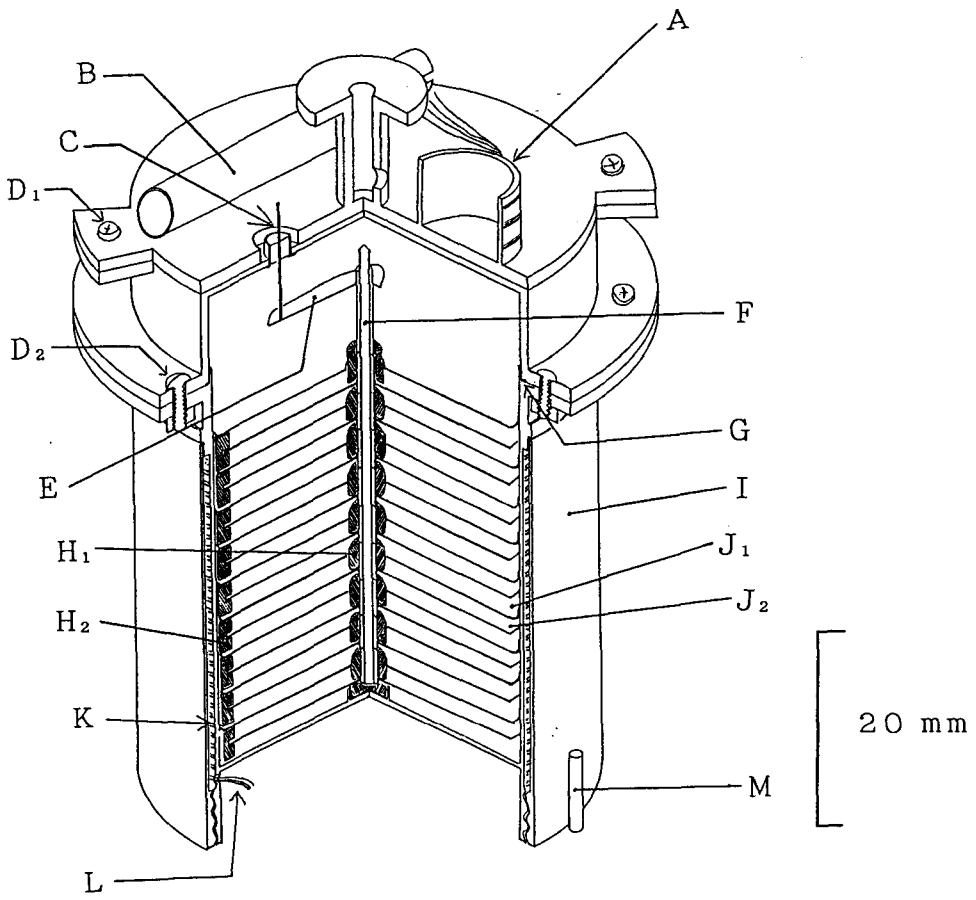

Fig. 2-2. Schematic drawing of the sample cell. A: thermal anchoring ring for leads of the thermometer, B: tubing in which the thermometer is fixed, C: hermetically sealed electrical feedthrough for the polarization current, D1,2: screws fastening the thermometer unit to the lid and the lid to the main body of the cell, E: electrical contact plate, F: central axle of electrodes HI (J2), G: indium sealing, H1,2: Teflon spacers, I: outer shell, J1: elsetrodes LO, J2: lectrodes HI, K: heater wire, L: leads of heater wire, M: copper tubing that accepts to differential thermocouple junction.

apply electric field to the sample and to measure the polarization change. The cell has been so designed that the electrodes do not deteriorate the thermal integrity of the cell but rather enhance it. This consideration was important because temperature should be as uniform as possible during heating as well as during the enthalpy and polarization relaxation observation. They are eighteen circular plates of copper placed horizontally in the cell. Nine of the plates have the same electrical potential as the main body of the cell (to be called the "electrode HI" below). The other nine have a different electrical potential (the "electrode LO"). Electrodes HI have teeth on their circumference. The teeth are bent down and touch the inner wall of the main body of the cell by their elasticity. These electrodes contact with the main body electrically as well as thermally. The central axle made of stainless steel passes through perforations of the electrodes. It is electrically connected with the electrodes LO but insulated from HI. An electric contact plate (E) is attached at the upper end of the axle and makes contact with the lower end of a hermetically sealed feedthrough (C) on the lid. The distance between one of the electrodes HI and the adjacent electrode LO is fixed to 1.8 mm by Teflon spacers (H1 and H2). One of the cables for polarization measurement is connected to the cell at D1 and the other soldered to the terminal (C).

The volume occupied by the sample is 34 cm^3. The electric field is homogeneous between the parallel electrode plates, but not near the edge of the plates. The sample volume in the homogeneous field is approximately 85 % of the whole sample volume. The

capacitance of this sample cell filled with helium gas at one atmospheric pressure was 84.0 pF.

The heat capacity of the sample cell is shown in Fig. 2-3. A polynomial function in T was fitted to the data. The peak at 290 K is due to the phase transition of 1.4 g of Teflon[1)] used for insulation of the electrodes. The resistance of the heating wire is shown in Fig. 2-4 between 20 and 200 K. The power of Joule heating on TSDC and TSPC measurements was calculated using this resistance value.

2-3 Instrumentation

The block diagram of the measurement system is shown in Fig. 2-5. It consists of the calorimetric section and the polarization measurement section. All electric instruments are interfaced to a personal computer (NEC PC-9801VF) which acts as a controller via the standard IEEE-488 and RS-232C buses. The computer operates the instruments, accepts data from them, processes these data and stores in the floppy disk. The measurements of temperature, energy and electric polarization are performed in the following way.

The temperature is measured with a Rhodium-Iron resistance thermometer (Cryogenic Calibrations Ltd.) whose nominal resistance at 273.15 K is 27 Ω . The ratio of the thermometer resistance to a standard resistance is determined by a seven-digit AC resistance bridge (Automatic Systems Laboratories, F-17). The resolu-

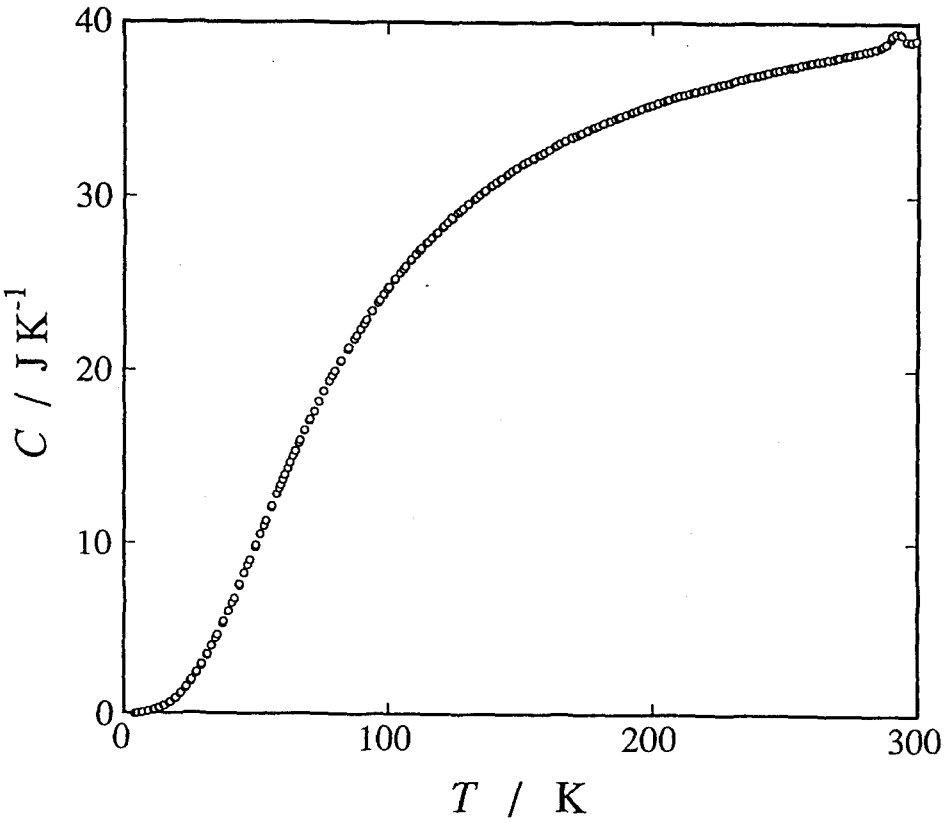

Fig. 2-3. Heat capacity of the sample cell.

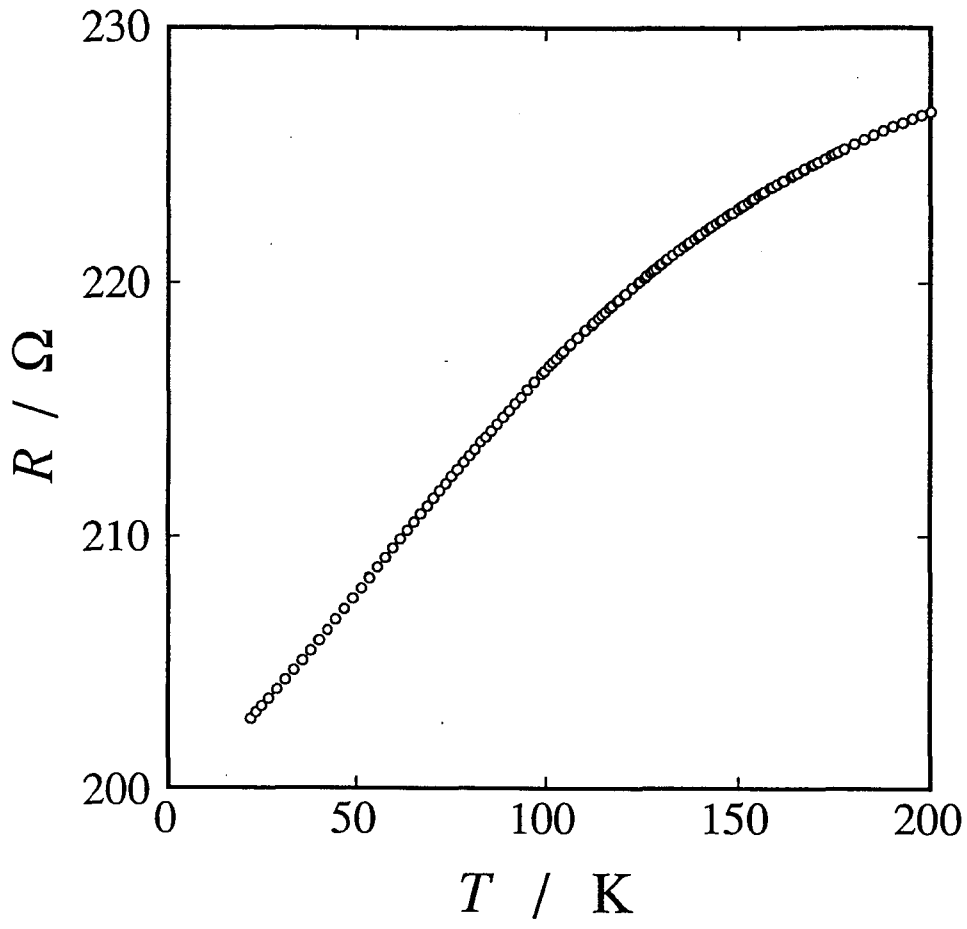

Fig. 2-4. Resistance of the heating wire of the sample cell.

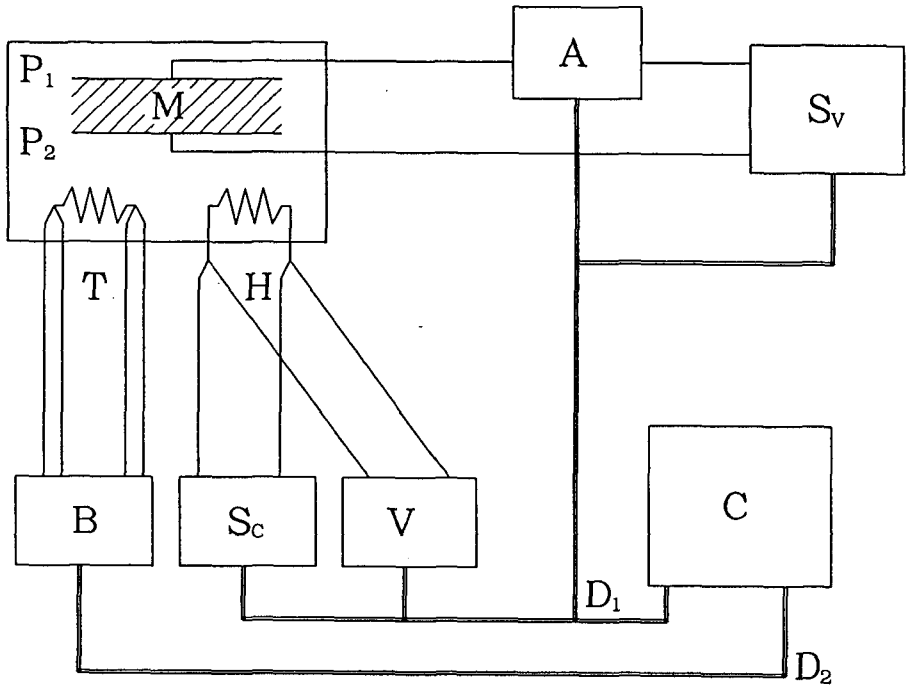

Fig. 2-5. Block diagram of the measurement system. B: automatic resistance bridge, S_C: programmable current source, V: digital voltmeter, A: digital electrometer, S_V: programmable voltage source, T: thermometer, H: heater, C: personal computer, M: sample, P_1: electrode HI, P_2: electrode LO , D_1: interface bus (IEEE-488), D_2: interface bus (RS-232C).

tion of the temperature is 0.1-0.3 mK between 4 and 300 K. The thermometer was calibrated on the basis of the IPTS-68.

Electrical energy supplied to the sample cell is determined by evaluating the integral

$$E = \int_0^{t_0} V\ I\ \mathrm{d}t, \tag{2.32}$$

where I is the current through the heater, V is the electrical potential across the heater and the integral is taken over time from the beginning of the heating period at $t = 0$ to the end at $t = t_0$. Constant current I is supplied by a current source (Advantest TR6142) and V is measured with a digital voltmeter (Keithley Instruments, Inc. Model 195A) every several seconds and averaged. Thus Eq. (2.32) is rewritten as

$$E = \langle V \rangle I\ t_0, \tag{2.33}$$

where $\langle V \rangle$ is the average value of V. The heater current is turned on and off by a relay operated by the computer.

The polarization measurement circuit consists of two instruments, a voltage source and an electrometer. The electrometer (Keithley Instruments, Inc. Model 617) can resolve current as low as 0.1 fA (10^{-16}A). However the electromagnetic noises of about 10 fA arising from various sources limited the actual sensitivity of the current measurement. A voltage is applied to the electrodes by the programmable voltage source built in the digital electrometer. This voltage source can be adjusted between -102.35 V and

+102.40 V in steps of 50 mV. The maximum electric field between electrodes, 55 kV m^{-1}, is determined by the highest source voltage.

A guarding technique is employed to achieve a high accuracy for the measurement of the polarizing process as well as the depolarizing process. The circuit of guarding is shown schematically in Fig. 2-6. When one makes a circuit consisting of a variable voltage source, an electrometer and a capacitor containing dielectric material, leakage resistance of about 1 GΩ is inevitable. The leakage path, R_L in the figure, is particularly detrimental in the polarizing current measurement. The leakage current flows in accordance with Ohm's law $I = V / R_L$. For example, the voltage of 100 V and the resistance of 1 GΩ results in the leakage current of 100 V/10 GΩ = 100 nA. This is a very huge current and entirely swamps the polarizing current which is of the order of 1 pA. Guarding as shown in Fig. 2-6(b) reduces to a great extent this leakage current. The "high" potential lead between the electrometer and capacitor is surrounded by a metallic shield. A high resistance insulator made of Teflon isolates the high potential lead and the conductor shield. The shield is kept at the "high" potential by the connection to the voltage source. There is still a leakage path between the shield and low potential line. But this leakage path does not disturb significantly the current measurement because the leakage current is not included in the current measured by the electrometer. This guarding technique keeps the leakage current smaller than 0.3 pA and thus permits the polarizing current to be measured accurately.

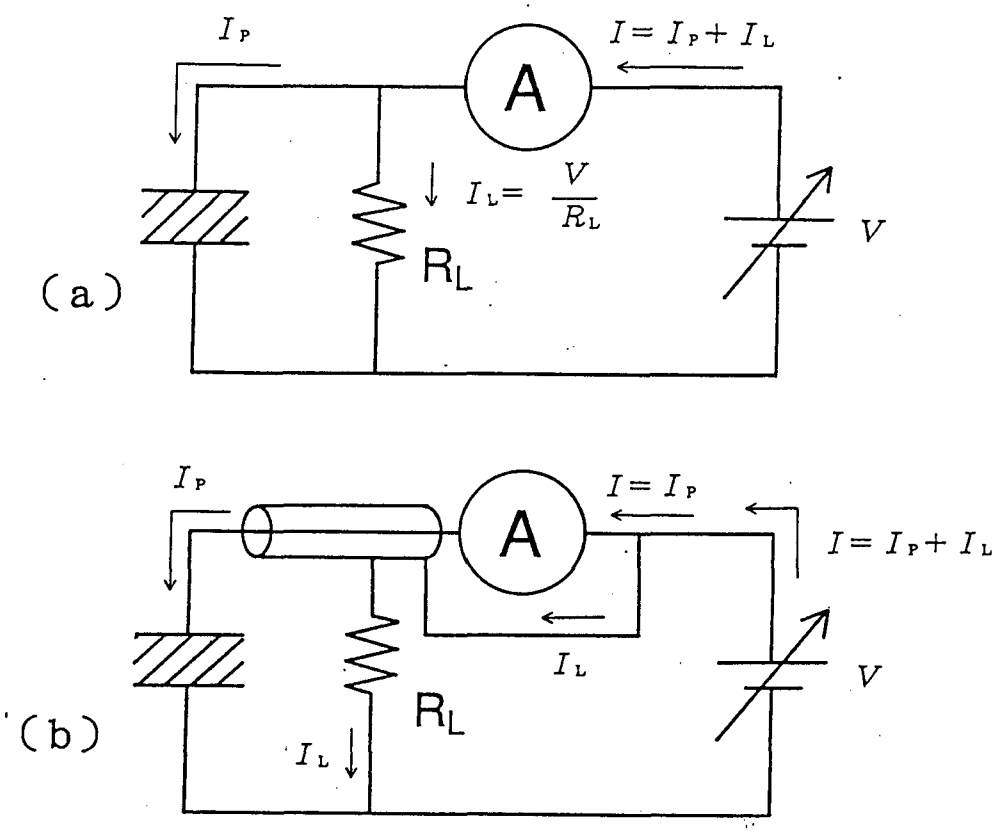

Fig. 2-6. Schematic diagram of the guarding technique for current measurement. (a)Without guarding, (b)with guarding. R_L: Resistance of leakage path, V: voltage generated by the voltage source, I: current measured by the electrometer, I_P: polarization current, I_L: leakage current.

2-4 Experimental Procedures

Because of the combination of two variable parameters, the temperature and electric field, various experimental procedures can be employed in the polaro-calorimetric experiment.

2-4-1 Heat Capacity

The intermittent heating method is employed for the heat capacity measurement. This is the standard method in adiabatic calorimetry. The actual measurement proceeds as follows. The temperature of the sample is measured as a function of time for 10–20 min. Under a normal condition, it remains constant or changes slowly with time (dT/dt < 10 mK h^{-1}). Then a definite amount of electrical energy E is introduced into the calorimeter cell. It takes 100–3000 s to increase the temperature of the sample by ~ 2 K (a normal temperature step for one heat capacity determination). After the heating, the calorimeter reaches new thermal equilibrium normally in 1–3 min. The temperature is measured again for 10–20 min. The heat capacity is given by the ratio $E/\Delta T$ where E is the Joule energy and $\Delta T = T_f - T_i$, T_i and T_f being the initial and final temperatures of the calorimeter, respectively. These temperatures are determined by linear extrapolation of the temperature vs. time plot to the middle point of the time interval of the Joule heating. The gross heat capacity thus determined is the sum of the heat capacities of the sample, sample cell and a small amount of helium gas at the average

temperature $T_{av} = (T_i + T_f)/2$. The heat capacity of the sample is calculated by subtracting the heat capacities of the cell and helium gas from the gross heat capacity. The heat capacity of the cell is determined in a separate experiment.

2-4-2 Thermally Stimulated Depolarization Current (TSDC) and Thermally Stimulated Polarization Current (TSPC)

The experimental scheme of thermally stimulated depolarization current (TSDC) method is shown in Fig. 2-7. The sample is polarized with a polarizing voltage V_p at a temperature T_p above the glass transition temperature T_g and is subsequently cooled to a temperature T_s with V_p being kept on. At T_s voltage is turned off and the sample is heated with a constant heating current I_h while the current released at the electrodes is measured by the electrometer. This current is called thermally stimulated depolarization current (abbreviated as TSDC). The TSDC measurement is continued to a temperature above T_g where there is no depolarization current anymore.

If an unpolarized state is first immobilized at a low temperature by cooling the sample without application of electric field and an electric field is then applied while the sample is heated subsequently, the thermally stimulated transition from a neutral to polarized state can be followed by registering the charging current as a function of time. It is thermally stimulated polarization current (TSPC). Its experimental scheme is shown in Fig. 2-8. TSPC curve is similar to TSDC, but not the same. The difference between TSDC and TSPC is due to the temperature dependence of

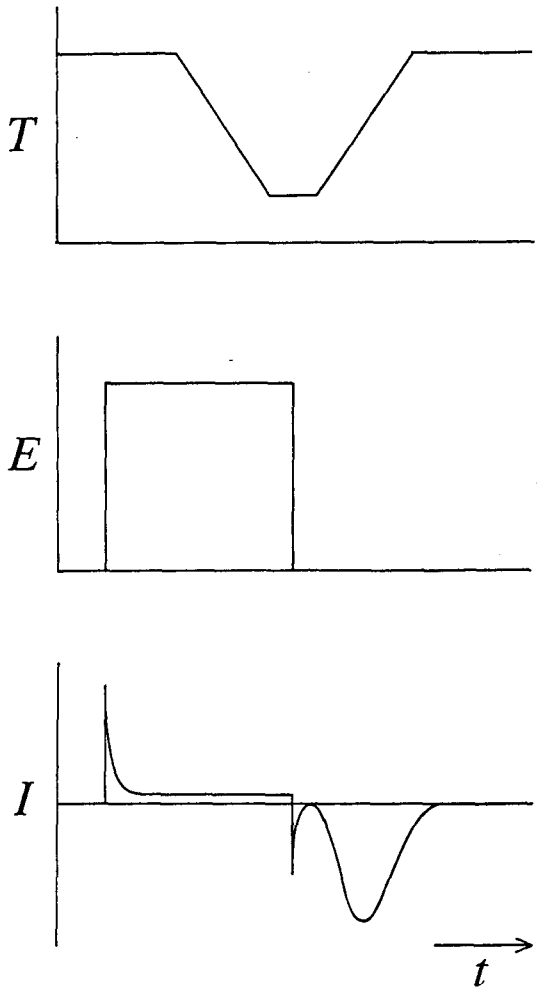

Fig. 2-7. Experimental procedure of TSDC measurement.

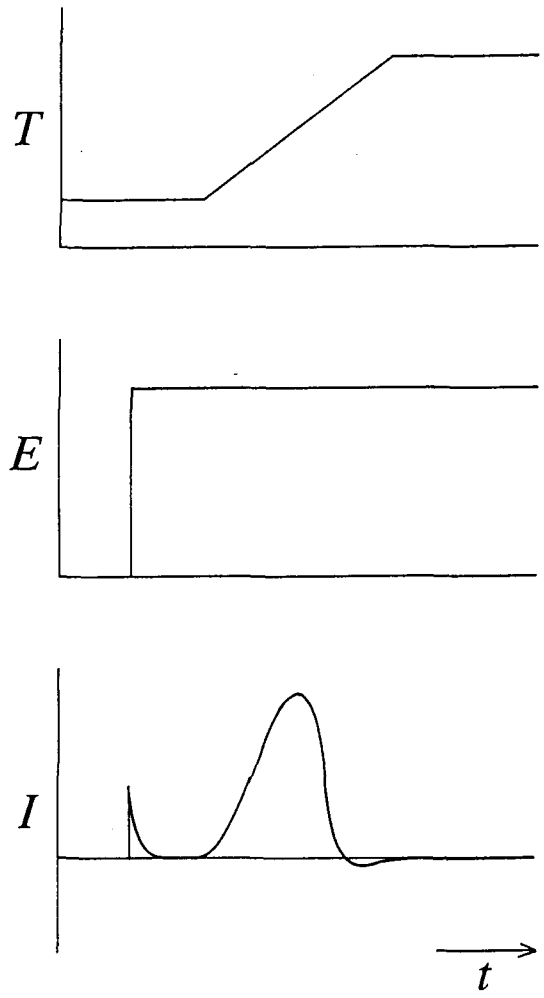

Fig. 2-8. Experimental procedure of TSPC measurement

equilibrium polarization $P_{eq}(E,T)$ and conduction current.

A constant heating rate scheme is normally employed in the TSDC and TSPC methods and is suitable for analysis of results. Here the heating by a constant current is employed because it is easier experimentally than the heating by constant rate. During the heating period, adiabatic shields are controlled as in the heat capacity measurement. Then the power supplied to the sample cell comes from the Joule heating. This power corresponds to $J(t)$ described in section 2-1-1. C_{vib} and $C_{c,eq}$ are obtained by the heat capacity measurement. By Eq. (2.16) the configurational enthalpy is determined in the TSDC and TSPC measurements. The apparent relaxation time of enthalpy $\tau_{H,ap}$ is determined by Eq. (2.20). At the same time apparent relaxation time of polarization $\tau_{P,ap}$ is determined by Eq. (2.31).

2-4-3 Enthalpy and Polarization Relaxations

There are two directions of enthalpy relaxation, exothermic and endothermic. There are also two directions of polarization relaxation, polarizing and depolarizing. Combination of the two pairs of the processes gives four types of simultaneous measurements on enthalpy and polarization relaxations: exothermic-polarizing, endothermic-polarizing, exothermic-depolarizing and endothermic-depolarizing relaxations. Because depolarizing current is measured more precisely than polarizing current (interfered by conducting current), simultaneous measurements were performed on exothermic-depolarizing and endothermic-depolarizing relaxations.

The experimental method on exothermic-depolarizing relaxation is illustrated in Fig. 2-9 and described as follows. The sample is cooled with a polarizing voltage V_p from higher temperature to just below T_g as in the TSDC experiment. The voltage is turned off synchronously with release of the thermal switch. Subsequently spontaneous temperature rise is observed under adiabatic condition while depolarization current is measured at the same time.

The experimental scheme on endothermic-depolarizing relaxation is shown in Fig. 2-10. After exothermic-depolarizing experiment, the sample is close to an equilibrium state. Then a constant voltage V_p is applied to the sample until the charging current is regarded as constant. Keeping the voltage on, the sample is heated rapidly by a few kelvin. The voltage is turned off at the same time as the heating is stopped. Subsequently spontaneous temperature fall is observed under adiabatic condition while depolarization current is measured at the same time.

2-4-4 Isothermal Polarization Relaxation

By the simultaneous measurements on enthalpy-polarization relaxation, it is difficult to observe the pure dielectric response because temperature is not constant. To observe the dielectric response at a constant temperature, the experiment only on polarization relaxation is carried out after enthalpy relaxation finishes. The experimental procedure consists of only two processes, polarization and depolarization as follows. The voltage V_p is applied to the sample until the charging current is regarded as constant.

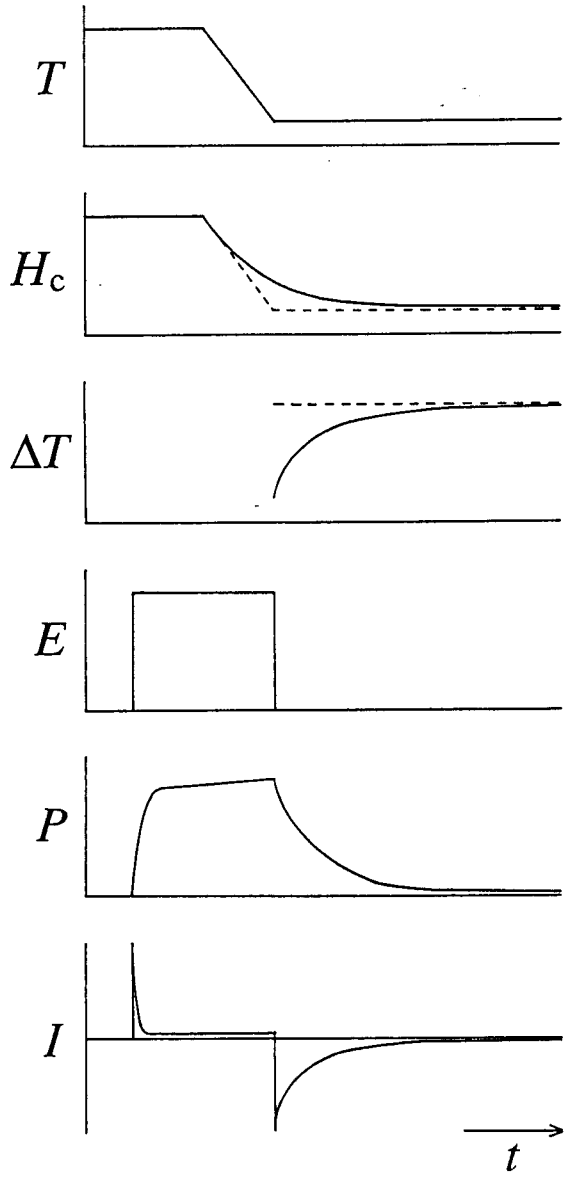

Fig. 2-9. Experiment on exothermic-depolarizing relaxation. *T*: temperature, H_C: configurational enthalpy, ΔT: spontaneous temperature change, *E*: electric field, *P*: polarization, *I*: polarization current.

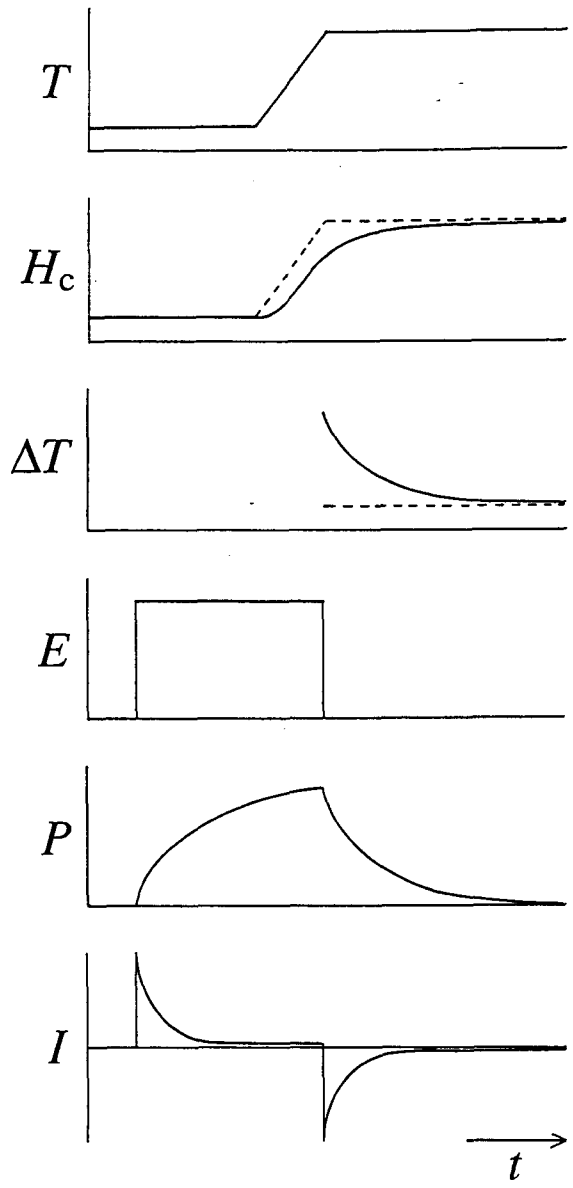

Fig. 2-10. Experiment on endothermic-depolarizing relaxation. T: temperature, H_C: configurational enthalpy, ΔT: spontaneous temperature change, E: electric field, P: polarization, I: polarization current.

During this time the polarizing response is recorded. Subsequently the voltage is turned off and the depolarizing response is recorded. The dielectric response function determined by this method should be the same as that determined by AC dielectric measurement. But the time scales of them differs much, *i.e.* 1 s—10 ns in usual AC measurement, 100 s—1 Ms in this method.

Reference

1. S. F. Lau, H. Suzuki and B. Wunderlich, *J. Polym. Sci., Polym. Phys. Ed.*, 22, 379 (1984).

Chapter 3 EXPERIMENT ON 1-PROPANOL

3-1 Sample

The commercial product from Tokyo Kasei Kogyo Co. Ltd. was purified by the following procedure: fractional distillation, drying with molecular sieve 3A and vacuum distillation. An impurity peak was detected by a gas chromatograph, but it was less than 0.03 % of the main peak. The amount of water in the sample was revealed to be 0.20 mol % by the Karl-Fischer test. Purity determined by the fractional melting method was 99.88 %.

The mass of the sample used for the polaro-calorimetric experiment was 22.0296 g (0.366574 mol).

3-2 Polaro-calorimetric Experiment

3-2-1 Heat Capacity

The purpose of the study on 1-propanol is the investigation of relaxation phenomena. Analysis of the calorimetric data for the enthalpy relaxation requires the experimental heat capacity separated into the vibrational and configurational contributions, as described in section 2-1-1. The heat capacities were measured between 55 and 210 K, and they are reproduced in Fig. 3-1 and Table 3-1. The heat capacity data of supercooled liquid between 120 and 150 K are not shown, since the heat capacity in the

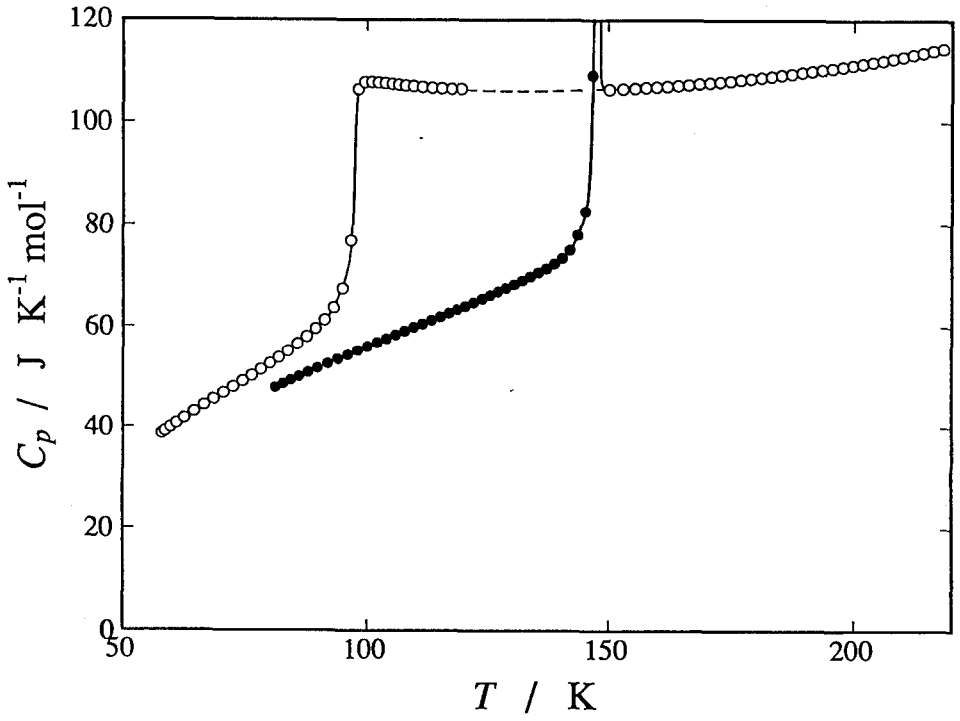

Fig. 3-1. Molar heat capacity of 1-propanol. ○ :liquid and glassy state, ● : crystalline state.

Table 3-1. Molar heat capacity of 1-propanol.

T_{av} / K	C_p / $JK^{-1}mol^{-1}$	T_{av} / K	C_p / $JK^{-1}mol^{-1}$	T_{av} / K	C_p / $JK^{-1}mol^{-1}$
(glass and super-		(liquid)		(crystal)	
cooled liquid)		150.18	106.4	81.05	47.96
57.98	38.70	152.90	106.5	82.67	48.69
58.65	39.16	155.34	106.6	84.27	49.41
59.80	39.92	157.50	106.8	86.00	50.18
60.93	40.71	159.66	106.9	87.85	50.98
62.52	41.78	161.81	107.0	89.85	51.83
64.53	43.14	163.96	107.2	91.98	52.71
66.51	44.44	166.11	107.3	94.07	53.58
68.48	45.68	168.24	107.5	96.13	54.43
70.43	46.91	170.38	107.7	98.16	55.26
72.37	48.11	172.50	107.9	100.15	56.06
74.26	49.27	174.63	108.0	102.12	56.82
76.11	50.40	176.74	108.3	104.07	57.59
77.99	51.57	178.86	108.5	105.99	58.34
79.90	52.76	180.96	108.7	107.89	59.07
81.77	53.90	183.07	108.9	109.76	59.79
83.69	55.18	185.16	109.2	111.62	60.51
85.64	56.57	187.26	109.4	113.45	61.22
87.55	58.00	189.35	109.7	115.27	61.92
89.42	59.55	191.43	110.0	117.07	62.62
91.24	61.30	193.51	110.2	118.85	63.33
93.11	63.67	195.58	110.6	120.62	64.01
95.01	67.47	197.65	110.8	122.37	64.73
96.77	76.93	199.71	111.1	124.10	65.43
98.20	106.4	201.77	111.5	125.83	66.13
99.55	107.7	203.82	111.8	127.53	66.85
100.97	107.8	205.87	112.1	129.23	67.54
102.40	107.7	207.91	112.5	130.91	68.27
103.81	107.6	209.95	112.8	132.57	69.01
105.23	107.4	211.98	113.2	134.23	69.81
106.64	107.2	214.01	113.6	135.87	70.59
108.05	107.1	216.03	114.0	137.50	71.42
109.68	107.0	218.04	114.4	139.11	72.37
111.54	106.8			140.71	73.50
113.50	106.7			142.29	75.08
115.56	106.6			143.85	78.05
117.61	106.5			145.36	82.65
119.74	106.5			146.82	109.1

temperature region could not be measured because of crystallization. The heat capacity increased abruptly around 98 K due to the glass transition.

The heat capacity of 1-propanol was measured by J. F. Counsell *et al.*[1] in 1968. To compare the present data with their results, the heat capacities of the liquid are plotted as a function of temperature in a magnified scale in Fig. 3-2. The discrepancy between the two sets of data is about 0.2 % of the heat capacity in the temperature range compared.

For the purpose of extrapolation, the experimental heat capacity data between 62 and 78 K were used to determine as assumed model linear function for the vibrational heat capacity $C_{vib,m}$, and the data between 102 and 110 K for the configurational heat capacity $C_{c,eq,m}$ below and above their respective temperature ranges, respectively. Figure 3.3 shows these functions and they are expressed numerically as

$$C_{vib,m}/\mathrm{J\ K^{-1}mol^{-1}} = 0.629612\ T/\mathrm{K} + 2.516, \quad (3.1)$$

and

$$C_{c,eq,m}/\mathrm{J\ K^{-1}mol^{-1}} = -0.729284\ T/\mathrm{K} + 115.365, \quad (3.2)$$

respectively. Although the assumed linear functions cannot be exact expressions for the heat capacities, they should be sufficiently accurate for short extrapolation.

3-2-2 TSDC and TSPC

Before the TSDC measurement the sample was cooled from

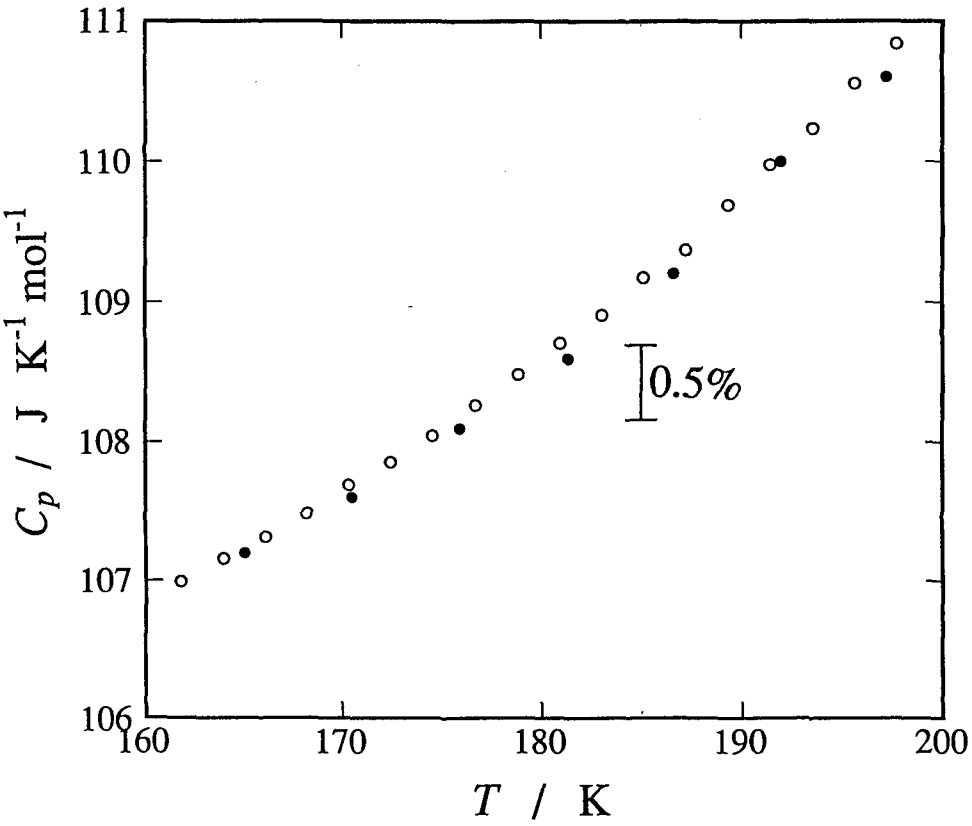

Fig. 3-2. Comparison of the present heat capacity (○) and the reference[1] (●).

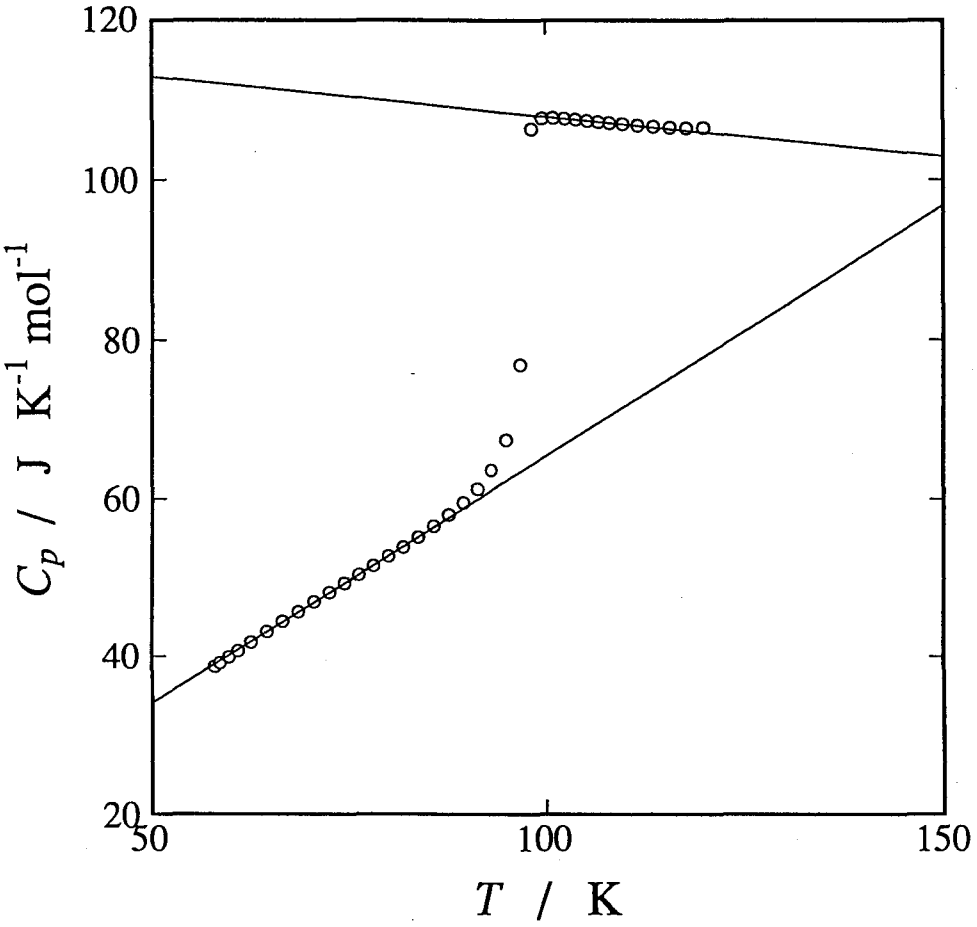

Fig. 3-3. Extrapolation of the heat capacities of glassy and liquid states.

109 K to 80 K in a polarizing voltage of 100 V. Temperature in the cooling process is shown in Fig. 3-4. At 80 K the voltage was turned off. The sample was heated from 80 K with heating current I_h of 20 mA. The temperature and the depolarization current were measured simultaneously as shown in Fig. 3-5. The peak of the depolarization current occurred at 101.0 K. The excess configurational enthalpy ΔH_c in the TSDC measurement was determined by means of Eq. (2.16), and the result is shown in Fig. 3-6. The configurational enthalpy in the TSDC measurement was also determined by Eq. (2.11) as shown in Fig. 3-7. Polarization decrease is shown in Fig. 3-8 as the charge amount on the electrodes.

For the TSPC measurement the sample was first cooled from 300 K to 83 K without application of polarizing voltage. Temperature in the cooling process between 110 K and 83 K is drawn in Fig. 3-9. The temperature change above 110 K is not shown because thermal history of the sample at temperatures much higher than the glass transition is irrelevant to the present experiment. The diagram of the temperature change was different from the TSDC measurement. The cooling rate of the TSPC measurement suddenly slowed down at 90 K due to a little accident of thermal switch. At 83 K the voltage 100 V was applied to the sample. The sample was heated from 83 K with heating current I_h of 20 mA. The temperature and the polarization current were measured simultaneously as shown in Fig. 3-10. The main peak of the polarization current occurred at 100.9 K. The excess configurational enthalpy ΔH_c in the TSPC measurement was determined as

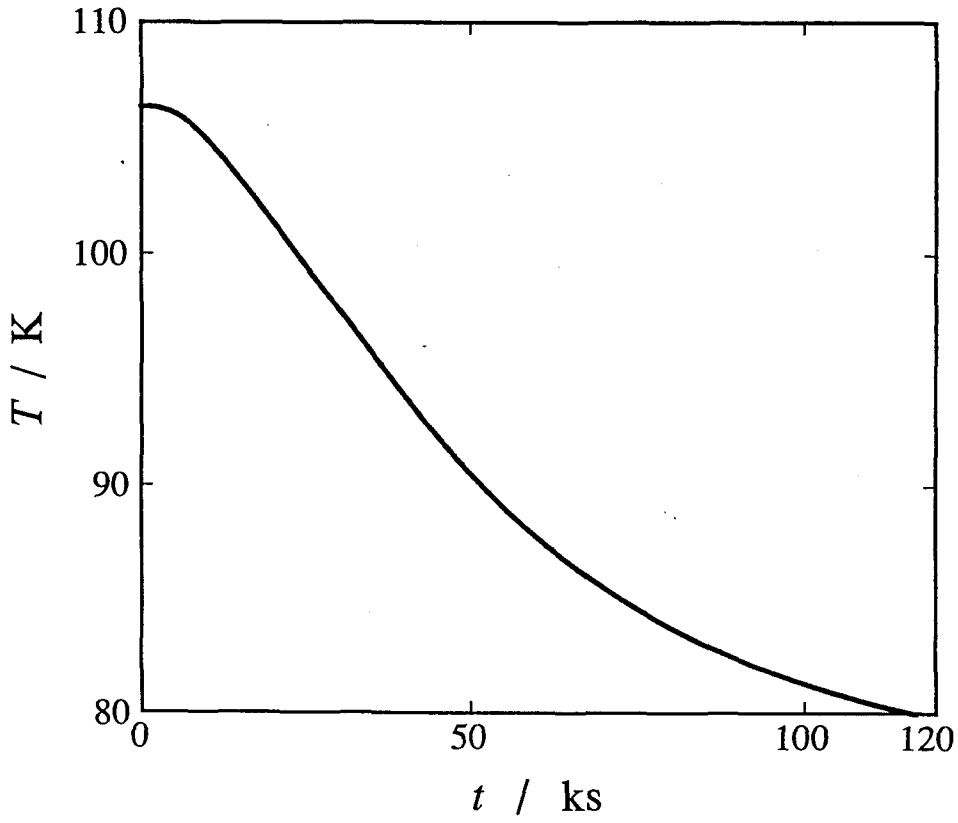

Fig. 3-4. Temperature as a function of time on cooling before TSDC measurement.

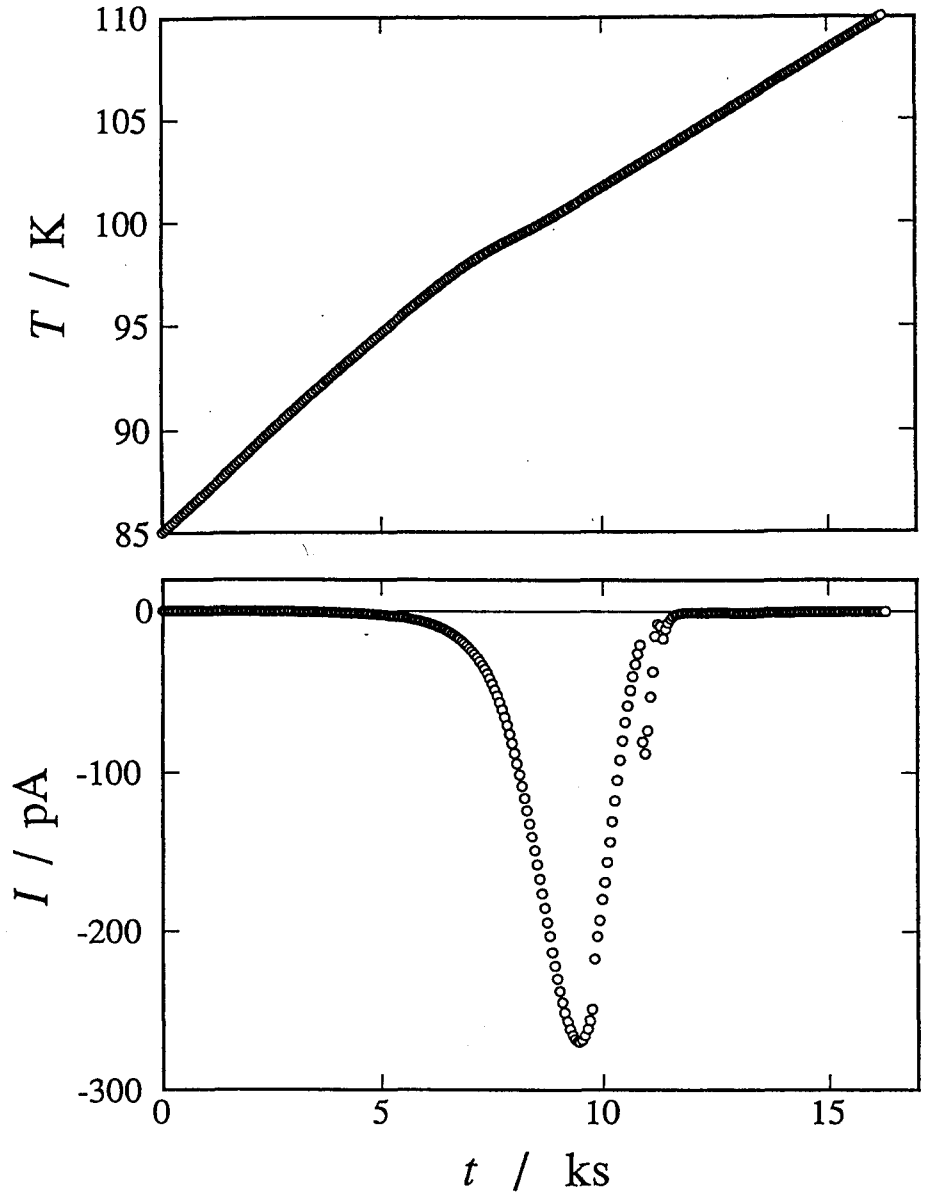

Fig. 3-5. Temperature and depolarization current as functions of time in TSDC measurement.

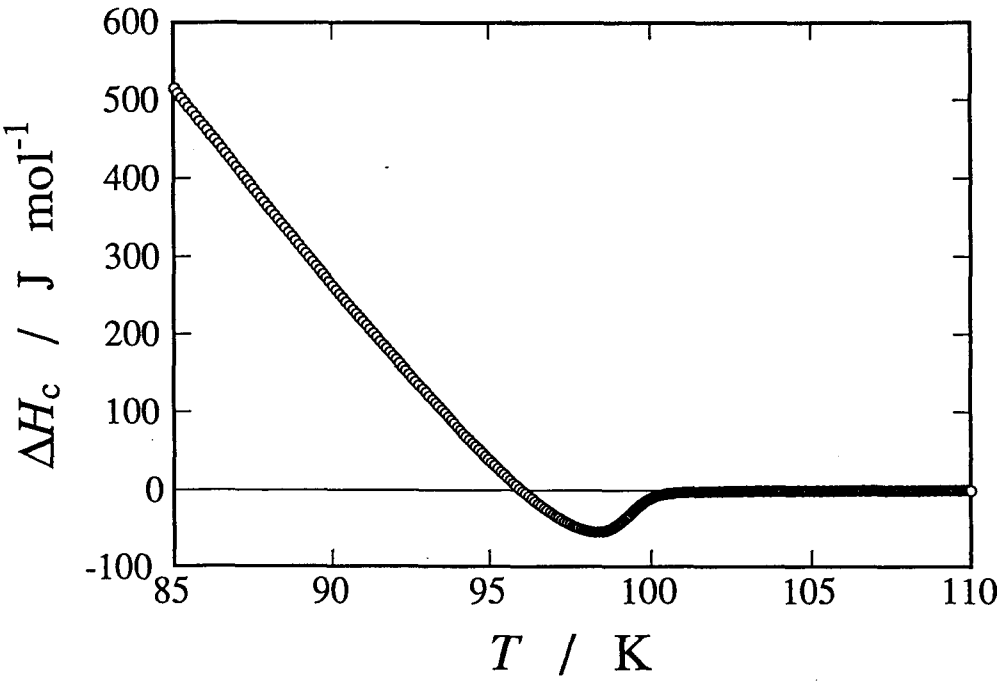

Fig. 3-6. Excess configurational enthalpy *vs.* temperature in TSDC measurement.

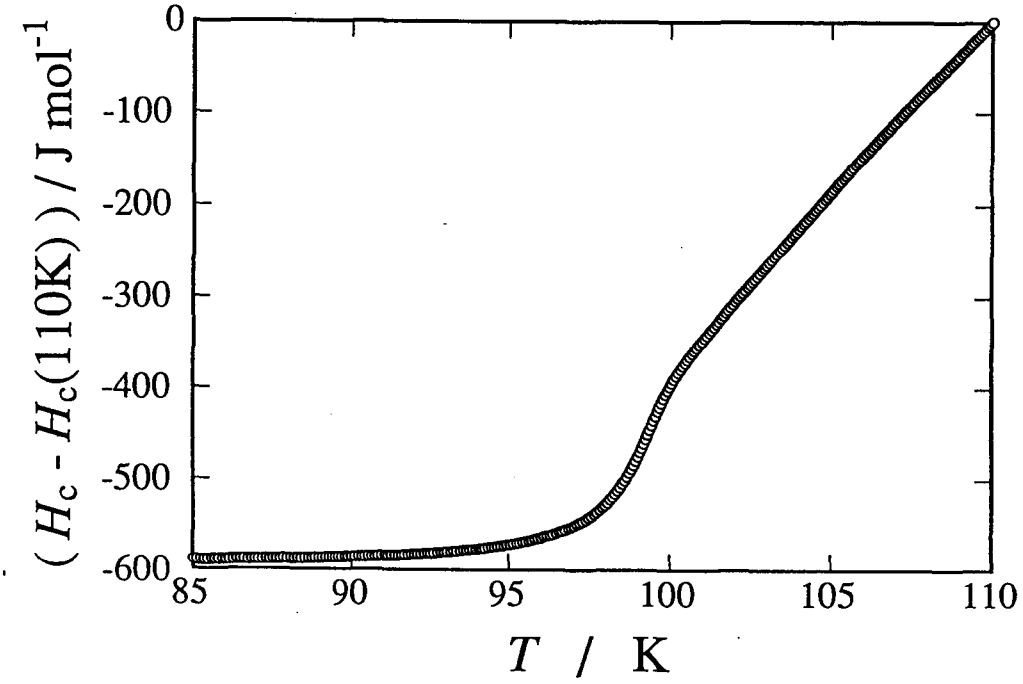

Fig. 3-7. Configurational enthalpy *vs.* temperature in TSDC measurement.

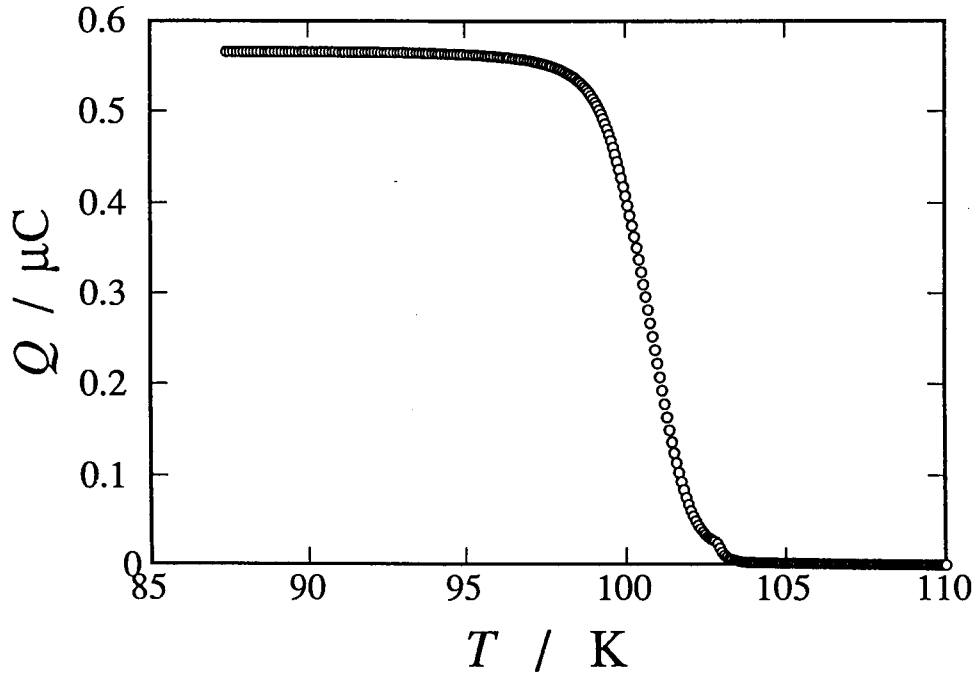

Fig. 3-8. Polarization decay in TSDC measurement.

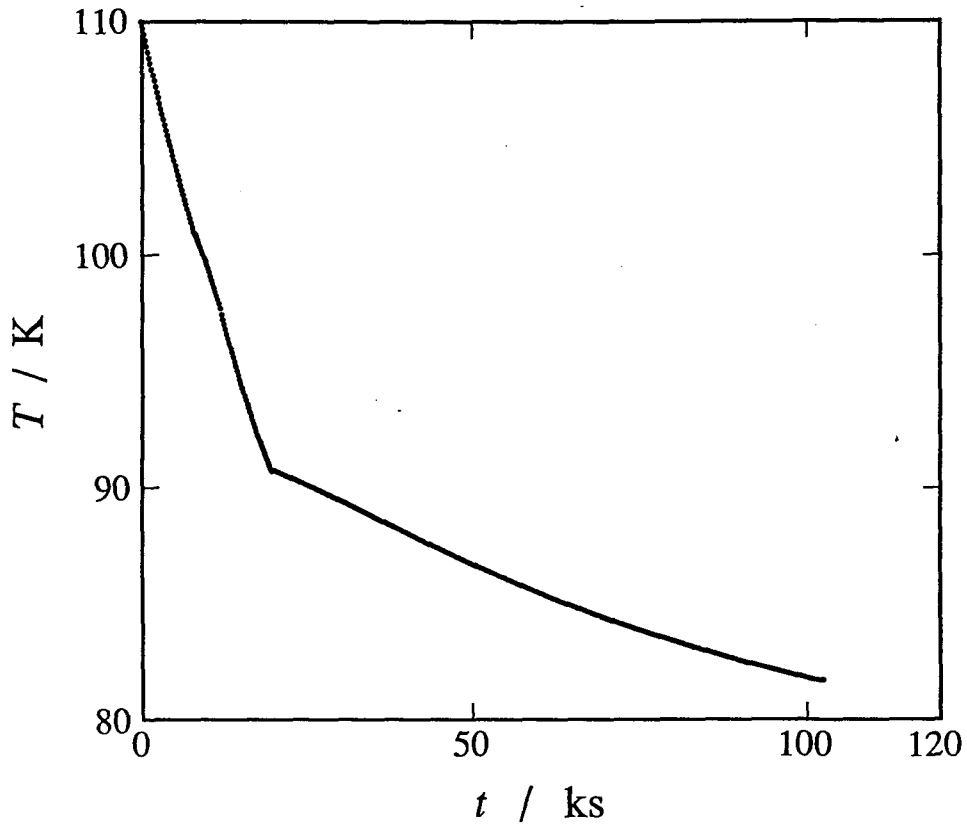

Fig. 3-9. Temperature as a function of time on cooling before TSPC measurement.

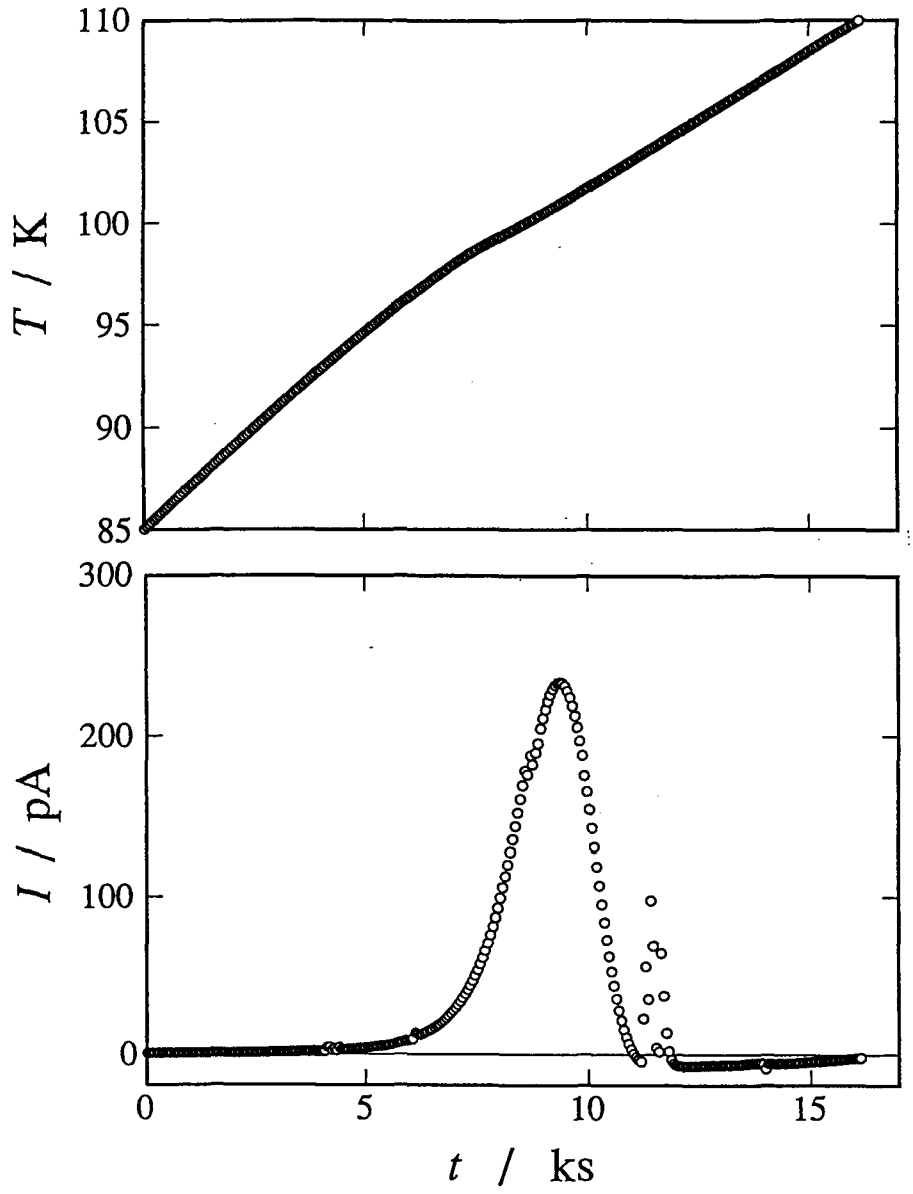

Fig. 3-10. Temperature and polarization current as functions of time in TSPC measurement.

shown in Fig. 3-11. The configurational enthalpy in the TSPC measurement was also determined as shown in Fig. 3-12. Integration of the polarization current with respect to time gave the amount of charge on the electrodes, and the quantity is plotted in Fig. 3-13.

An unexpected peak was found just above the main peak in the TSDC and TSPC measurements. Their origin is not understood. It may have been caused by flow of the sample in the cell because the thermal expansion of the sample generates internal stress which will be released by the flow of the sample when the viscosity of the sample decreases above the glass transition region. However, the electric charge associated with the spurious peak was about 10 nC, or 1.8 % of the charge of the main peak in both of the TSDC and TSPC measurements.

3-2-3 Enthalpy and Polarization Relaxations

Experiments on exothermic-depolarizing relaxation were carried out at three temperatures, 95.7 K, 96.7 K and 97.6 K. Only the experimental result at 95.7 K is shown here. The sample was cooled as indicated in Fig. 3-14. The polarizing voltage was turned on at 110 K. When the temperature reached 95.48 K, the polarizing voltage and the thermal switch were turned off. The spontaneous temperature increase and depolarization current were recorded simultaneously. The temperature increase is shown in Fig. 3-15 and the depolarization current in Fig. 3-16. The excess configurational enthalpy calculated from the spontaneous temperature increase is shown in Fig. 3-17. Decrease of the polarization

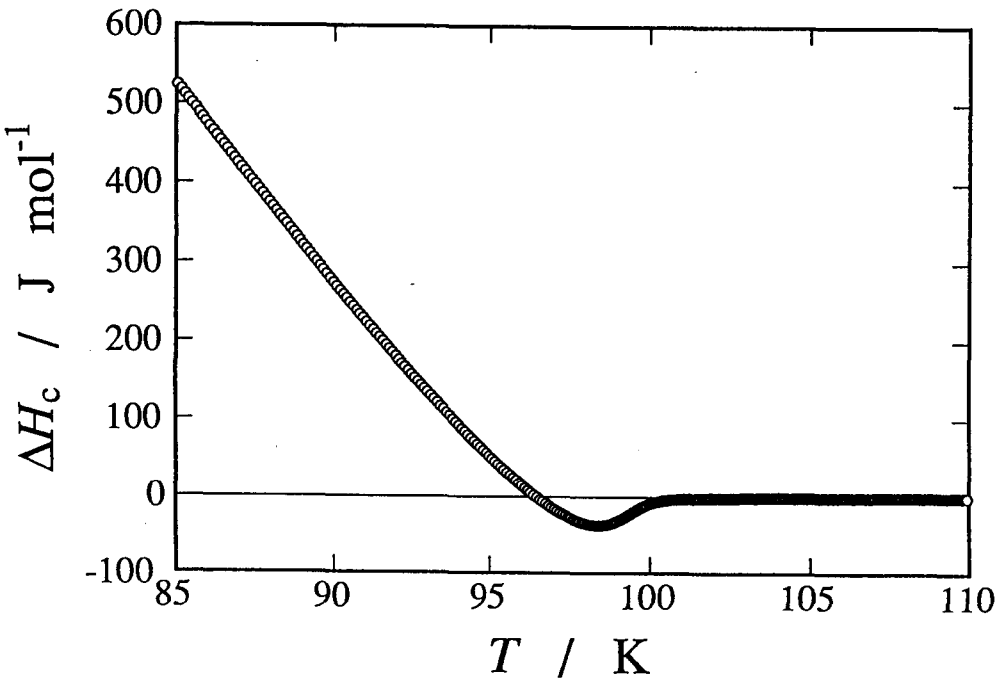

Fig. 3-11. Excess configurational enthalpy *vs.* temperature in TSPC measurement.

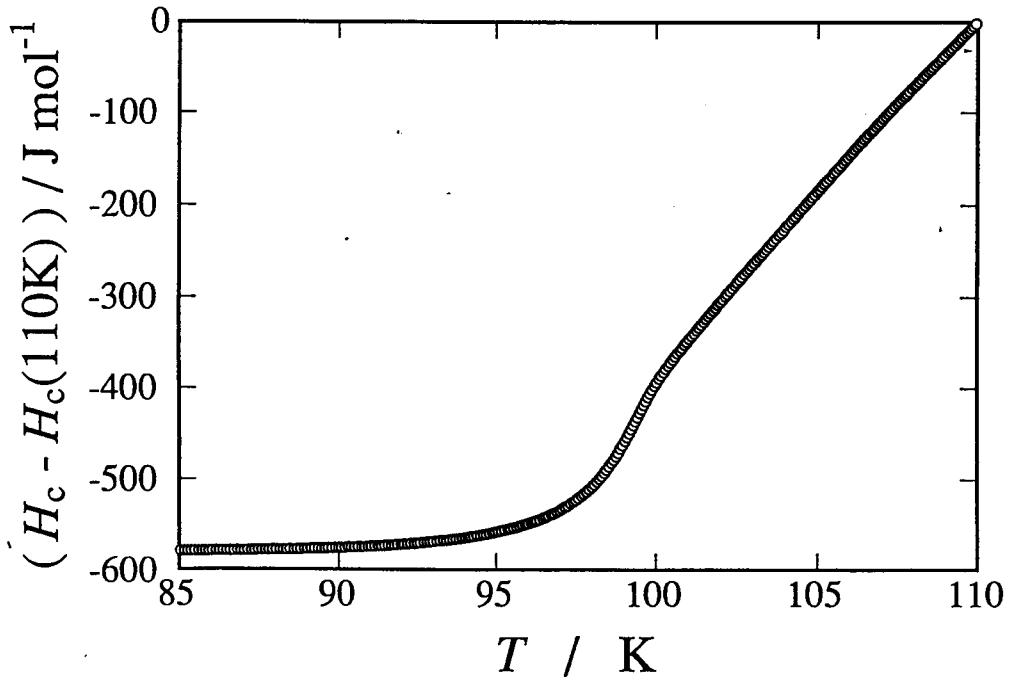

Fig. 3-12. Configurational enthalpy *vs.* temperature in TSPC measurement.

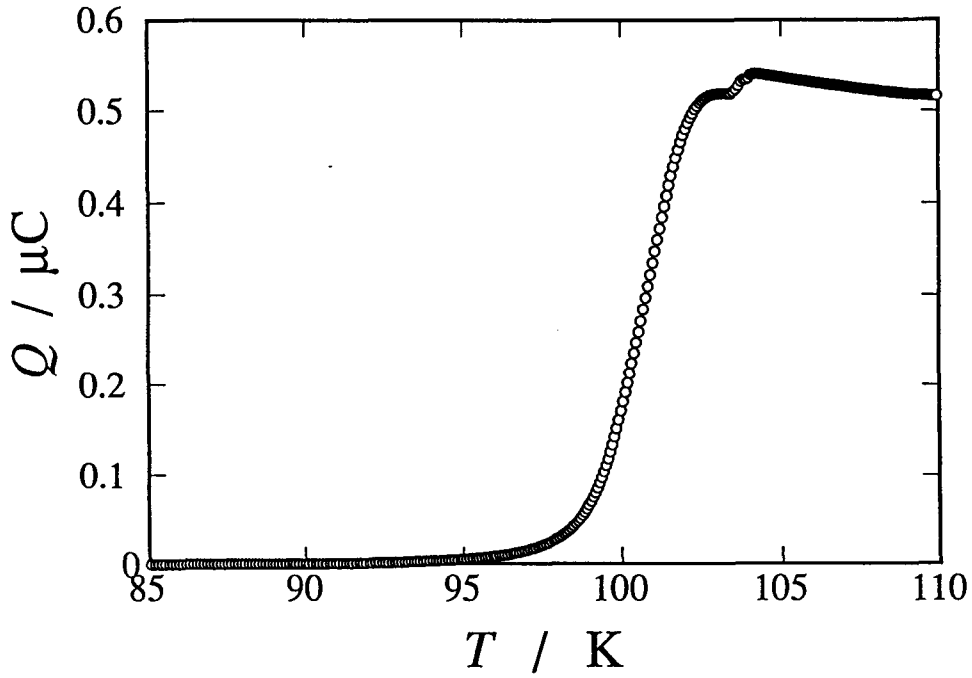

Fig. 3-13. Increase of polarization in TSPC measurement.

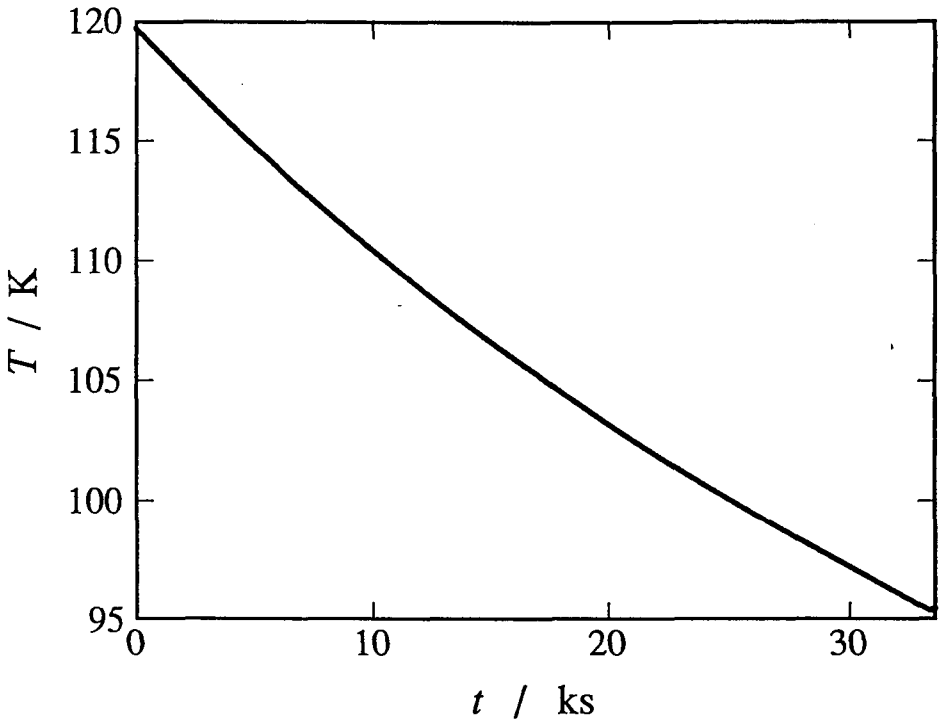

Fig. 3-14. Temperature as a function of time before the experiment of exothermic-depolarizing relaxation.

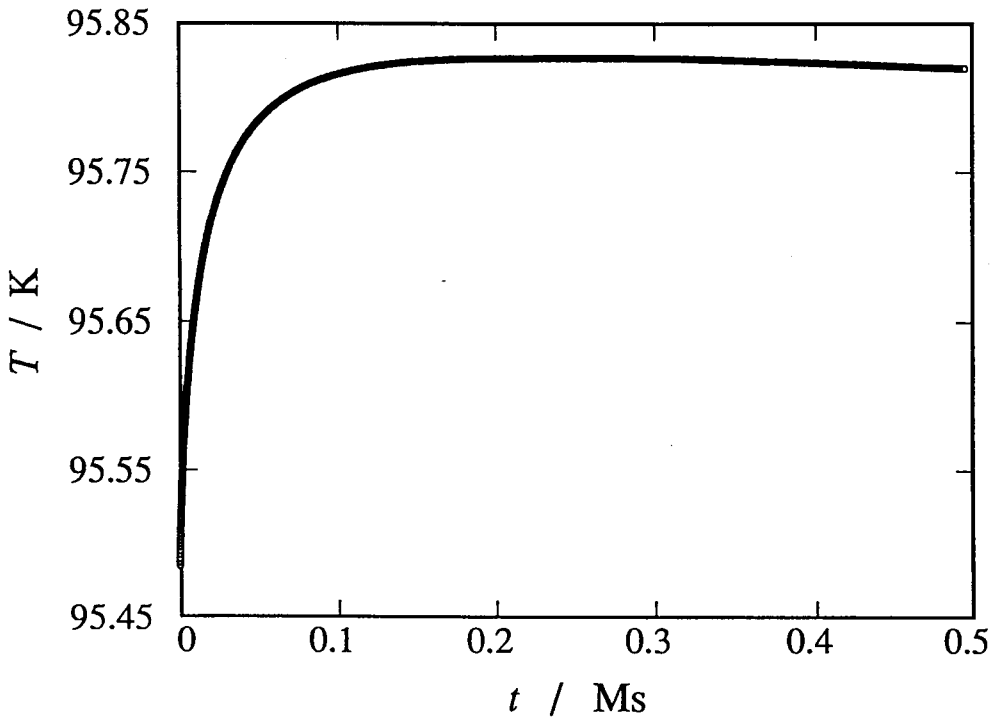

Fig. 3-15. Spontaneous temperature rising in the experiment of exothermic-depolarizing relaxation around 95.6 K.

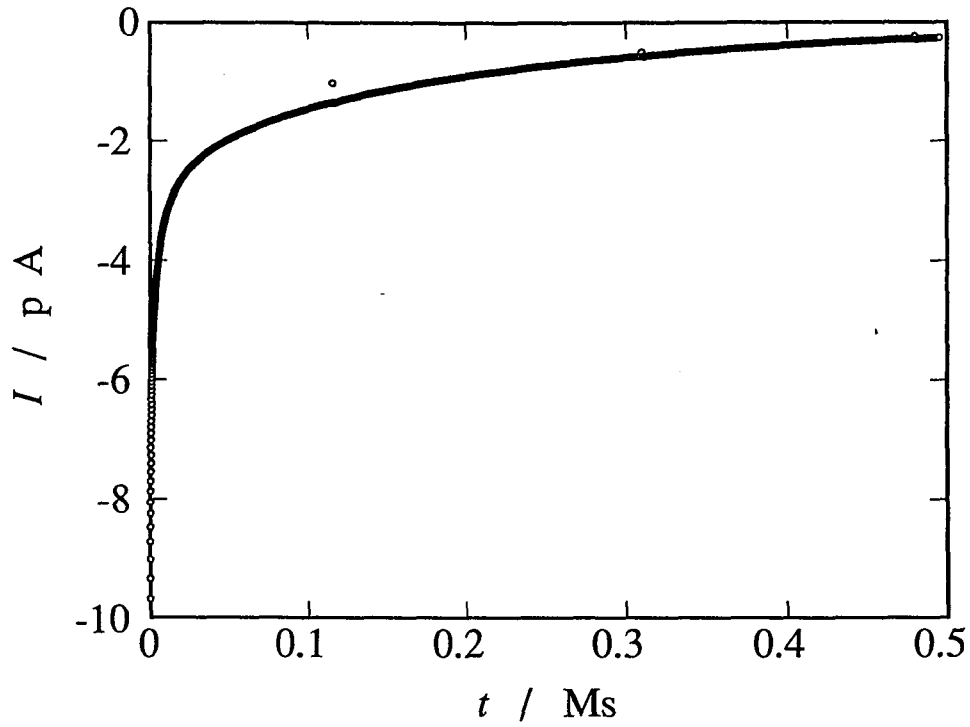

Fig. 3-16. Depolarization current in the experiment of exothermic-depolarizing relaxation around 95.6 K.

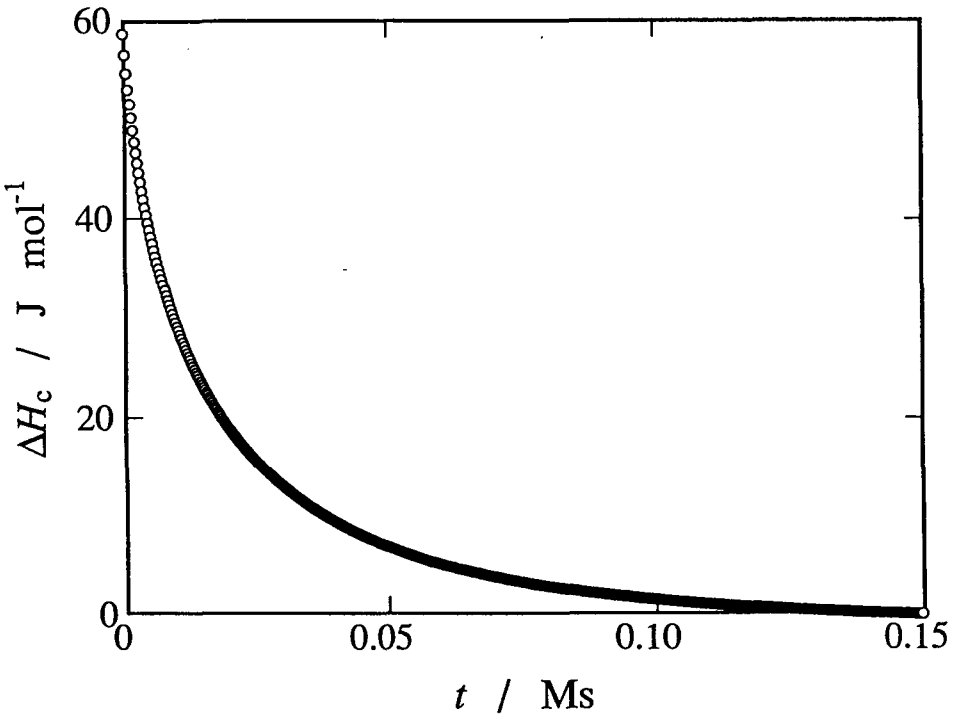

Fig. 3-17. Decay of the excess configurational enthalpy in the exothermic-depolarizing relaxation whose temperature change is shown in Fig. 3-15.

is shown as integration of the depolarization current with respect to time. The asymptotic value of the electric charge drawn in Fig. 3-18 corresponds to the zero point of the polarization.

Experiment on endothermic-depolarizing relaxation was carried out only at 99.0 K. After the sample relaxed thermally, the sample was polarized by 100 V for 0.16 Ms at 97.56 K. Then the sample was heated to 99.2 K as shown in Fig. 3-19 while the polarizing voltage was kept on. When the heating was finished, the polarizing voltage was turned off. The spontaneous temperature decrease and depolarization current were observed simultaneously. The temperature decrease is shown in Fig. 3-20 and the depolarization current in Fig. 3-21. The excess configurational enthalpy derived from the spontaneous temperature decrease is shown in Fig. 3-22. The polarization change is shown as integration of the depolarization current with time. The asymptotic value (-580 nC) of the electric charge in Fig. 3-23 gives the initial value of the zero point of the polarization.

3-2-4 Isothermal Polarization Relaxation

Experiments on isothermal polarization relaxation were carried out at four temperatures, 95.74 K, 97.58 K, 98.85 K and 100.29 K. The temperature change during measurement of polarization relaxation was smaller than 20 mK at each temperature. Here the result in detail was shown only at 97.58 K. The polarization current with an applied voltage of 100 V is shown in Fig. 3-24. After the sample was polarized for 0.15 Ms, the voltage was turned off and the measurement of the depolarization current was

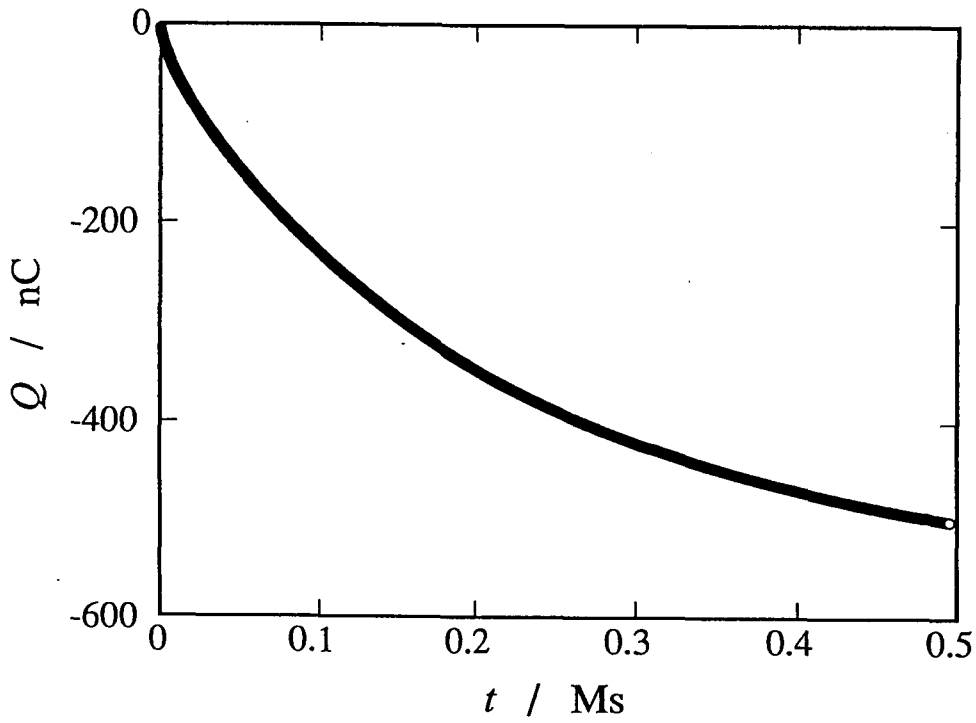

Fig. 3-18. Decay of polarization in the exothermic-depolarizing relaxation. Integration of depolarization current in Fig. 3-16 is shown as a function of time.

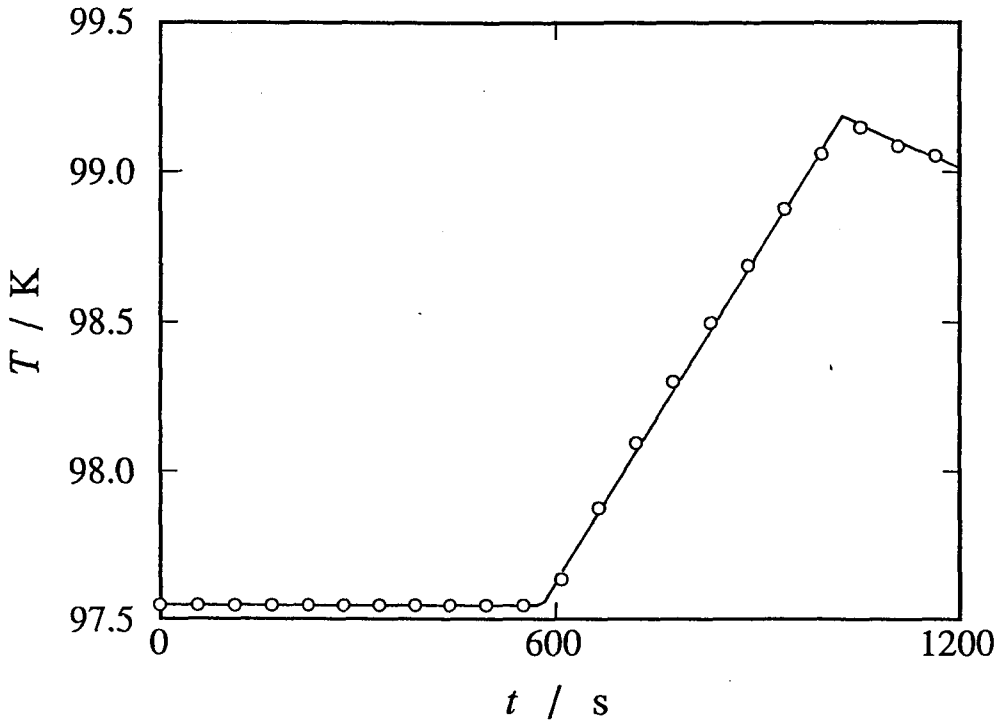

Fig. 3-19. Temperature as a function of time before the experiment of endothermic-depolarizing relaxation. The sample was heated in the period between 580 s and 1000 s.

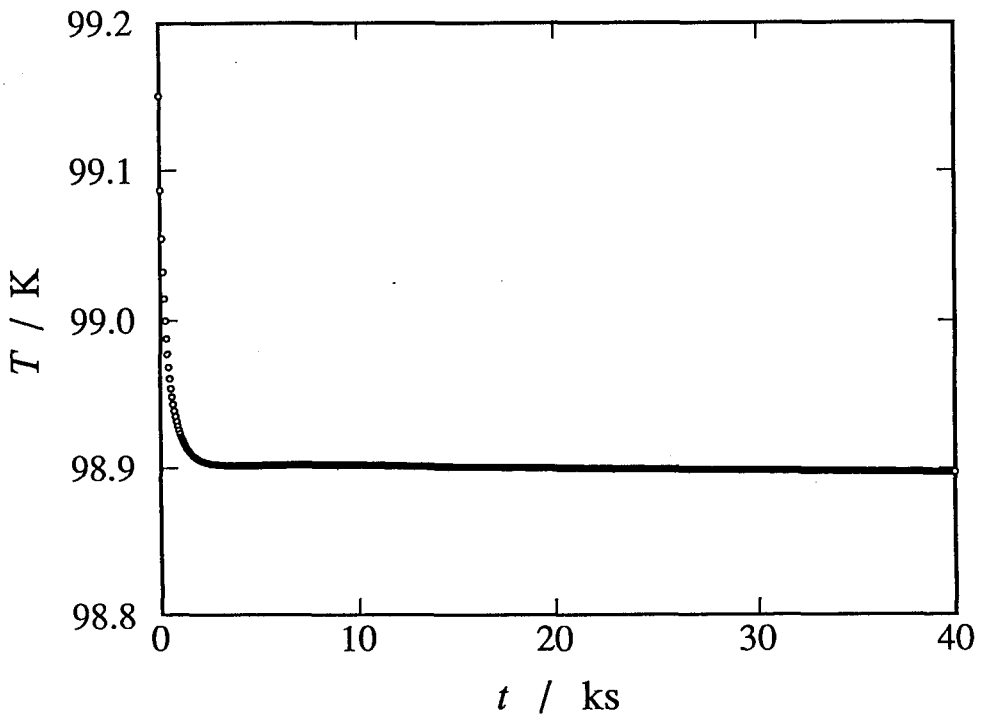

Fig. 3-20. Spontaneous temperature fall in the experiment of endothermic-depolarizing relaxation.

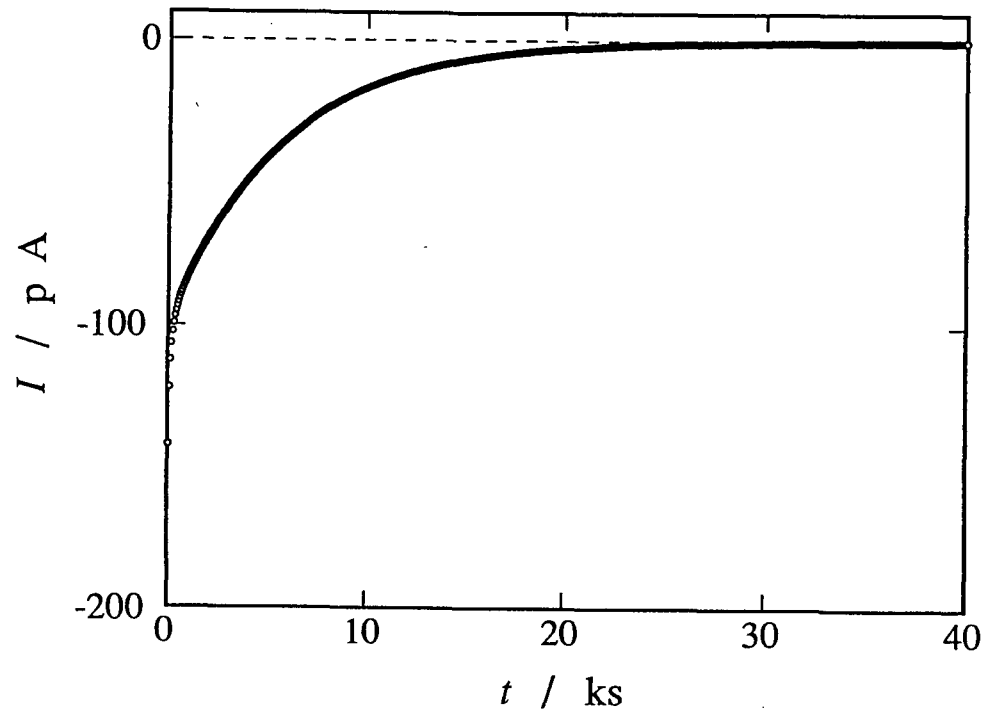

Fig. 3-21. Depolarization current in the experiment of endothermic-depolarizing relaxation.

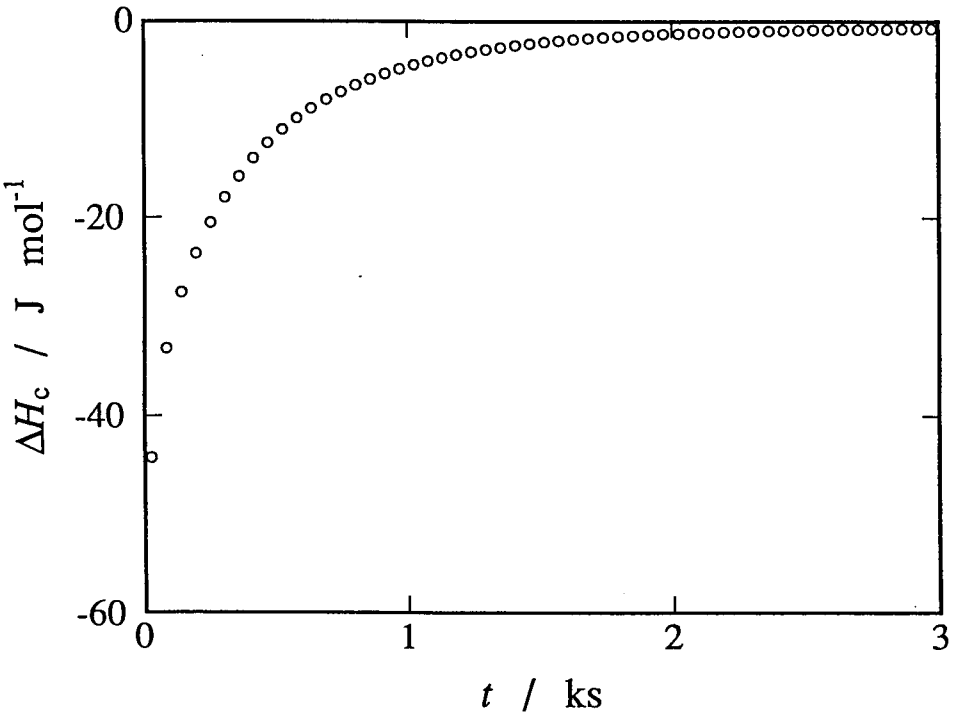

Fig. 3-22. Decay of the excess configurational enthalpy in the endothermic-depolarizing relaxation whose temperature is shown in Fig. 3-20.

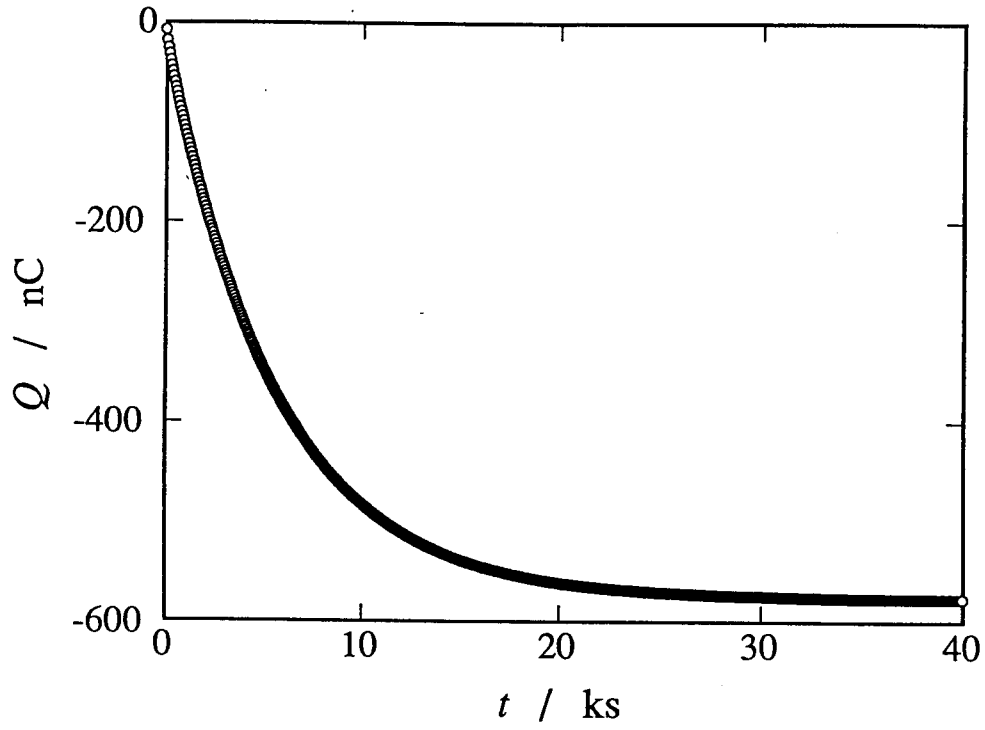

Fig. 3-23. Decay of the polarization in the endothermic-depolarizing relaxation. Integration of depolarization current drawn in Fig. 3-21 is shown as a function of time.

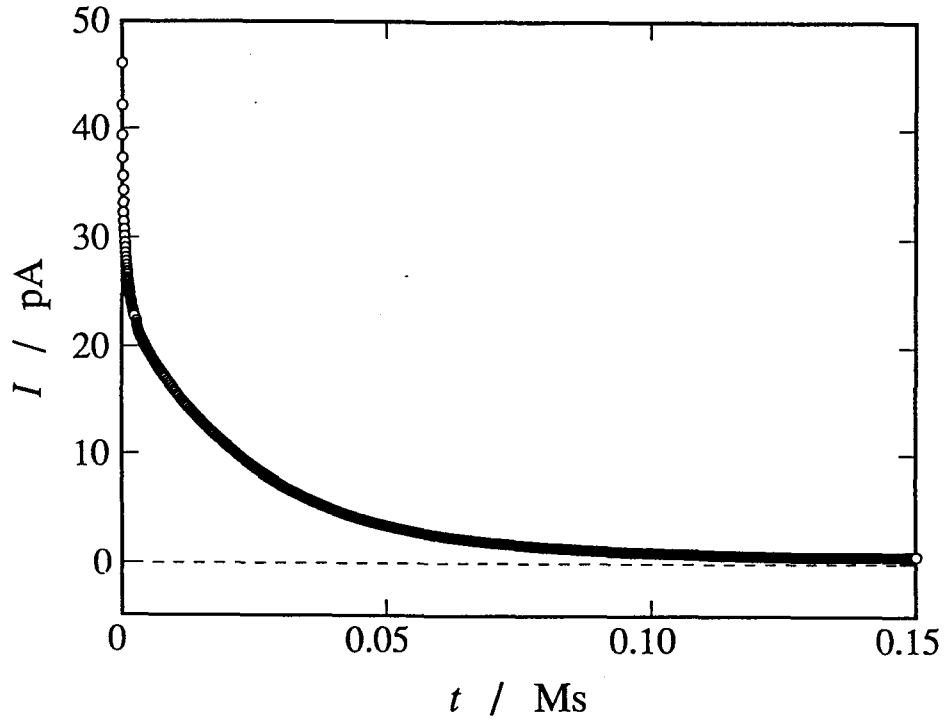

Fig. 3-24. Polarization current in the experiment of isothermal polarization relaxation at 97.58 K.

started. The depolarization current is shown in Fig. 3-25. Integrations of the polarization and depolarization currents with time are shown in Figs. 3-26 and 3-27, respectively. Because the integration of the polarization current includes the conduction current, the electric charge is larger than the contribution from the polarization of the sample itself. The integration of the depolarization current corresponds solely to the polarization change. Temperature dependence of the depolarization current is shown in Fig. 3-28.

Reference

1. J. F. Counsell, E. B. Lees and J. F. Martin, *J. Chem. Soc.*, A 1819 (1968).

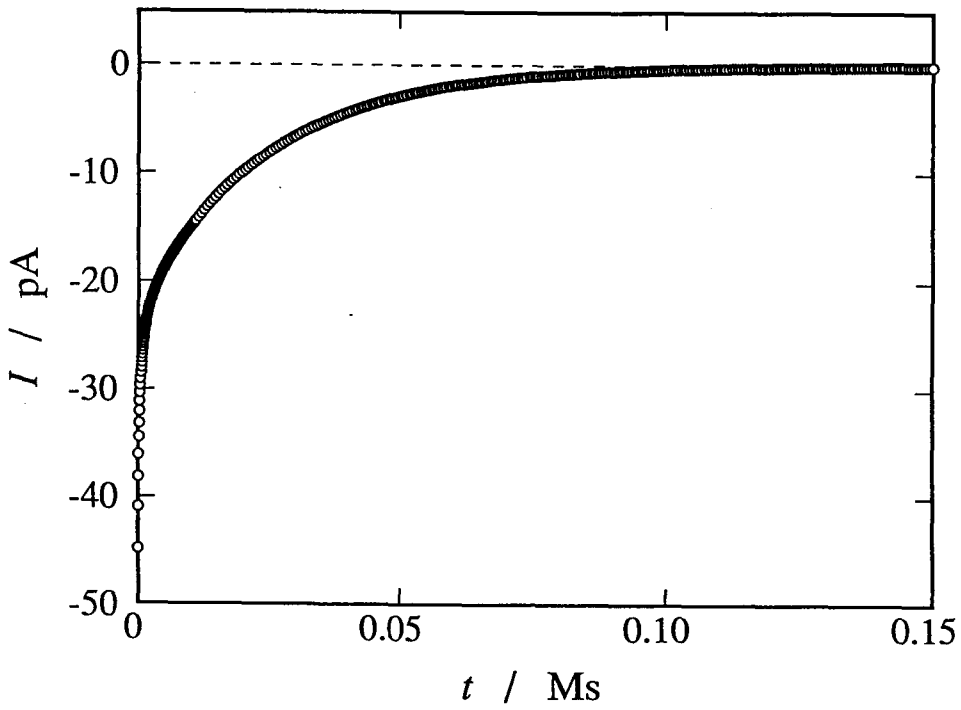

Fig. 3-25. Depolarization current in the experiment of isothermal polarization relaxation at 97.58 K.

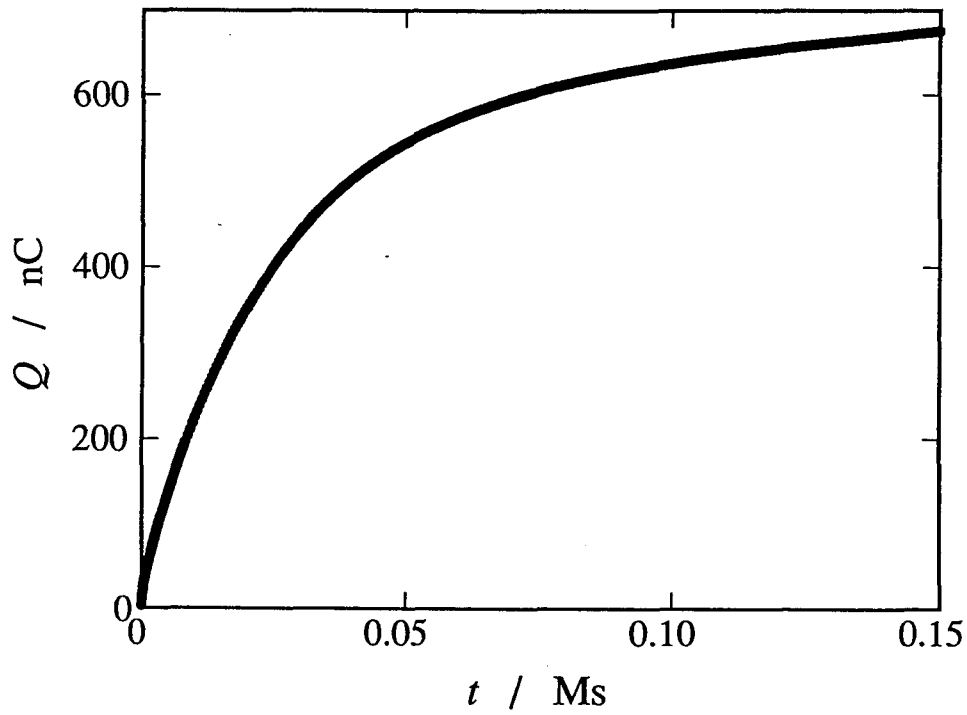

Fig. 3-26. Polarization increase at a constant temperature. Integration of polarization current in Fig. 3-24 is shown as a function of time.

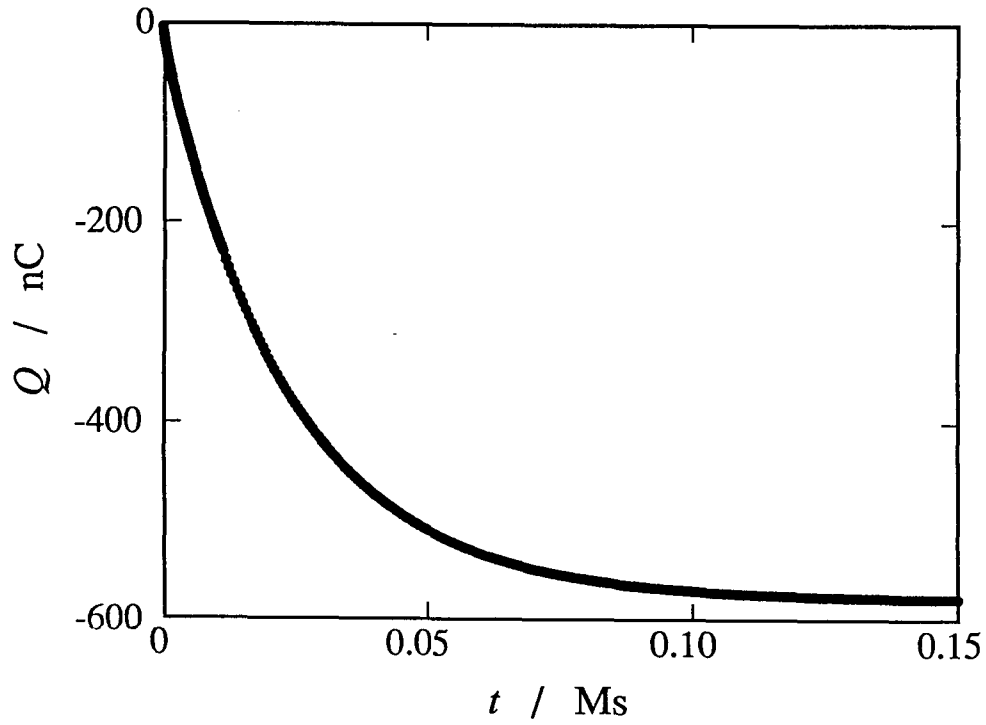

Fig. 3-27. Polarization decay at a constant temperature. Integration of depolarization current in Fig. 3-25 is shown as a function of time.

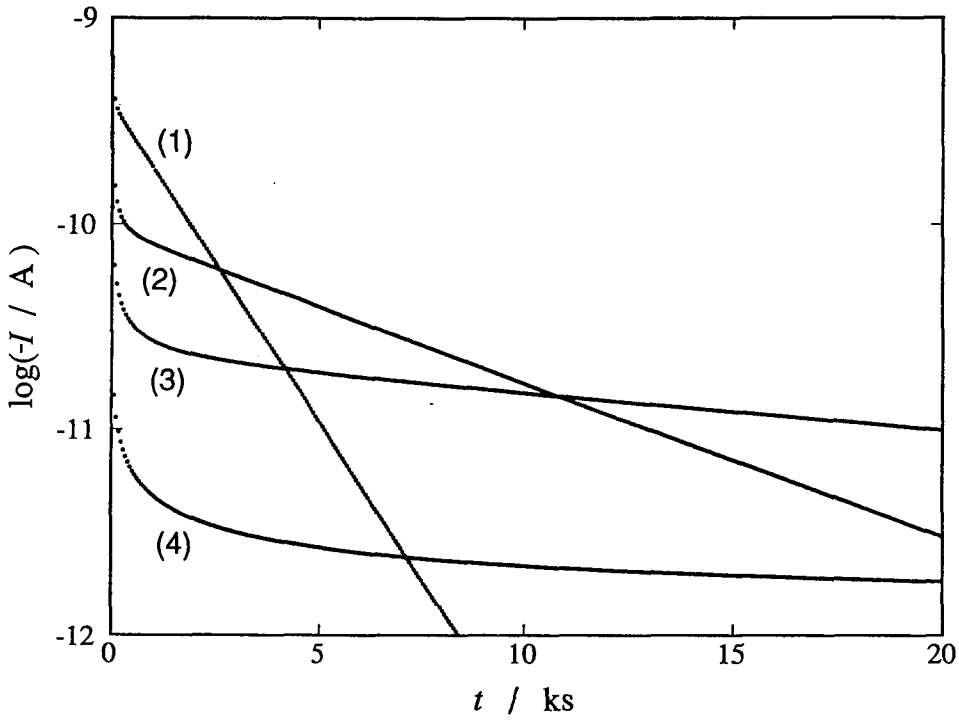

Fig. 3-28. Common logarithm of depolarization current *vs.* time plots at constant temperatures, (1): 100.29 K, (2): 98.85 K, (3): 97.58 K and (4): 95.74 K.

Chapter 4 EXPERIMENT ON ISOCYANOCYCLOHEXANE

4-1 Sample

The commercial product from Fluka was purified by the following procedure: fractional distillation under reduced pressure, drying with molecular sieve 4A and vacuum distillation. Test of purity by a gas chromatograph did not detect any volatile organic impurities. The amount of water in the sample was 0.04 mol % by Karl-Fischer test. Purity was determined to be 99.965 % by the fractional melting method in the polaro-calorimeter.

The mass of the sample used for the polaro-calorimetric experiment was 24.6573 g (0.225859 mol).

The glassy crystalline phase of isocyanocyclohexane was easily obtained even at a relatively slow cooling rate ($\approx$ 0.2 K min^{-1}). The relaxation experiments were performed on this phase. The low-temperature ordered phase was obtained fully by annealing the crystal at 175 K for three weeks *in situ* in the polaro-calorimeter.

4-2 Polaro-calorimetric Experiment

4-2-1 Heat Capacity

The heat capacity of isocyanocylohexane was measured between 5 and 300 K. The results are drawn in Fig. 4-1 and

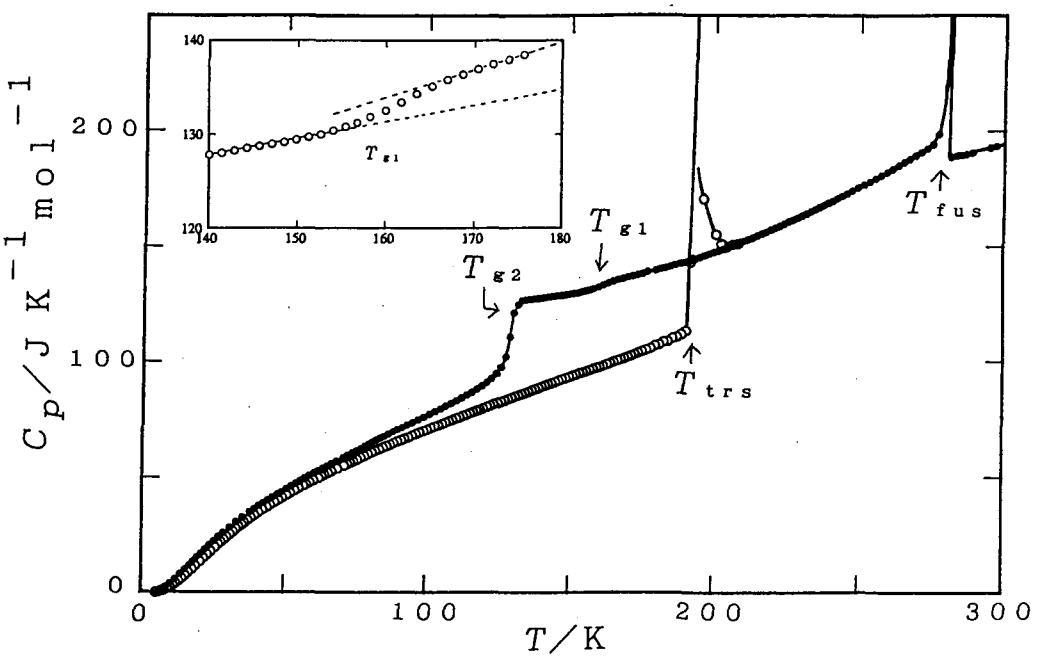

Fig. 4-1. Molar heat capacity of isocynanocyclohexane. ● : plastic crystal and glassy crystal, ○ : ordered crystal.

tabulated in Table 4-1. The heat capacity curve has anomalies at four temperatures (T_{fus}, T_{trs}, T_{g1} and T_{g2}). Thermodynamic quantities associated with the phase transition and fusion are given in Table 4-2.

The heat capacity of the supercooled sample increased markedly around 130 K (T_{g2}) by $\Delta C_p \approx 30$ J $K^{-1}mol^{-1}$. A similar change, but smaller in magnitude, occurred around 160 K (T_{g1}). During the equilibration period of measurement, spontaneous temperature change of the calorimetric cell was observed around T_{g1} and T_{g2}. It was exothermic below each of T_{g1} and T_{g2} and endothermic above, respectively.

For the purpose of extrapolation, the heat capacity data between 95 and 109 K were used to determine the coefficients of an assumed linear function for the vibrational heat capacity $C_{vib,m}$. In this temperature region, the temperature drift was normal indicating that only vibrational heat capacity was responding there. Similarly, the data between 136 and 148 K were used to determine the high temperature heat capacity ($C_{c,eq,m}+C_{vib,m}$) associated with T_{g2}. Figure 4-2 shows these functions and they are expressed numerically as

$$C_{vib,m}/J\ K^{-1}mol^{-1} = 0.620968\ T/K + 14.897, \qquad (4.1)$$

and

$$C_{c,eq,m}/J\ K^{-1}mol^{-1} = -0.461934\ T/K + 90.708, \qquad (4.2)$$

respectively.

Table 4-1. Molar heat capacity of isocyanocyclohexane.

T_{av} / K	C_p / J K^{-1} mol^{-1}	T_{av} / K	C_p / J K^{-1} mol^{-1}	T_{av} / K	C_p / J K^{-1} mol^{-1}
(glassy crystal		72.07	59.94	138.71	127.7
and		73.66	60.94	140.12	127.9
plastic crystal)		75.22	61.92	141.53	128.1
		76.74	62.87	142.93	128.3
5.13	0.6330	78.24	63.79	144.32	128.6
5.90	0.9633	79.71	64.70	145.72	128.8
7.14	1.651	81.16	65.59	147.11	129.0
8.56	2.652	82.59	66.51	148.50	129.2
10.19	4.068	83.99	67.31	149.88	129.5
12.17	6.099	85.37	68.13	151.26	129.7
14.08	8.264	86.89	69.06	152.63	130.0
15.75	10.25	88.53	70.06	154.00	130.4
17.31	12.16	90.15	71.03	155.35	130.8
18.68	13.87	91.75	71.99	156.70	131.3
20.04	15.54	93.32	72.93	158.26	131.9
21.44	17.24	95.11	74.01	160.01	132.6
22.26	18.27	97.11	75.21	161.76	133.4
23.66	19.95	99.08	76.40	163.51	134.4
25.16	21.68	101.02	77.57	165.25	135.2
27.01	23.80	102.93	78.74	166.98	135.8
29.21	26.18	104.82	79.90	168.71	136.4
31.44	28.46	106.69	81.07	170.43	137.0
33.66	30.82	108.53	82.23	172.15	137.5
35.84	32.80	110.35	83.39	173.86	138.0
38.00	34.77	112.15	84.54	175.56	138.5
40.17	36.65	113.93	85.79	180.14	140.0
42.38	38.50	115.69	87.03	181.83	140.6
44.65	40.33	117.43	88.33	183.51	141.2
46.92	42.11	119.15	89.69	185.18	141.7
49.13	43.79	120.84	91.18	186.85	142.4
51.31	45.42	122.52	92.91	188.51	143.0
53.47	47.07	124.17	95.01	190.17	143.6
55.61	48.70	125.79	97.82	191.82	144.3
57.71	50.24	127.34	102.3	193.46	144.9
59.72	51.66	128.81	111.0	195.10	145.7
61.66	53.01	130.19	121.4	196.74	146.4
63.52	54.31	131.61	124.8	198.37	147.1
65.33	55.53	133.04	126.8	199.99	147.8
67.08	56.68	134.47	127.0	201.61	148.5
68.79	57.80	135.89	127.3	203.22	149.3
70.45	58.87	137.30	127.5	204.83	150.1

Table 4-1. Continued.

T_{av} / K	C_p / J K^{-1} mol^{-1}	T_{av} / K	C_p / J K^{-1} mol^{-1}	T_{av} / K	C_p / J K^{-1} mol^{-1}
206.44	150.9	276.88	198.8	29.58	23.26
208.03	151.7	278.40	281.0	30.57	24.32
209.63	152.4	279.17	1059	31.62	25.42
211.21	153.3			32.72	26.61
212.80	154.0			33.75	27.69
214.37	154.8	(liquid)		34.74	28.67
215.95	155.7			35.68	29.63
217.51	156.6	281.36	188.9	36.57	30.51
219.08	157.4	282.82	189.4	37.64	31.52
220.63	158.2	286.40	190.1	38.86	32.64
222.18	159.0	288.50	190.7	40.03	33.70
223.73	159.9	290.59	192.2	41.14	34.67
225.27	160.8	292.66	192.6	42.20	35.55
226.81	161.6	294.74	193.0	43.23	36.40
228.34	162.5	296.82	193.6	44.22	37.22
229.87	163.4			45.29	38.13
231.39	164.3	(ordered		46.45	39.02
232.91	165.3	crystal)		47.56	39.88
234.42	166.2			48.63	40.66
235.93	167.1	5.36	0.3208	49.79	41.50
237.43	168.0	6.41	0.5172	51.02	42.43
238.93	168.9	7.61	0.8816	52.21	43.35
240.42	169.8	8.70	1.350	53.36	44.21
241.98	170.9	9.75	1.928	54.49	45.03
243.61	171.9	10.73	2.575	55.58	45.79
245.23	172.8	11.70	3.312	56.65	46.54
247.07	174.1	12.70	4.166	57.69	47.26
249.12	175.5	13.76	5.157	58.71	47.99
251.17	176.8	14.86	6.270	59.77	48.66
253.20	178.2	16.04	7.538	60.85	49.36
255.23	179.6	17.27	8.918	61.92	50.02
257.24	181.0	18.52	10.37	62.96	50.66
259.25	182.3	19.77	11.86	63.99	51.31
261.25	183.7	20.97	13.29	87.14	64.21
263.24	185.2	21.32	13.69	88.54	64.94
265.21	186.6	22.59	15.22	89.94	65.67
267.18	188.1	23.85	16.72	91.31	66.37
269.14	189.5	25.04	18.11	92.67	67.05
271.10	190.9	26.20	19.43	94.01	67.70
273.04	192.5	27.39	20.88	95.34	68.42
274.97	194.4	28.52	22.16	96.65	69.07

Table 4-1. Continued.

T_{av} / K	C_p / J K^{-1} mol^{-1}	T_{av} / K	C_p / J K^{-1} mol^{-1}
97.96	69.69	147.38	92.58
99.25	70.34	148.61	93.11
100.53	70.97	149.84	93.63
101.79	71.57	151.06	94.16
103.05	72.17	152.28	94.64
104.30	72.76	153.49	95.20
105.53	73.36	154.69	95.60
106.76	73.95	155.89	96.07
107.98	74.55	157.09	96.56
109.19	75.13	158.29	97.06
110.39	75.70	159.48	97.57
111.58	76.23	160.67	98.04
112.76	76.81	161.88	98.53
113.94	77.38	163.12	99.09
115.11	77.92	164.35	99.61
116.27	78.45	165.58	100.2
117.43	78.95	166.81	100.7
118.58	79.47	168.03	101.2
119.75	80.07	169.25	101.8
121.00	80.67	170.46	102.3
122.25	81.28	171.67	102.9
123.49	81.84	172.87	103.5
124.72	82.38	174.07	104.1
125.94	82.94	175.27	104.6
127.16	83.48	176.46	105.2
128.37	84.04	178.50	106.2
129.57	84.63	180.00	107.3
130.77	85.17	181.49	107.7
131.96	85.70	182.97	108.8
133.15	86.27	184.49	109.1
134.33	86.78	186.04	110.4
135.51	87.27	187.57	111.0
136.68	87.80	189.10	112.2
137.85	88.32	190.62	113.7
139.01	88.83	192.02	143.4
140.16	89.42		
141.31	89.93		
142.46	90.42		
143.66	90.95		
144.90	91.49		
146.15	92.04		

Table 4-2. Thermodynamic quantities associated with the phase transition and fusion of isocyanocyclohexane.

T_{trs}/K	192.6
$\Delta_{trs}H$ / kJ mol^{-1}	6.177
$\Delta_{trs}S$ / J K^{-1}mol^{-1}	32.07
T_{fus}/K	279.6
$\Delta_{fus}H$ / kJ mol^{-1}	4.227
$\Delta_{fus}S$ / J K^{-1}mol^{-1}	15.12

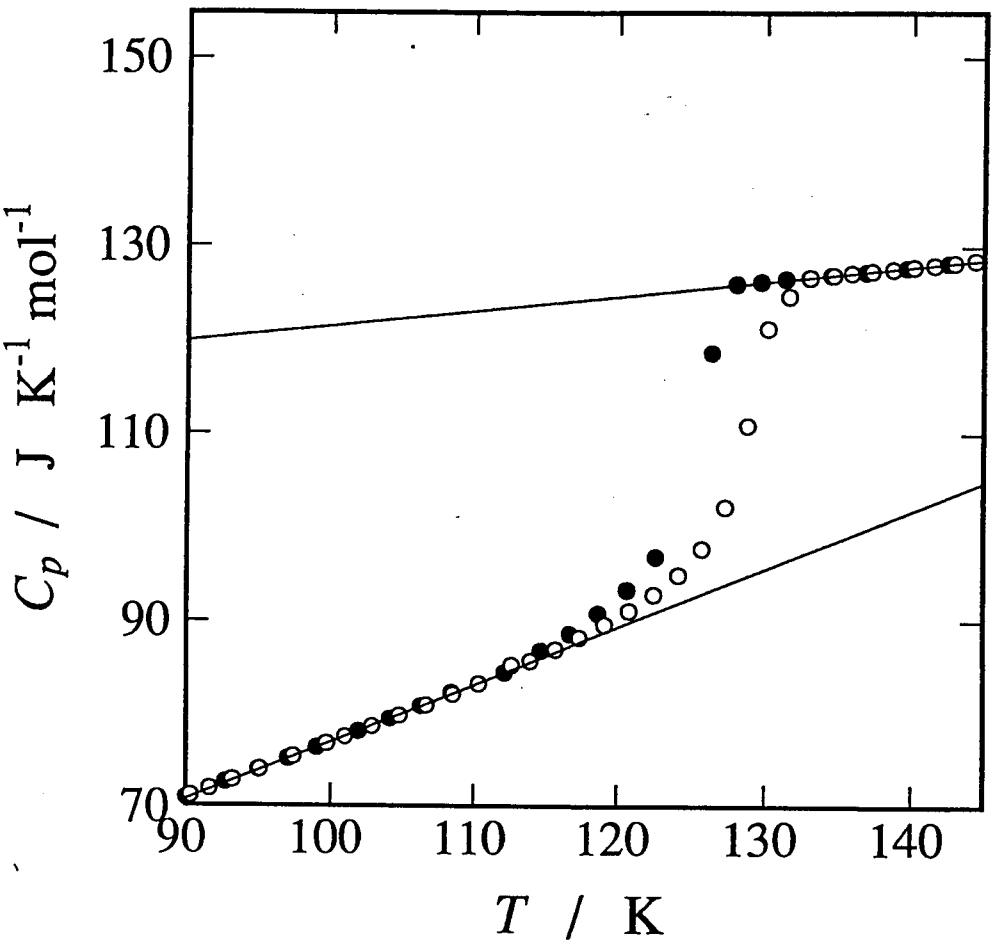

Fig. 4-2. Extrapolation of the heat capacities of glassy and platstic crystal. ● and ○ are in different experimental series with different heating rates.

4-2-2 TSDC and TSPC

For the TSDC measurement, the sample was cooled from 230 K to 80 K in a polarizing voltage of 100 V. Temperature of the sample in the cooling process is shown in Fig. 4-3. At 80 K the voltage was turned off. The sample was heated from this temperature with heating current I_h of 35 mA. The temperature and the depolarization current were measured simultaneously, and they are summarized in Fig. 4-4. The peak of the depolarization current occurred at 129.40 K. The current reversed its sign around 140 K and reversed again around 150 K. At higher temperature the current increased and reached the maximum of 2 μA at the fusion temperature. Amount of the electric charge released above 150 K was about 10 mC. This amount was very large compared with the charge released around T_{g2} of 110 nC. The origins of the current reversal and the large charge are not clear. It may be caused by an electrochemical effect at the electrodes.

After an exothermic-depolarizing experiment recorded at 125.6 K, the sample was cooled to 80 K without polarizing voltage. At 80 K the voltage of 100 V was turned on. The sample was heated them from that temperature with heating current I_h of 35 mA. The temperature and the polarization current were measured simultaneously as shown in Fig. 4-5. The main peak of the polarization current appeared at 129.90 K.

The excess configurational enthalpy ΔH_c in the TSDC and TSPC measurements was determined by means of Eq. (2.16), and the result is shown in Fig. 4-6. The minimum of the excess con-

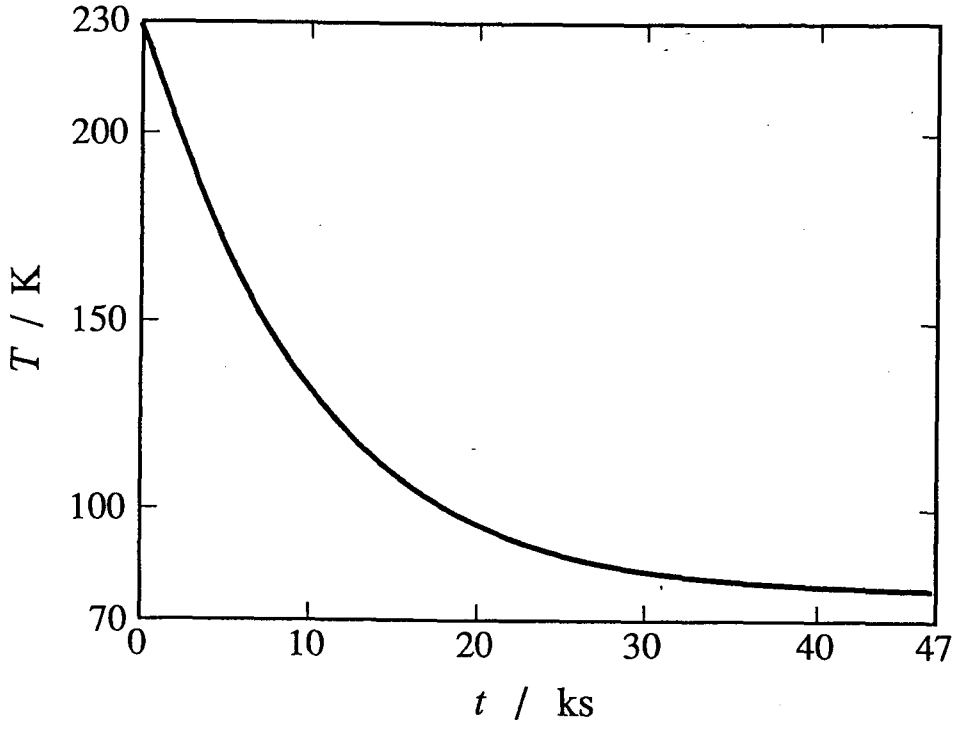

Fig. 4-3. Temperature as a function of time during cooling before TSDC measurement.

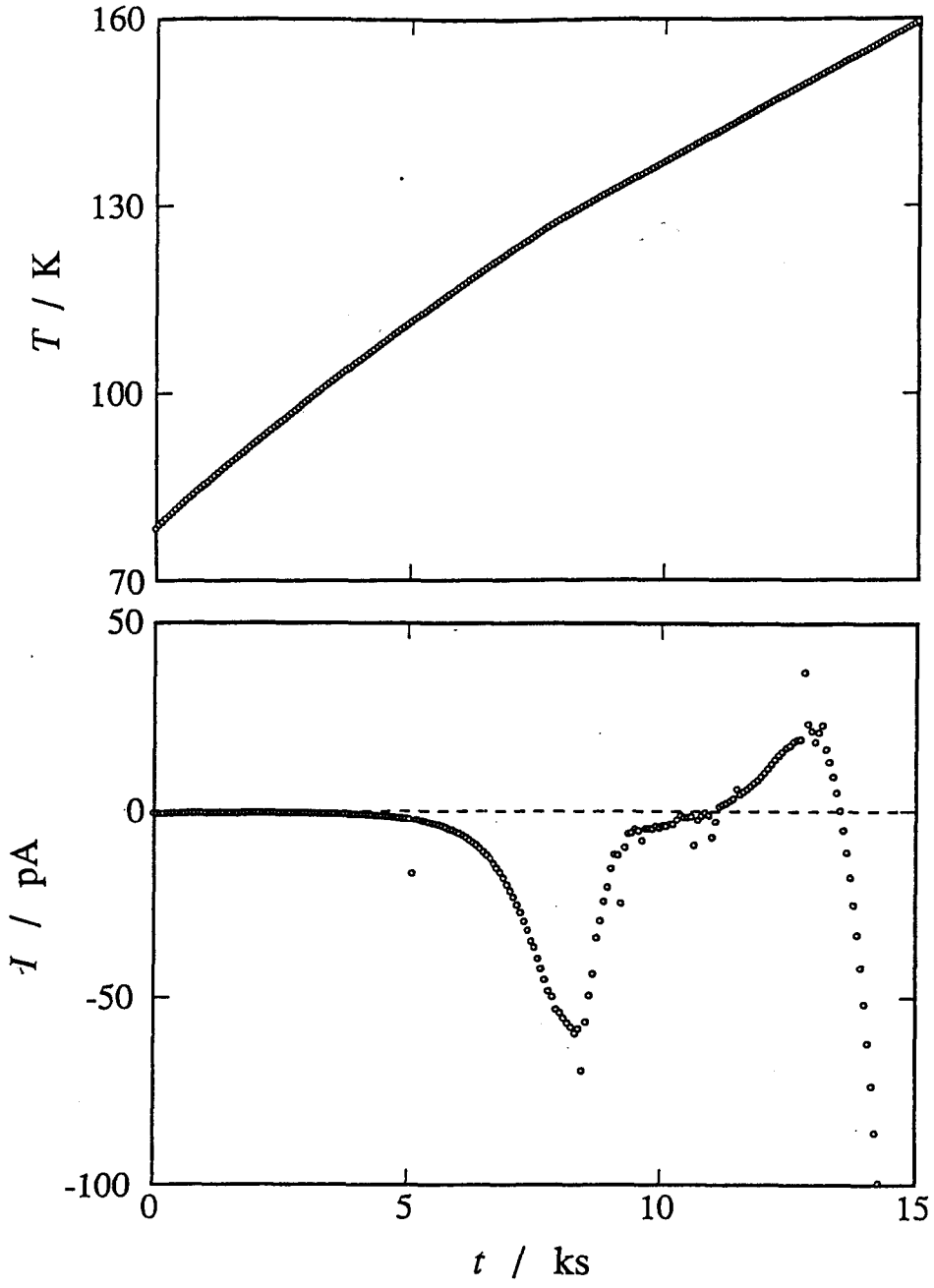

Fig. 4-4. Temperature and depolarization current as functions of time in TSDC measurement.

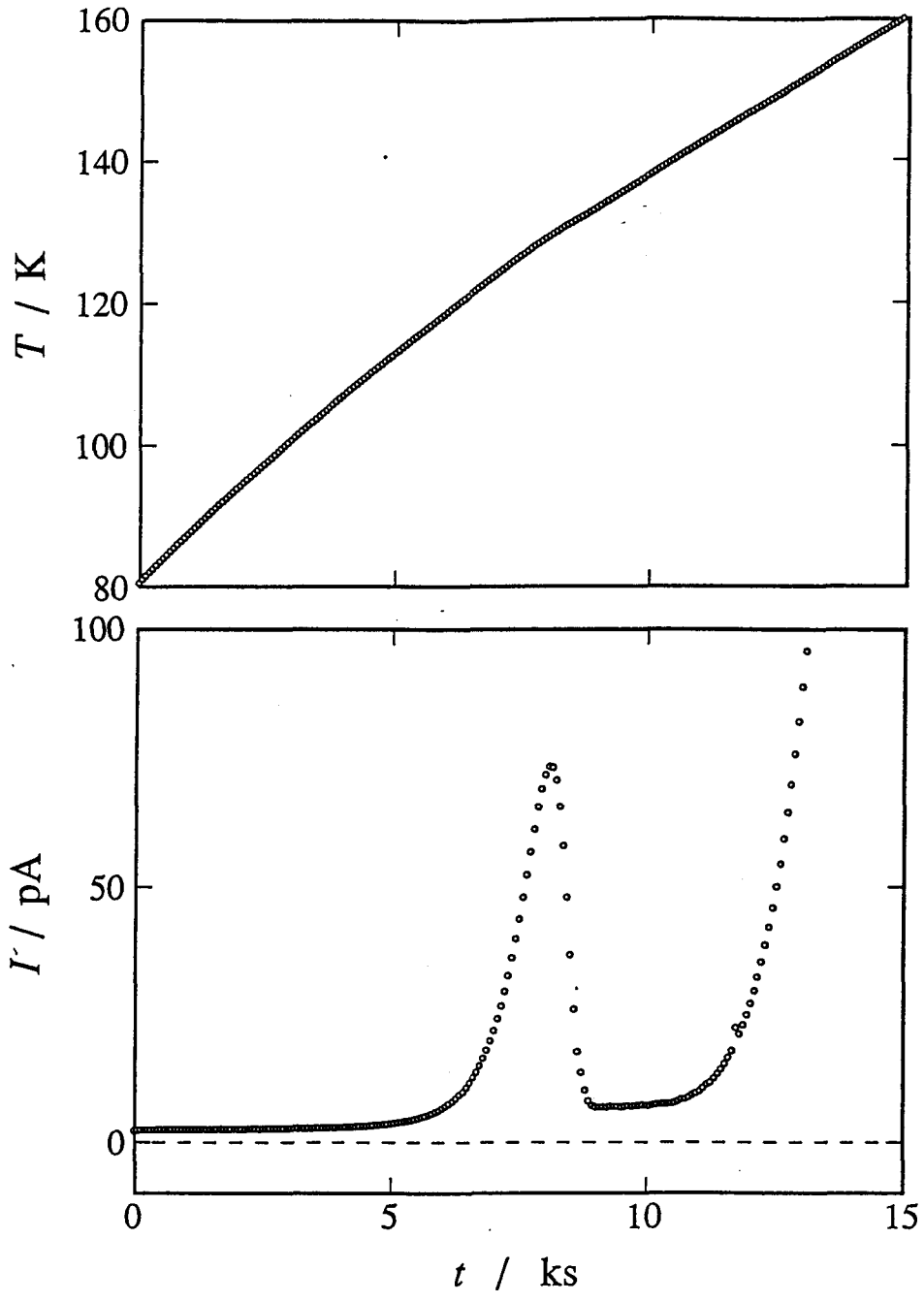

Fig. 4-5. Temperature and polarization current as functions of time in TSPC measurement.

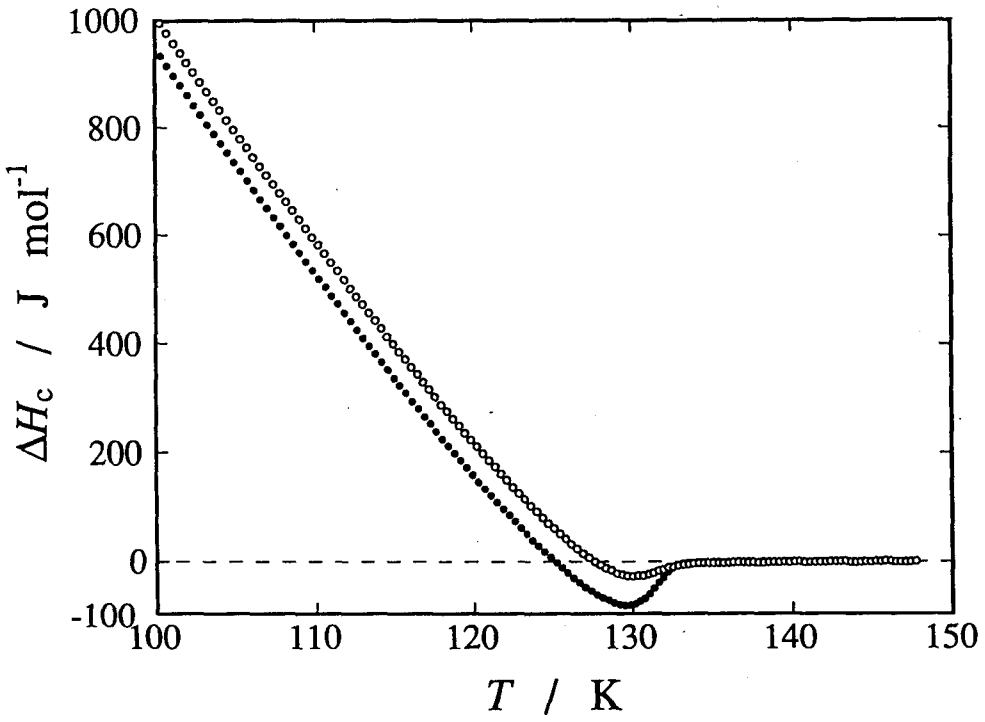

Fig. 4-6. Excess configurational enthalpy *vs.* temperature in the TSDC (○) and TSPC (●) measurements.

figurational enthalpy was approximately the same as the peak temperatures of the TSDC and TSPC. Both peaks were caused by the activation of the molecular reorientation.

Strikingly different behavior was found for the ordered phase of isocyanocylohexane. The ordered phase was obtained by annealing the supercooled sample at 175 K (see 4-1). For the TSDC measurement the sample was cooled from 178 K to 60 K in a polarizing voltage of 100 V. At 60 K the voltage was turned off. The sample was heated with heating current 30 mA. The TSDC recorded during the heating period is plotted in Fig. 4-7. The observed current was less than 0.05 pA, and was much small compared with the peak value of 60 pA found in the TSDC run on the glassy crystalline phase (Fig. 4-4).

4-2-3 Enthalpy and Polarization Relaxations

Experiments on exothermic-depolarizing relaxation were carried out at six temperatures, 123.1 K, 125.4 K, 126.0 K, 126.8 K, 126.9 K and 127.7 K around the glass transition T_{g2}. Here only the result at 126.9 K is described. The sample was cooled as shown in Fig. 4-8. The polarizing voltage was turned on at 147 K. When the temperature reached 126.85 K, the polarizing voltage and the thermal switch were turned off. The spontaneous temperature increase and depolarization current were observed simultaneously. The temperature increase is shown in Fig. 4-9 and the depolarization current in Fig. 4-10. The excess configurational enthalpy derived from the spontaneous temperature increase is plotted in Fig. 4-11. Decrease of the polarization is obtained as integration

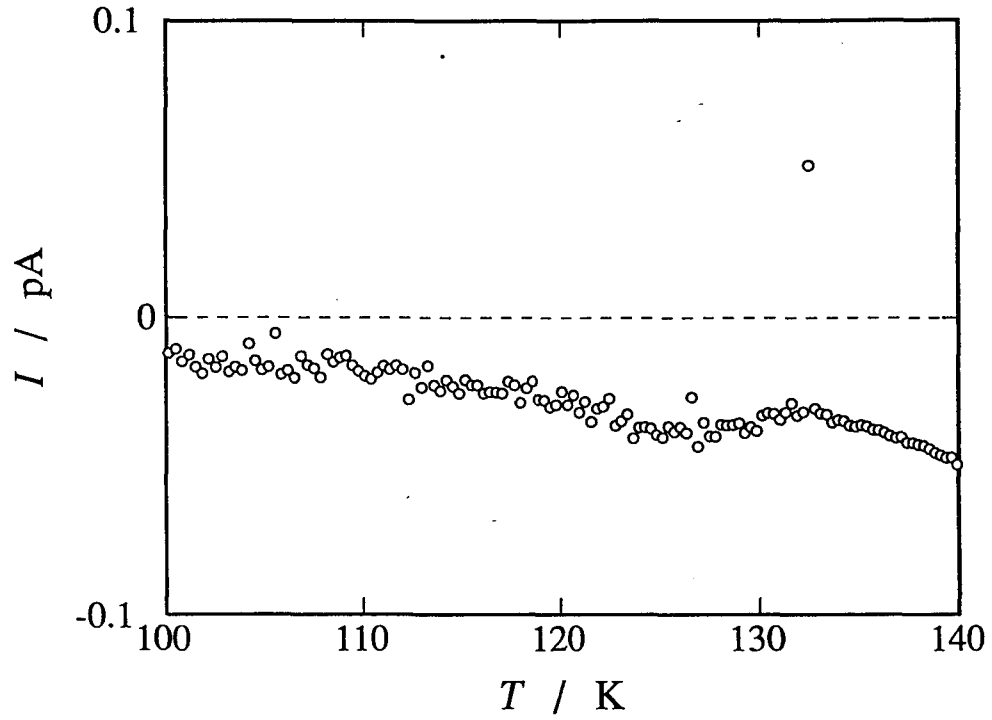

Fig. 4-7. Temperature and depolarization current as functions of time in TSDC measurement for the ordered crystal phase.

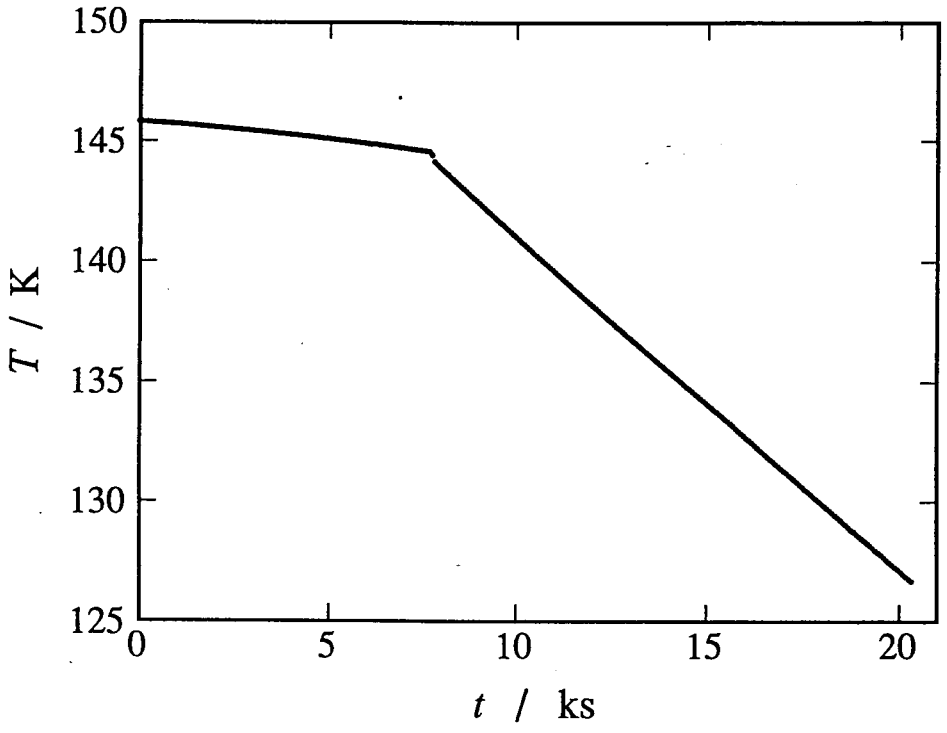

Fig. 4-8. Temperature as a function of time before the experiment of exothermic-depolarizing relaxation.

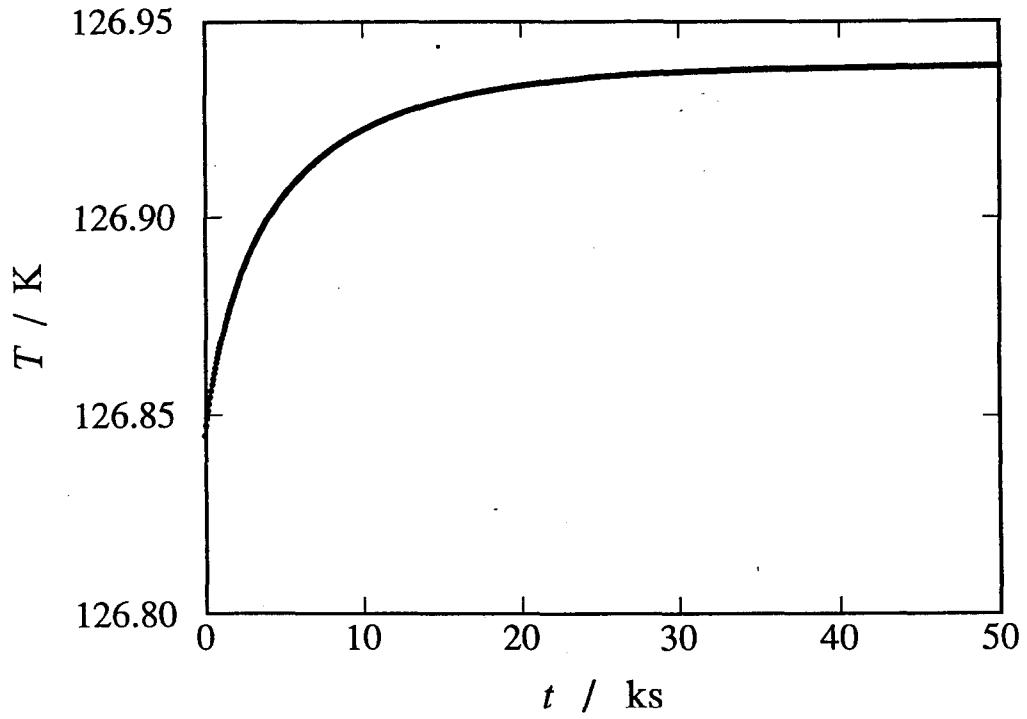

Fig. 4-9. Spontaneous temperature rising in the experiment of exothermic-depolarizing relaxation around 126.9 K.

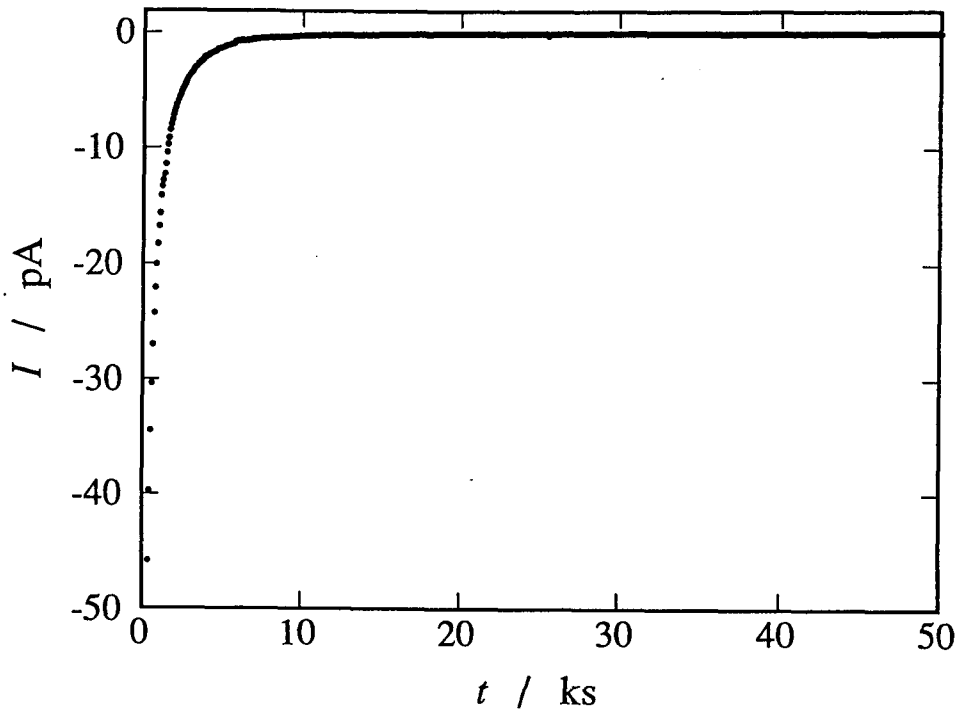

Fig. 4-10. Depolarization current in the experiment of exothermic-depolarizing relaxation around 126.9 K.

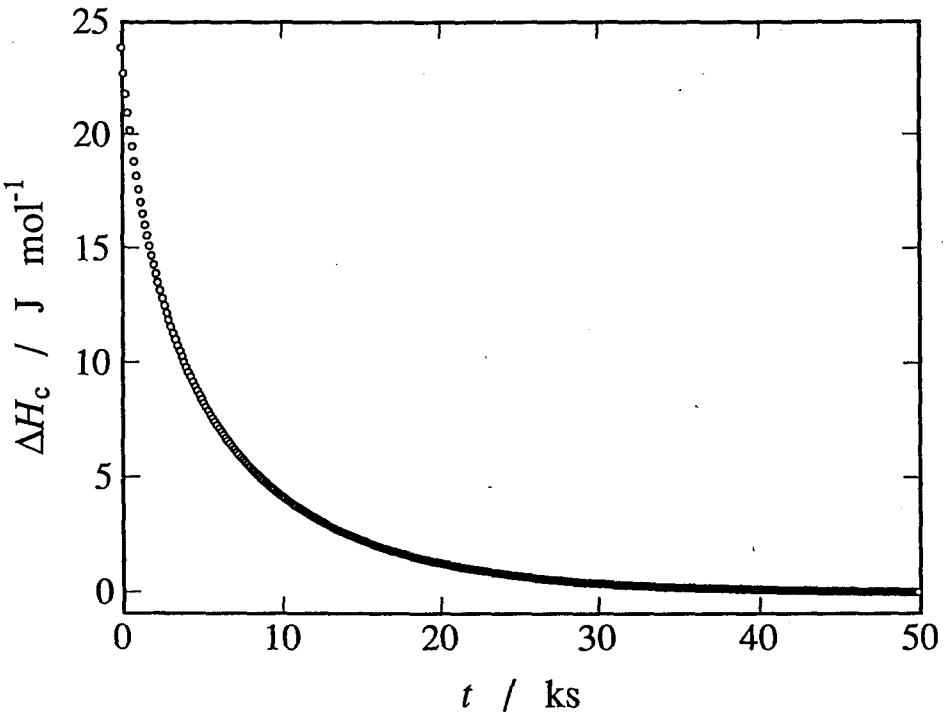

Fig. 4-11. Decay of the excess configurational enthalpy in the exothermic-depolarizing relaxation. The corresponding temperature change is shown in Fig. 4-9.

of the depolarization current with respect to time. The asymptotic value of the electric charge shown in Fig. 4-12 corresponds to the zero point of the polarization.

Experiments on enthalpy relaxation were carried out for the glass transition T_{g1}. Exothermic relaxations were observed at 144.6 K and 149.8 K. Endothermic relaxations were observed at 154.8 K, 157.5 K, 160.18 K and 162.8 K, respectively. Only the exothermic relaxation measured at 149.8 K is shown here. The sample was cooled from 199 K by the rate of 0.16 K min^{-1} and subsequently kept at the target temperature of 149.8 K under adiabatic condition. The spontaneous temperature rise is shown in Fig. 4-13 as a function of time. Low resistivity of the sample in this temperature region made it impossible to do the polarization measurement for this glass transition.

4-2-4 Isothermal Polarization Relaxation

Experiments on isothermal polarization relaxation were carried out at eight temperatures, 124.09 K, 125.60 K, 126.16 K, 126.72 K, 126.83 K, 126.94 K, 127.70 K and 128.24 K around the glass transition T_{g2}. The temperature change during measurement of polarization relaxation was smaller than 20 mK at each temperature. Here only the experimental result measured at 126.16 K is described in detail. The polarization current with an applied voltage of 100 V is shown in Fig. 4-14. After the sample was polarized for 0.14 Ms, the voltage was turned off and measurement of the depolarization current started. The depolarization current is shown in Fig. 4-15. Integrations of the polarization and depo-

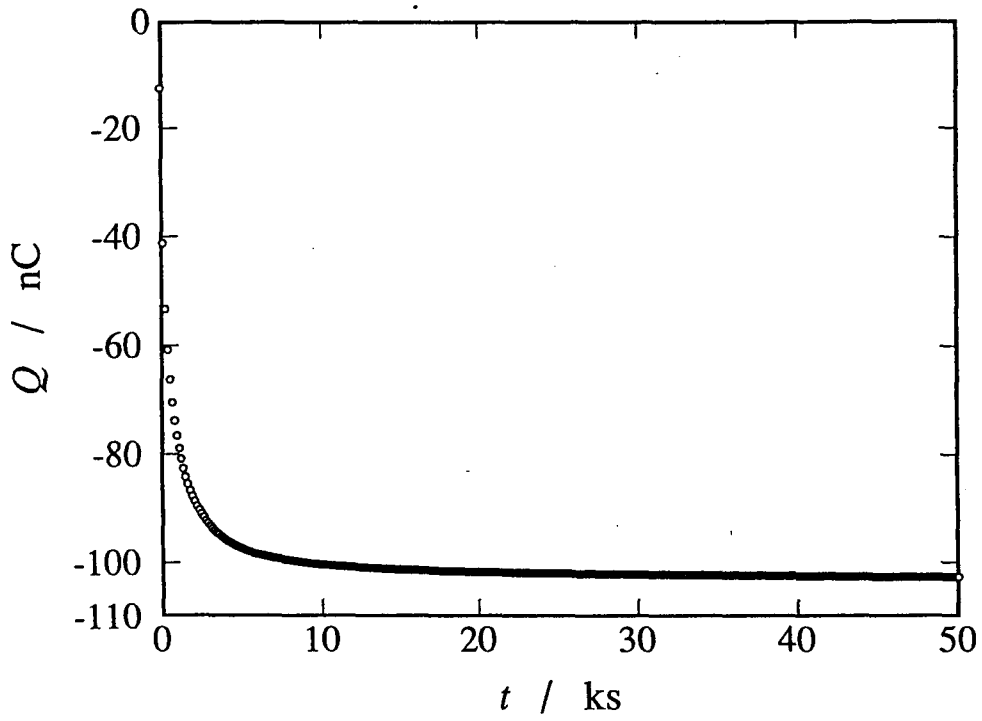

Fig. 4-12. Decay of polarization in the exothermic-depolarizing relaxation. Integration of depolarization current in Fig. 4-10 is shown as a function of time.

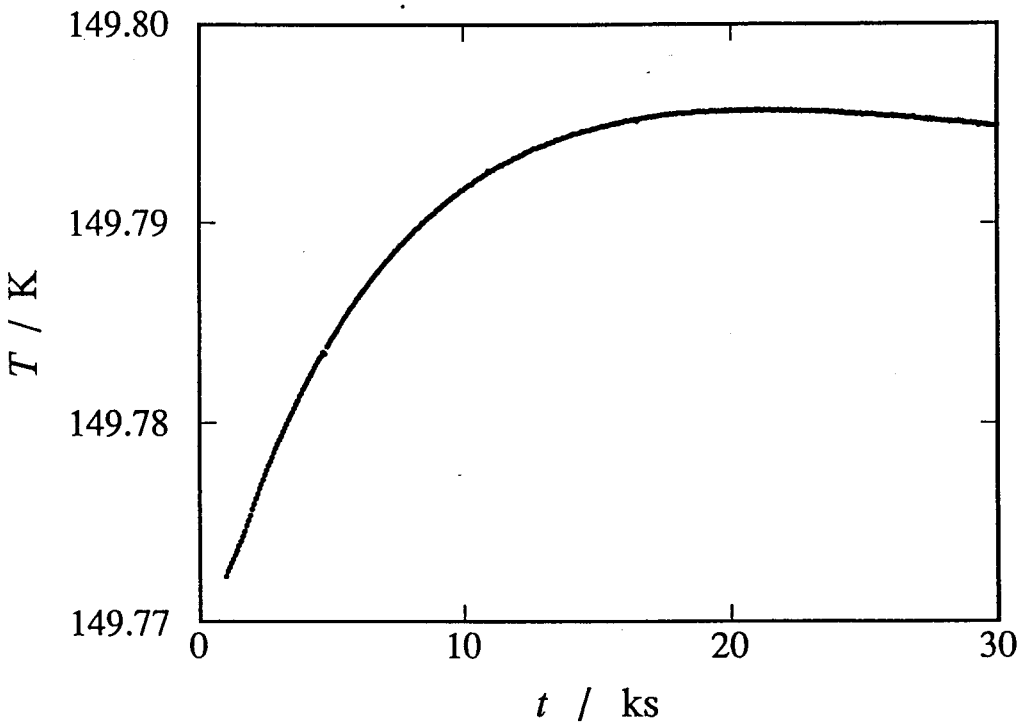

Fig. 4-13. Spontaneous temperature rising around T_{g1}.

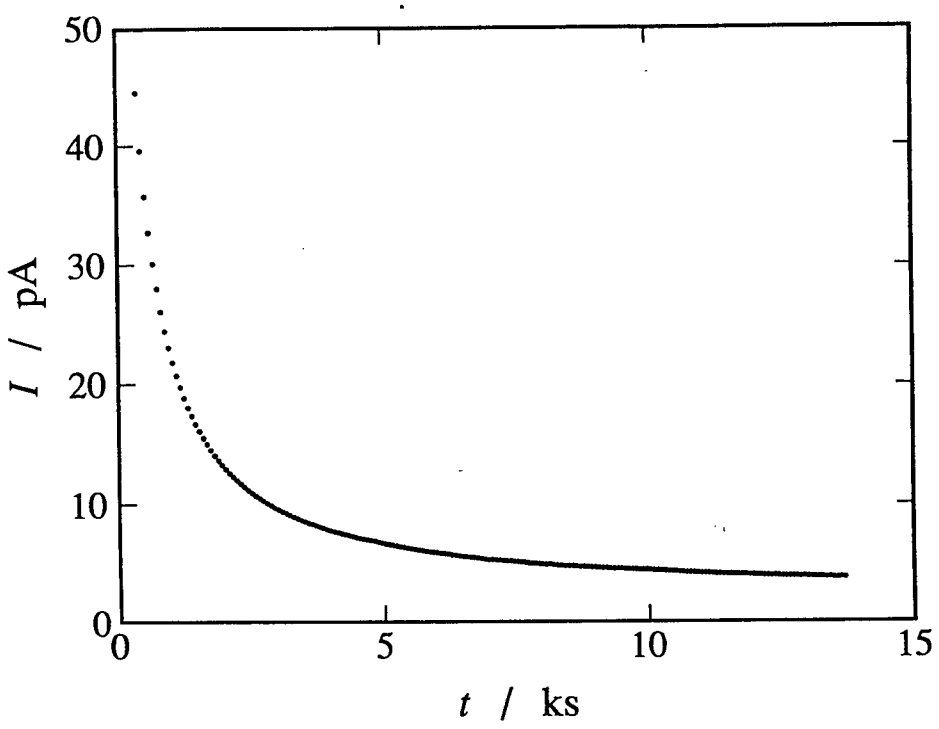

Fig. 4-14. Polarization current in the experiment of isothermal polarization relaxation at 126.16 K.

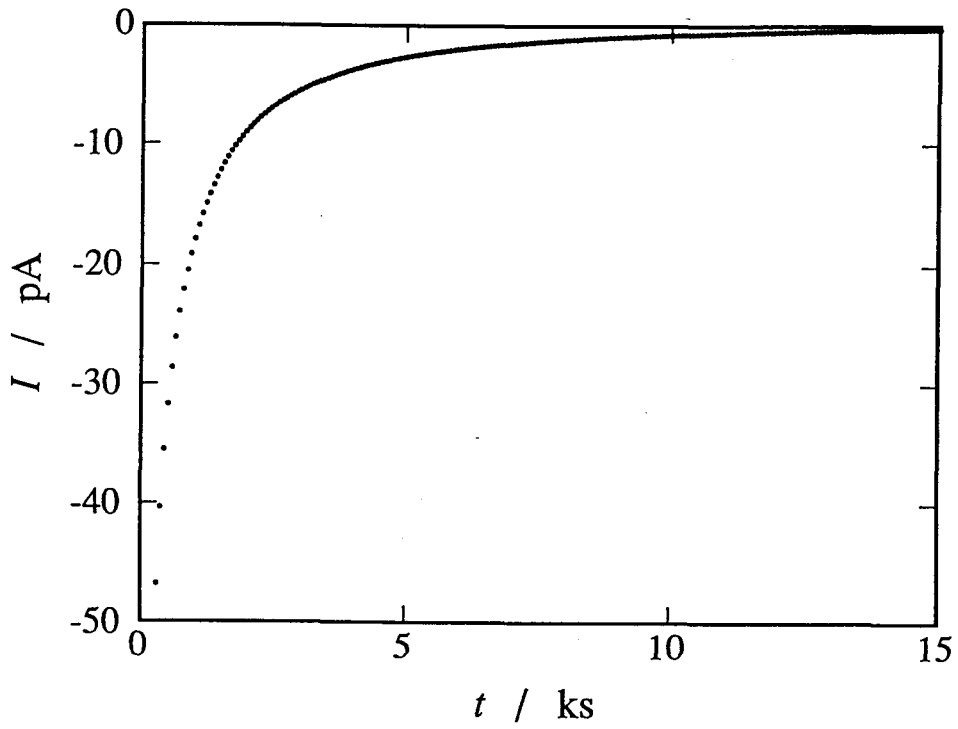

Fig. 4-15. Depolarization current in the experiment of isothermal polarization relaxation at 126.16 K.

larization currents with respect to time are shown in Figs. 4-16 and 4-17, respectively. Because the integration of the polarization current includes the conduction current, the electric charge is larger than the contribution of the polarization of the sample. The integration of the depolarization current corresponds solely to the polarization change. Temperature dependence of the depolarization current is shown in Fig. 4-18.

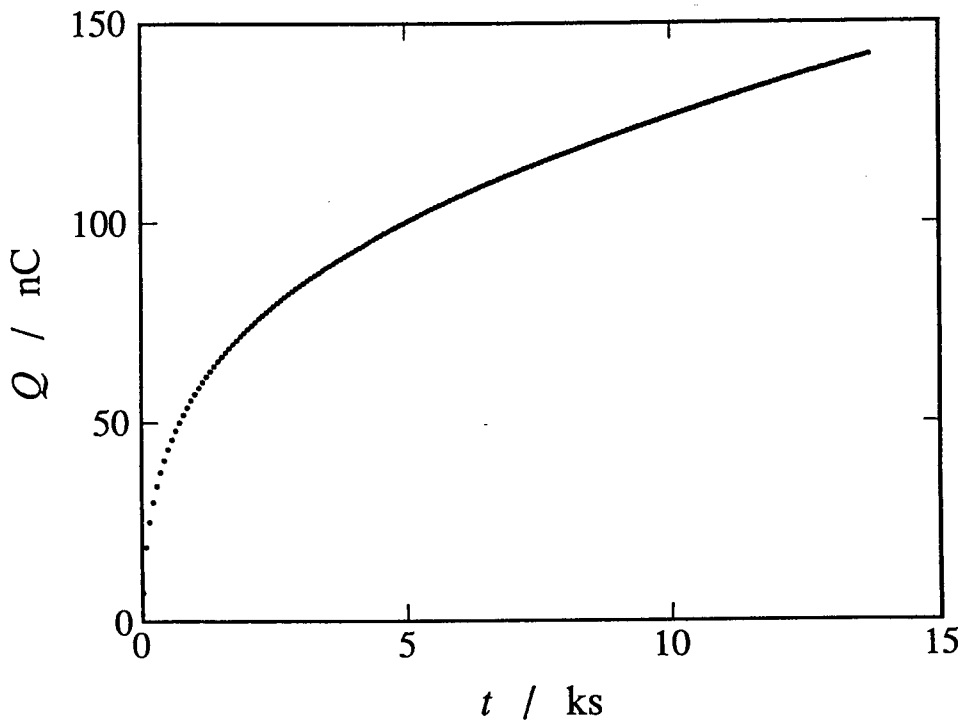

Fig. 4-16. Polarization increase at a constant temperature. Integration of polarization current given in Fig. 4-14 is recorded as a function of time.

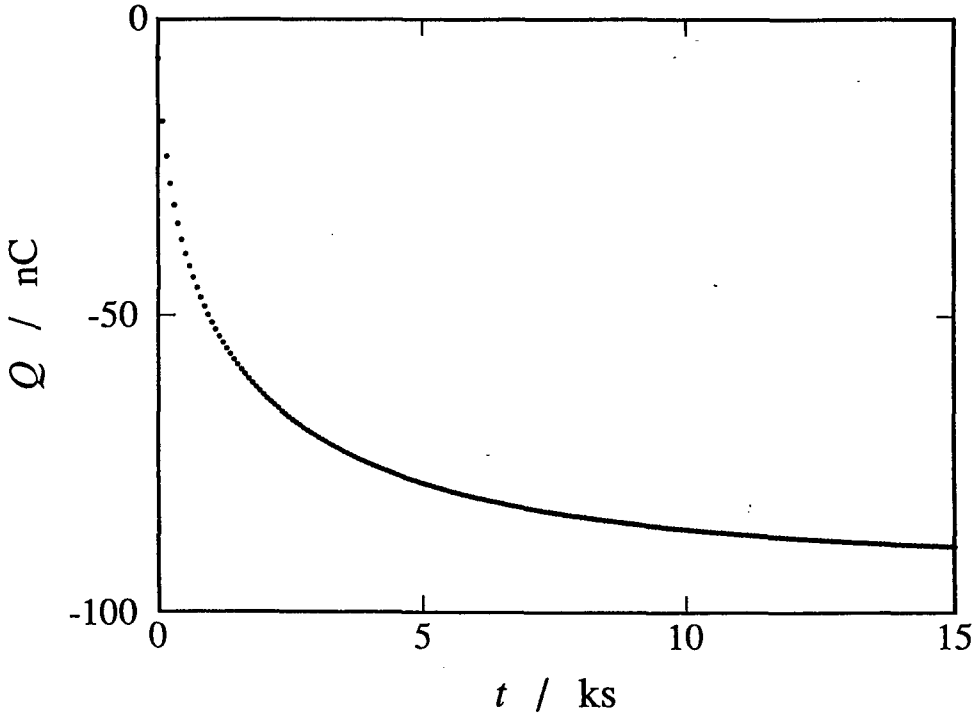

Fig. 4-17. Polarization decay at a constant temperature. Integration of depolarization current in Fig. 4-15 is shown as a function of time.

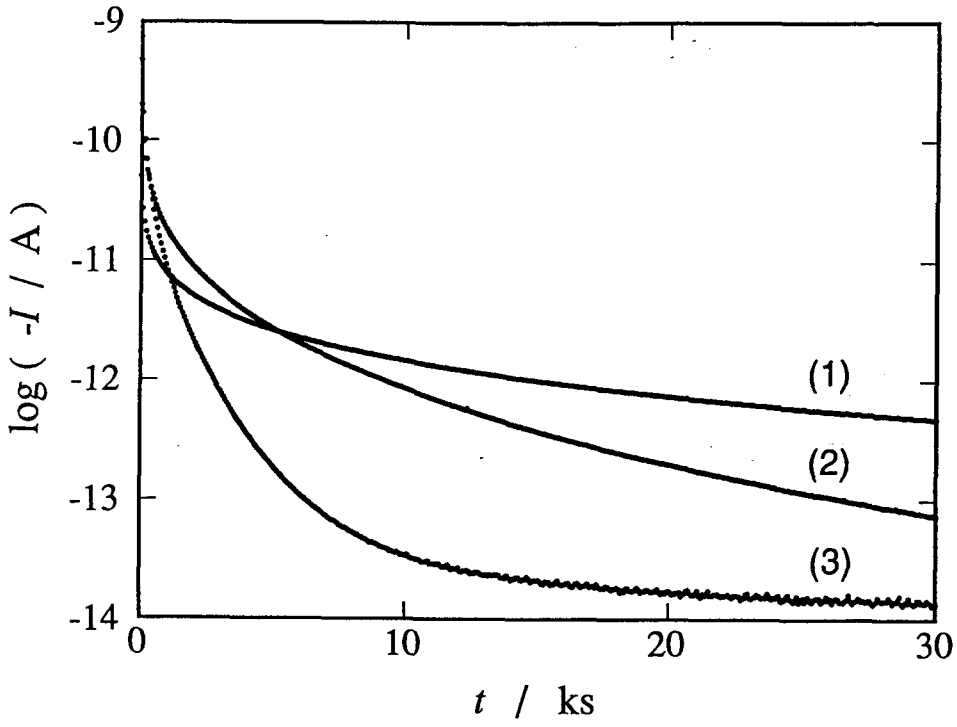

Fig. 4-18. Common logarithm of depolarization current *vs.* time plots at constant temperatures, (1): 124.09 K, (2): 126.16 K and (3): 128.24 K.

Chapter 5 DISCUSSION

5-1 Phenomenological Description of Glass Transition

As described in the following section, non-Debye relaxation was observed in common thermally and electrically in both of the liquid 1-propanol and crystalline isocyanocylohexane. There are some ways to interpret the non-Debye type relaxation. One of the general interpretations is superposition of the Debye type relaxations which have the distributed relaxation times. In the present study this interpretation was attempted.

The configurational enthalpy freezes around the glass transition temperature as the relaxation time increases by cooling. Amount of the excess configurational enthalpy depends on cooling rate as well as on the temperature dependence of the relaxation time. A general equation for the excess configurational enthalpy with respect to the temperature change is formulated based on the Debye law. A modified equation including the distributed relaxation times is then formulated. Similar equations are formulated for the electric polarization.

[Enthalpy relaxation with a single relaxation time]

Supposed that the configurational enthalpy obeys the Debye law defined by the following equation.

$$\frac{dH_C}{dt} = -\frac{\Delta H_C}{\tau_H(T)}. \qquad (5.1)$$

Here τ_H is the relaxation time and ΔH_c the excess configurational enthalpy which is the difference between the actual configurational enthalpy H_c and the equilibrium configurational enthalpy $H_{c,eq}$,

$$\Delta H_c = H_c - H_{c,eq}. \tag{5.2}$$

By this relation, H_c in Eq. (5.1) is replaced by $H_{c,eq} - \Delta H_c$ and Eq. (5.1) is rewritten as

$$\frac{d\Delta H_c}{dt} = - \frac{\Delta H_c}{\tau_H(T)} - \frac{dH_{c,eq}}{dt}. \tag{5.3}$$

The configurational heat capacity $C_{c,eq}$ $(=dH_{c,eq}/dT)$ is introduced and Eq. (5.3) is written as

$$\frac{d\Delta H_c}{dt} = - \frac{\Delta H_c}{\tau_H(T)} - \frac{dT}{dt} C_{c,eq}. \tag{5.4}$$

The term $-dT/dt$ is simply the cooling rate α,

$$\alpha(t) = - \frac{dT(t)}{dt}. \tag{5.5}$$

Equation (5.4) is thus written as

$$\frac{d\Delta H_c}{dt} = -\frac{\Delta H_c}{\tau_H(T)} + \alpha(t)\, C_{c,eq}(T). \qquad (5.6)$$

This differential equation is solved under the initial condition that ΔH_c is equal to $\Delta H_c(t_i)$ at the initial time t_i. The excess configurational enthalpy at the final time t_f is represented by the following equation.

$$\Delta H_c(t_f) = \exp\left(-\int_{t_i}^{t_f} \frac{ds}{\tau_H(T(s))}\right) \times \left[\int_{t_i}^{t_f} \alpha(t) C_{c,eq}(T(t)) \exp\int_{t_i}^{t} \frac{ds}{\tau_H(T(s))}\, dt + \Delta H_c(t_i)\right]. \qquad (5.7)$$

If the relaxation time $\tau_H(T)$ and the configurational heat capacity $C_{c,eq}$ are known as functions of temperature, the configurational enthalpy at any temperature T and any time t is determined by this equation.

[Enthalpy relaxation with distributed relaxation times]

Consider that the system consists of an assembly of Debye type relaxors which have different relaxation times, and the relaxors do not interact with each other. A parameter x characterizing the relaxation time in introduced here. For example, x is the activation energy in the Arrhenius law. The parameter x is added to Eq. (5.7) as

$$\Delta H_c(x, t_f) = \exp\left(-\int_{t_i}^{t_f} \frac{ds}{\tau_H(x, T(s))}\right) \times \left[\int_{t_i}^{t_f} \alpha(t) C_{c,eq}(x, T(t)) \exp \int_{t_i}^{t} \frac{ds}{\tau_H(x, T(s))} dt + \Delta H_c(x, t_i)\right]. \quad (5.8)$$

In such system the excess configurational enthalpy observed experimentally is the sum of configurational enthalpy brought by the relaxors. The fraction of the relaxor characterized by the parameter x is denoted as $g(x)$.

$$\Delta H_c(t_f) = \int g(x) \Delta H_c(x, t_f) \, dx. \quad (5.9)$$

The experimental configurational heat capacity is summation of the configurational heat capacities contributed from each relaxors.

$$C_{c,eq}(T) = \int g(x) C_{c,eq}(x, T) dx. \quad (5.10)$$

The apparent relaxation time of enthalpy defined by Eq. (2.18) is related to the distribution of the relaxation time by the following equation.

$$\tau_{H,ap}(t) = \frac{\int g(x) \Delta H_c(x, t) dx}{\int \{g(x) \Delta H_c(x, t)/\tau_H(x, T)\} dx}. \quad (5.11)$$

[Polarization relaxation with a single relaxation time]

For the electric polarization, the equation representing the relaxation and freeze associated with cooling is formulated similarly. The next equation represents the Debye law for the polarization.

$$\frac{dP}{dt} = -\frac{\Delta P}{\tau_p(T)}. \tag{5.12}$$

ΔP is the difference between the equilibrium and actual polarization under an electric field E.

$$\Delta P = P - P_{eq}(E, T) \tag{5.13}$$

Equation (5.12) is rewritten as

$$\frac{d\Delta P}{dt} = -\frac{\Delta P}{\tau_p(T)} - \frac{dP_{eq}(E, T)}{dt}. \tag{5.14}$$

As the configurational heat capacity was introduced above, the temperature derivative of the equilibrium polarization is introduced and Eq.(5.13) is

$$\frac{d\Delta P}{dt} = -\frac{\Delta P}{\tau_p(T)} + \alpha(t)\ Y(T), \tag{5.15}$$

where $Y(T)$ is defined by

$$Y(T) = \frac{dP_{eq}(E, T)}{dT}. \tag{5.16}$$

The differential equation (5.15) is solved under the initial condition is $\Delta P(t_i)$ at the initial time t_i. It gives the equation similar to Eq. (5.8),

$$\Delta P(t_f) = \exp\left(-\int_{t_i}^{t_f} \frac{ds}{\tau_p(T(s))}\right) \times \left(\int_{t_i}^{t_f} \alpha(t) Y(T(t)) \exp \int_{t_i}^{t} \frac{ds}{\tau_p(T(s))} dt + \Delta P(t_i) \right) . \quad (5.17)$$

If the relaxation and the equilibrium polarization Y are known as functions of temperature, the polarization can be determined by this equation.

[Polarization relaxation with distributed relaxation times]

For the polarization process, consider again an assembly of relaxors. Assume that there is no interaction among relaxors in order to simplify the model. Of course the electric interaction between polarizations can never be neglected.

$$\Delta P(x, t_f) = \exp\left(-\int_{t_i}^{t_f} \frac{ds}{\tau_p(x, T(s))}\right) \times \left(\int_{t_i}^{t_f} \alpha(t) Y(x, T(t)) \exp \int_{t_i}^{t} \frac{ds}{\tau_p(x, T(s))} dt + \Delta P(x, t_i) \right) . \quad (5.18)$$

The excess polarization observed experimentally is the sum of the polarization of each relaxor.

$$\Delta P(t_f) = \int g(x)\ \Delta P(x, t_f)\ dx. \qquad (5.19)$$

The temperature dependence of equilibrium polarization is also the sum.

$$Y(T) = \int g(x)\, Y(x, T)\, dx. \qquad (5.20)$$

The apparent relaxation time of polarization defined by Eq. (2.28) is related to the distribution of the relaxation time by the following equation.

$$\tau_{P,ap}(t) = \frac{\int g(x)\, \Delta P(x, t)\, dx}{\int \{ g(x)\, \Delta P(x, t)/\tau_P(x, T) \}\, dx}. \qquad (5.21)$$

The configurational enthalpy change is not measured directly in the present experiment of the exothermic or endothermic relaxation. It is measured as the spontaneous temperature increase or decrease. This temperature increase or decrease is accompanied by the decrease or increase of the equilibrium configurational enthalpy. Because the excess configurational enthalpy ΔH_C is $H_C - H_{C,eq}$, the excess configurational enthalpy decreases by decrease of H_C and by increase of $H_{C,eq}$. The former is the *relaxation* and the latter is due to the temperature rise. The relaxation time τ_T, which is determined by regarding the temperature increase as the relaxation function as if it were measured

isothermally, is shorter than the enthalpy relaxation time τ_H hypothetically measured at a constant temperature. The transformation from τ_T to τ_H for the Debye relaxation can be formulated. [For the polarization, distinction between two relaxation times is not necessary. The equilibrium polarization without electric field is constant (=0) with respect to temperature. The relaxation time determined by regarding the electric charge as the relaxational quantity is the polarization relaxation time in the exothermic-depolarizing or endothermic-depolarizing experiment.]

First the temperature change caused by the enthalpy relaxation is calculated. Equation (2.11) is used to relate the configurational enthalpy at a time t with the temperature. $J(t) = 0$, $t_f = \infty$ and $t_i = t$ are substituted into Eq. (2.11). It is assumed that C_{vib} is constant for the narrow temperature range where the enthalpy relaxation takes place actually.

$$H_c(\infty) - H_c(t) = -\{T(\infty) - T(t)\}C_{vib}. \qquad (5.22)$$

This is rewritten in the following form to represent the temperature variation with time,

$$T(t) = \frac{H_c(\infty) - H_c(t)}{C_{vib}} + T(\infty). \qquad (5.23)$$

The change in equilibrium configurational enthalpy caused by this temperature change is derived as follows. Assume that $C_{c,eq}$ is constant. This assumption is valid for a small temperature interval. Because $C_{c,eq}$ is $dH_{c,eq}/dT$,

$$H_{c,eq}(t) - H_{c,eq}(\infty) = C_{c,eq}\{T(t) - T(\infty)\}. \quad (5.24)$$

This equation is rewritten as the expression of the equilibrium configurational enthalpy as follow.

$$H_{c,eq}(t) = H_{c,eq}(\infty) + C_{c,eq}T(t) - C_{c,eq}T(\infty). \quad (5.25)$$

Substitution Eq. (5.23) into Eq. (5.25) gives the following equation.

$$H_{c,eq}(t) = \frac{C_{c,eq}}{C_{vib}} \{H_c(\infty) - H_c(t)\} + H_{c,eq}(\infty). \quad (5.26)$$

Now consider the simplest relaxation of the Debye type. The next equation is equivalent to Eq. (5.1).

$$\frac{dH_c}{dt} = -\frac{1}{\tau_H}\{H_c(t) - H_{c,eq}(t)\}. \quad (5.27)$$

The equilibrium enthalpy obtained as Eq. (5.26) is substituted to Eq. (5.27) and rearranged to give the next expression.

$$\frac{dH_c}{dt} = -\frac{C_{c,eq}/C_{vib} + 1}{\tau_H}\{H_c(t) - H_{c,eq}(\infty)\}. \quad (5.28)$$

This differential equation is solved as follows.

$$H_C(t) - H_{C,eq}(\infty) = \{H_C(0) - H_{C,eq}(\infty)\}\exp(-t/\tau_T), \tag{5.29}$$

where

$$\tau_T = \frac{\tau_H}{(C_{C,eq}/C_{vib} + 1)}. \tag{5.30}$$

Substitution Eq. (5.29) to Eq. (5.23) gives the temperature as a function of time in the following equation.

$$T(t) = T(\infty) - A_H \exp(-t/\tau_T), \tag{5.31}$$

where

$$A_H = \{H_C(0) - H_{C,eq}(\infty)\}/C_{vib}. \tag{5.32}$$

For the Debye relaxation with a single characteristic time, transformation from τ_T to τ_H is thus given by Eq. (5.30). For the system with the distributed relaxation times, transformation corresponding to Eq. (5.30) cannot be represented analytically. In the following sections only τ_T is experimentally determined and discussed.

5-2 1-Propanol

The configurational enthalpy and polarization in exothermic-

depolarizing experiment are shown in Figs. 3-17 and 3-18, respectively. They show clear difference in relaxational behavior of enthalpy and polarization. In terms of the half life, the polarization persists longer than the enthalpy (~150 ks for the polarization and ~10 ks for enthalpy at 95.6 K). To determine the relaxation times for each processes, an attempt was made to fit exponential functions of time to the enthalpy and polarization data for the entire time region (0-290 ks). It turned out that the exponential function did not reproduce the data of both the enthalpy and polarization relaxations. In order to examine its departure from exponential function, the depolarization current which is equivalent to time-derivative of the polarization is plotted in logarithmic scale with respect to time as shown in Fig. 5-1. It shows a good linearity after t = 0.1 Ms. The linearity of logarithm of depolarization current means the exponential decay of the polarization, as the following equations show.

If the polarization decays exponentially, the electric charge on electrodes is described as

$$Q = Q \exp(-t/\tau_p). \qquad (5.33)$$

Since the depolarization current is the derivative of the charge with respect to time, it follows

$$I = -Q/\tau_p \exp(-t/\tau_{p1}). \qquad (5.34)$$

The logarithm of the current is described by

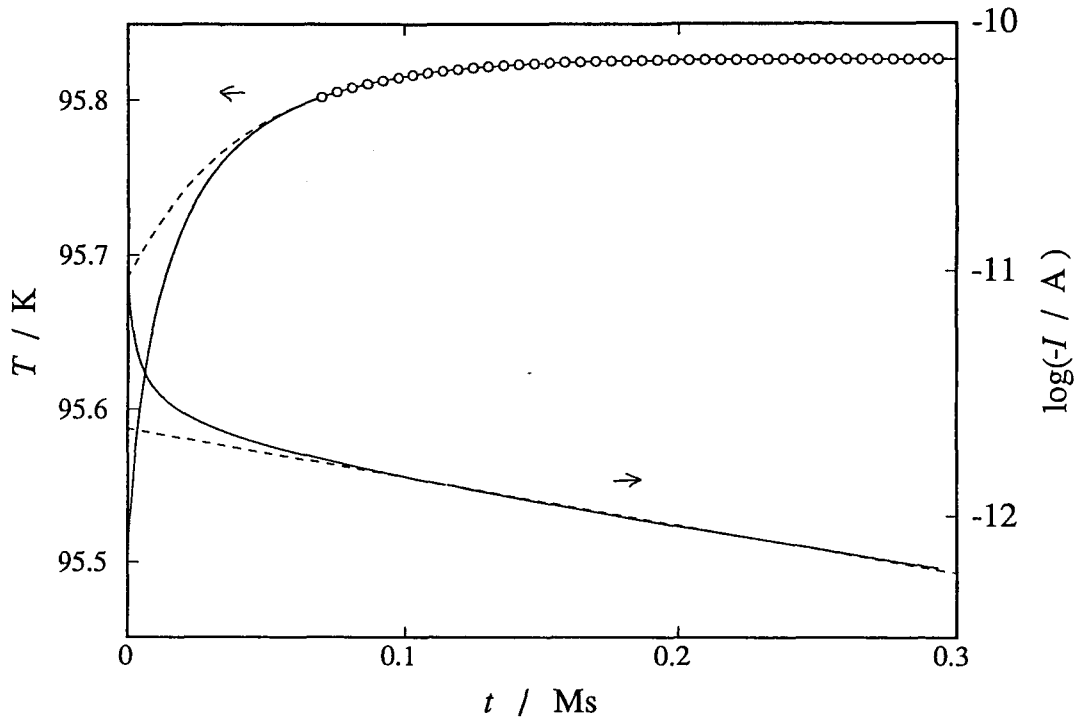

Fig. 5-1. The spontaneous temperature increase and the depolarization current (in logarithmic scale) in the exothermic-depolarizing experiment around 95.6 K. Dashed lines indicate contribution of the long-time relaxations.

$$\ln(-I/A) = \ln((Q/\tau_p)/A) - t/\tau_p. \qquad (5.35)$$

If the depolarization current is linear in the logarithmic plot, the slope of the line is equal to $-1/\tau_p$.

The relaxation time τ_{p1} for the polarization was determined using the slope of the logarithm of the current with respect to the time. Here the subscript 1 was added to τ_p to distinguish it from the shorter-time relaxation component. The data between 70 and 290 ks were used for the result at 95.6 K to determine τ_{p1}, and the result is shown in Fig. 5-1. The relaxation time for the enthalpy was determined using the temperature data in the same time interval as used for the determination of τ_{p1}. The temperature is represented by the following equation with the optimal parameters,

$$T(t) = T_\infty - A_{T1} \exp(-t/\tau_{T1}) + ct, \qquad (5.36)$$

where T_∞ is the convergence temperature, A_{T1} the magnitude of the relaxation (for exothermic $A_{T1}>0$, and for endothermic $A_{T1}<0$), τ_{T1} the relaxation time of the spontaneous temperature increase or decrease and c temperature drift rate due to the heat leakage. The calorimetric temperature was described by Eq. (5.36) satisfactorily within the experimental error. The relaxation times for the temperature and polarization were determined by the exothermic-depolarizing relaxation and endothermic-depolarizing relaxation experiments, as listed in Table. 5-1. The Arrhenius plots of the relaxation times are shown in Fig. 5-2. The relaxation time of the polarization is 5 to 12 times longer than that of the temperature change.

Table 5-1. Relaxation times of temperature and polarization in exothermic-depolarizing and endothermic-depolarizing experiments.

	T	τ_{T1}	τ_{P1}
	K	ks	ks
exothermic	95.82	41.2	219.2
	96.72	13.9	69.8
	97.60	2.74	22.5
endothermic	98.90	0.47	5.5

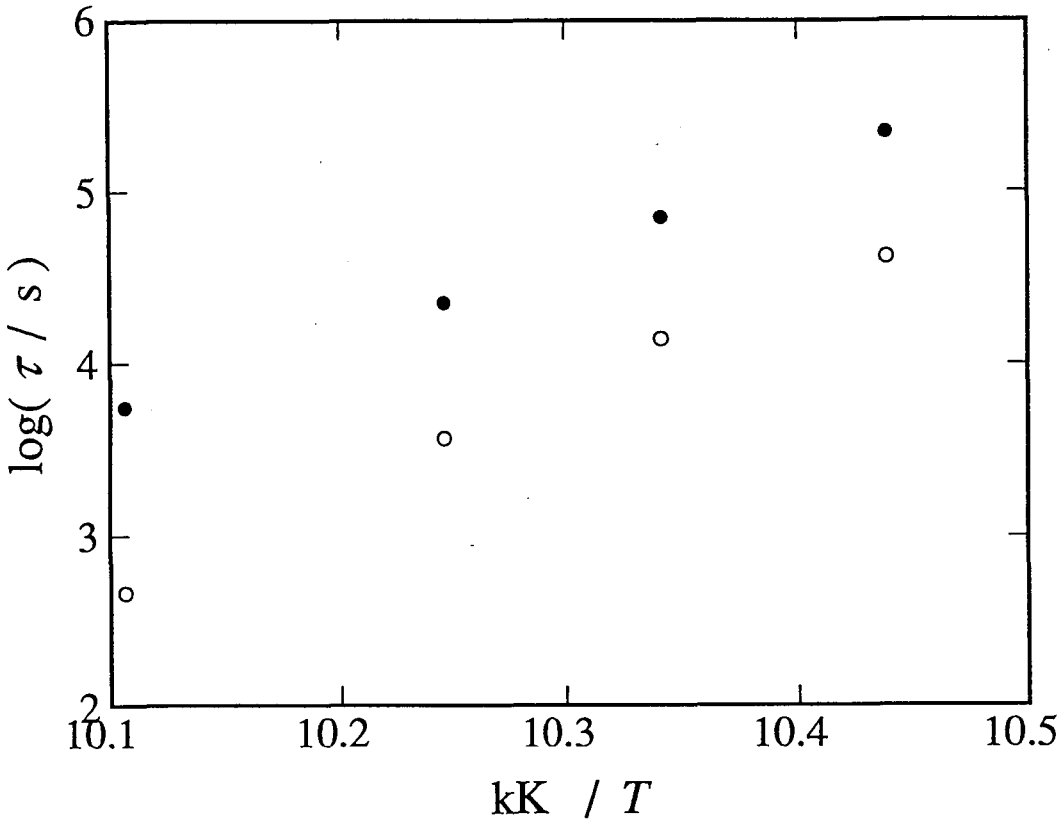

Fig. 5-2. Arrhenius plot of the relaxation time of long-time relaxation process. ● : polarization relaxation time τ_{P1}, ○ : enthalpy relaxation time τ_{T1}.

The relaxation time for the polarization obtained by the isothermal depolarization experiment was determined in the same way. The isothermal relaxation times determined at several temperatures are listed in Table. 5-2. They are also plotted in Fig. 5-3, together with the relaxation times determined from the enthalpy-depolarizing experiments. The two sets of relaxation times agree very well. The relaxation time in the enthalpy-depolarizing experiment was determined for the thermally non-equilibrium state. The relaxation time of this process is not necessarily the same as the isothermal relaxation time at the same temperature. However, the experiment showed that they do agree actually.

For the short-time exothermic-depolarizing relaxation, the contributions of the exponential relaxations assigned above are subtracted from the temperature and electric charge data, respectively. The residual contributions to the relaxation are shown in Figs. 5-4 and 5-5 for the temperature and polarization, respectively. The description by the exponential function was attempted for the residual components of relaxations. The following functions were used for the residual temperature change,

$$\Delta T(t) = T_0 - A_{T2} \exp(-t/\tau_{T2}), \qquad (5.37)$$

and for the residual polarization,

$$\Delta Q(t) = Q_0 + Q_2 \exp(-t/\tau_{P2}). \qquad (5.38)$$

Here A_{T2} and Q_2 are the magnitudes of the residual enthalpy and polarization relaxations, respectively. τ_{T2} and τ_{P2} are the relaxation times of the enthalpy and polarization. Although the optimal

Table 5-2. Polarization relaxation time under isothermal condition.

T / K	τ_{P1} / ks
95.74	266.0
97.58	24.6
98.85	5.90
100.29	1.42

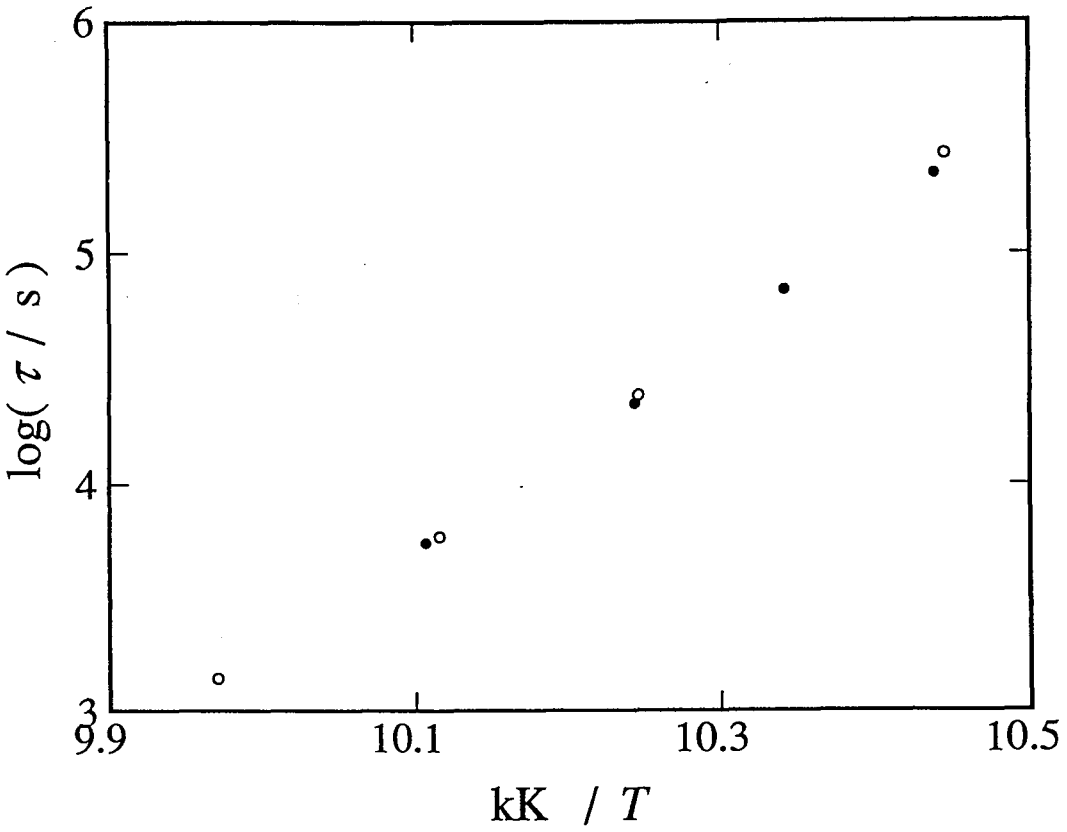

Fig. 5-3. Arrhenius plot of the polarization relaxation time. ○ : in thermally equilibrium state, ● : accompanied with enthalpy relaxation.

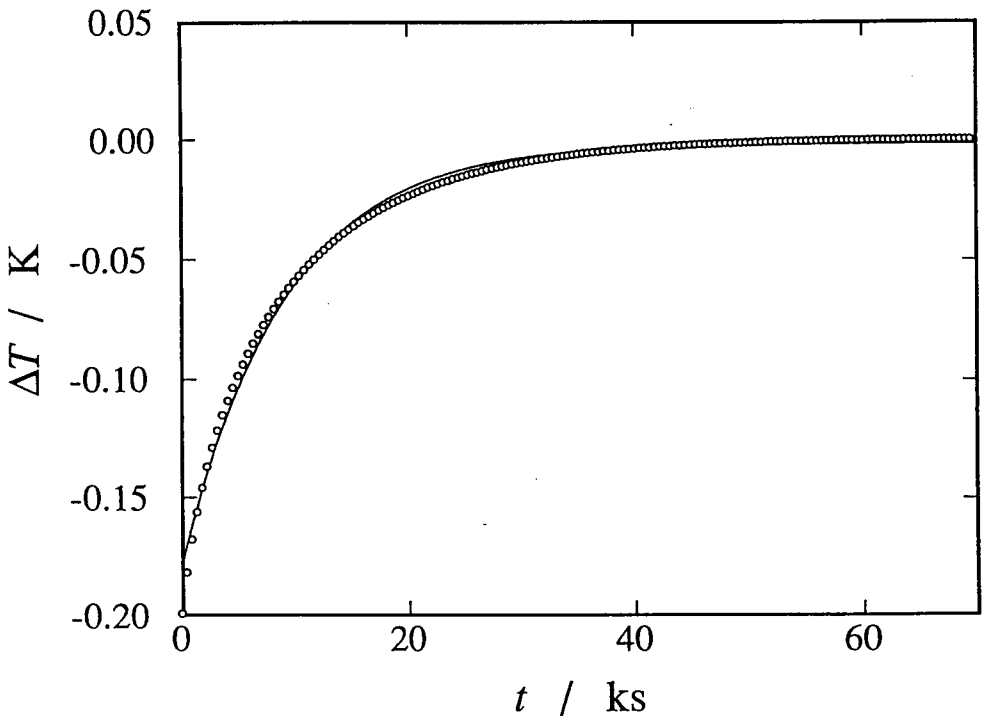

Fig. 5-4. Residual temperature increase in the exothermic-depolarizing experiment.

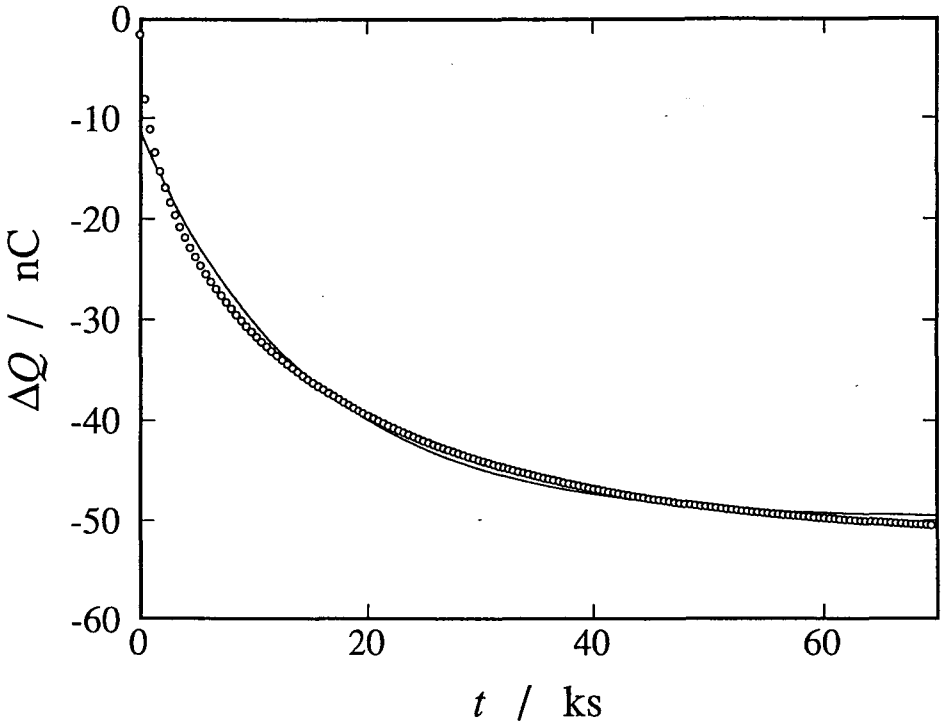

Fig. 5-5. Residual polarization relaxation in the exothermic-depolarizing experiment.

functions slightly differ from the data for both quantities, yet the relaxation times could be determined as shown in Table 5-3. The relaxation times τ_{T2} and τ_{P2} are plotted in Fig. 5-6, along with the data for τ_{T1} and τ_{P1}. It is obvious that τ_{T2} is close to τ_{P2}. Although τ_{T2} and τ_{P2} are smaller than τ_{T1} and τ_{P1}, the slopes of the curves in the log τ *vs.* $1/T$ plot are roughly the same for all relaxation times.

The apparent relaxation times for the polarization and configurational enthalpy are shown in Fig. 5-7. These were determined by means of Eqs. (2.20) and (2.31) using the data recorded in the TSDC measurement (Fig. 4-4). The apparent relaxation time of the enthalpy behaved in an unexpected way: it decreased as the temperature is lowered below about 97 K. This unexpected behavior can be understood, however, by the superposition of relaxation processes assigned above. The apparent relaxation time is based on the assumption of single relaxation process. The long-time process is expected to be dominant at 100 K. The difference in apparent relaxation times for the polarization and enthalpy at 100 K is due to the difference in the relaxation time of enthalpy and depolarization arising from the long-time process.

The Debye relaxation in 1-propanol observed by Davidson and Cole[1] corresponds to the long-time exponential relaxation. Figure 5-8 shows the isothermal relaxation time obtained in this study and the dielectric relaxation time obtained by Davidson and Cole. Both sets of the relaxation times are described commonly by a VTF function $\tau(T) = \tau_0 \exp[A/R(T-T_0)]$ with the following parameters: $\tau_0 = 1.78 \times 10^{-12}$, $A = 11.8$ kJ mol^{-1} and $T_0 = 59.4$ K. High fre-

Table 5-3. Relaxation times of temperature and polarization determined for the short-time components in the exothermic-depolarizing experiment.

T	τ_{T2}	τ_{P2}
K	ks	ks
95.60	8.89	14.7
96.65	3.76	3.90
97.60	0.85	0.71

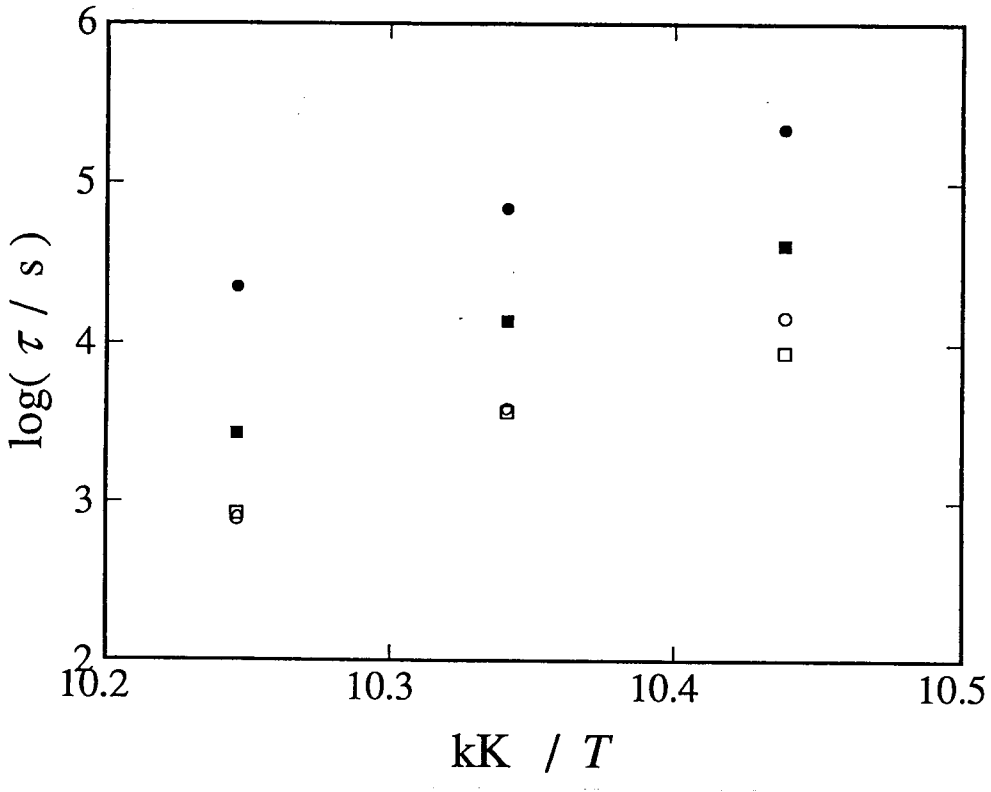

Fig. 5-6. Relaxation times of the enthalpy and polarization. Short-time process □ : τ_{T2}, ○ : τ_{P2}. Long-time process ■ : τ_{T1}, ● : τ_{P1}.

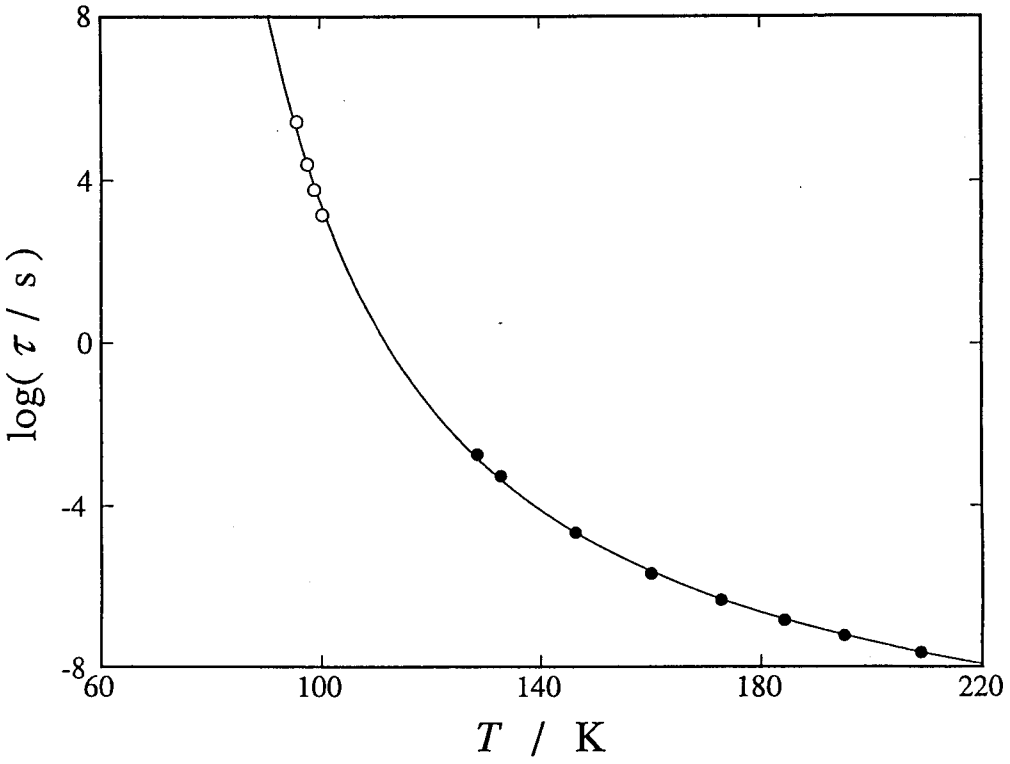

Fig. 5-7. Polarization relaxation times. ● : Determined by dielectric measurement[1], ○: determined in this study.

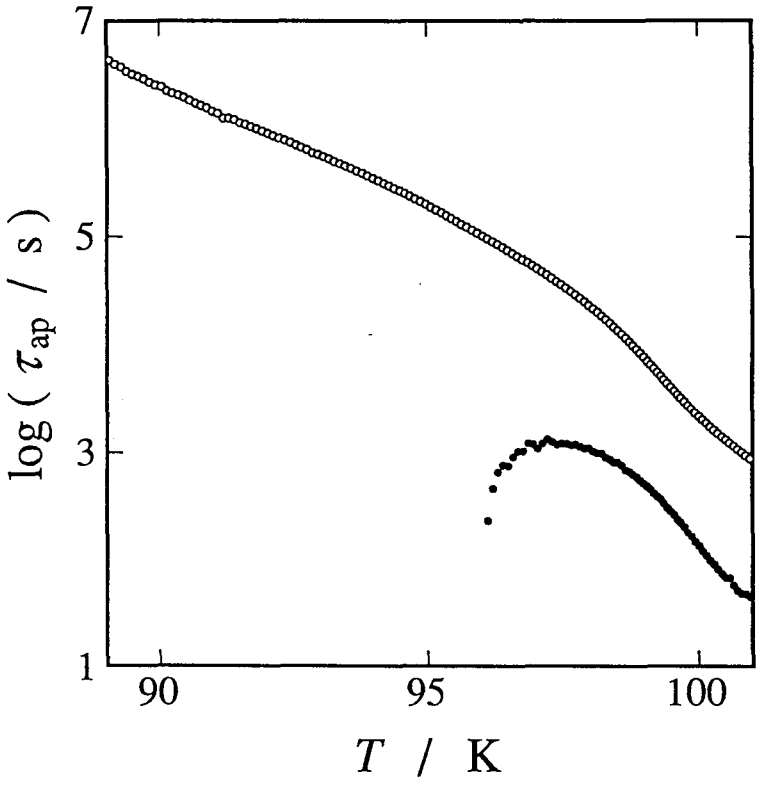

Fig. 5-8. Apparent relaxation times of the configurational enthalpy (●) and polarization (○) in the TSDC measurement.

quency dispersion was observed by Cole and Davidson[2] and they analyzed it as the overlap of two Cole-Cole type dispersions. This high frequency dispersion was observed as the short-time residual relaxation in this study for the polarization and enthalpy. In the enthalpy-depolarizing experiment the large difference of relaxation time between enthalpy and polarization was found. The ultrasonic[3] and dielectric experiment showed the difference between dielectric and volume relaxations. The mechanism of the relaxations was suggested by Floriano and Angell[4]. They explained that the long-time relaxation is due to a clustering. But still the origin of the relaxation is not clear and the difference between the different quantities is not understood.

5-3 Isocyanocyclohexane

Isocyanocyclohexane has a small entropy of fusion which is one of characteristic properties of the plastic crystal. In contrast, the entropy change at the phase transition from the ordered to plastically crystalline phase is large. Temperature dependence of the heat capacity of isocyanocyclohexane is very similar to that of cyanocyclohexane[5]. Obviously this reflects similarity of the molecular structures, which differ only by the chemical transpose of the nitrile group. It is interesting to note that the entropies of fusion of the two compounds differ by 2.4 $J\ K^{-1}mol^{-1}$ and the entropies of transition differ by almost the same magnitude in the opposite way (see Table 5-4). Thus, the

Table 5-4. Comparison of thermodynamic quantities associated with the phase transitions and fusions of isocyanocyclohexane ($C_6H_{11}NC$) and cyanocyclohexane ($C_6H_{11}CN$). *) determined by J.-J. Pinvidic[5].

	$C_6H_{11}NC$	$C_6H_{11}CN$(*)
T_{trs}/K	192.6	215.0
$\Delta_{trs}H$ / kJ mol^{-1}	6.177	7.425
$\Delta_{trs}S$ / J K^{-1}mol^{-1}	32.07	34.5
T_{fus}/K	279.6	285.1
$\Delta_{fus}H$ / kJ mol^{-1}	4.227	3.635
$\Delta_{fus}S$ / J K^{-1}mol^{-1}	15.12	12.75
$(\Delta_{trs}H+\Delta_{fus}H)$/ kJ mol^{-1}	10.40	11.09
$(\Delta_{trs}S+\Delta_{fus}S)$/ J K^{-1} mol^{-1}	47.19	47.25

sum of the entropies of fusion and phase transition agrees remarkably closely to each other.

In reference to the low temperature ordered phase, the supercooled crystal has the calorimetrically determined residual entropy of 6.30 J K^{-1} mol^{-1}.

The spontaneous temperature changes around T_{g1} could be described by the Debye type relaxation. The enthalpy relaxation times were determined as listed in Table. 5-5. The Arrhenius plot of the relaxation time is shown in Fig. 5-9. The temperature dependence of the relaxation time is represented satisfactorily well by the Arrhenius law. The activation energy E_a was determined as 53.6 kJ mol^{-1} and τ_0 as 1.3×10^{-15} s.

Gonthier-Vassal *et al.*[6] suggested a molecular explanation for the two glass transitions of isocyanocyclohexane. T_{g1} is the glass transition associated with freezing of the interconversion between the axial and equatorial conformers and T_{g2} is associated with freezing of the reorientational motion of the molecule as a whole. On the basis of this interpretation, the activation energy determined above is the barrier height hindering the conversion between the axial and equatorial conformers in the lattice.

The relaxational behavior of enthalpy and polarization around T_{g2} are shown in Figs. 4-9 and 4-12. The relaxational behavior of both quantities at all experimental temperatures showed the following two characters. One is that the curve of electric charge converges faster than the temperature. The other is that both curves cannot be represented by the simple exponential function satisfactorily. To compare the relaxational behavior

Table 5-5. The relaxation time of enthalpy around T_{g1}.

	T / K	τ_H / ks
Exothermic	144.56	28.94
	149.78	6.89
Endothermic	154.81	1.49
	157.50	0.74
	160.18	0.38
	162.84	0.21

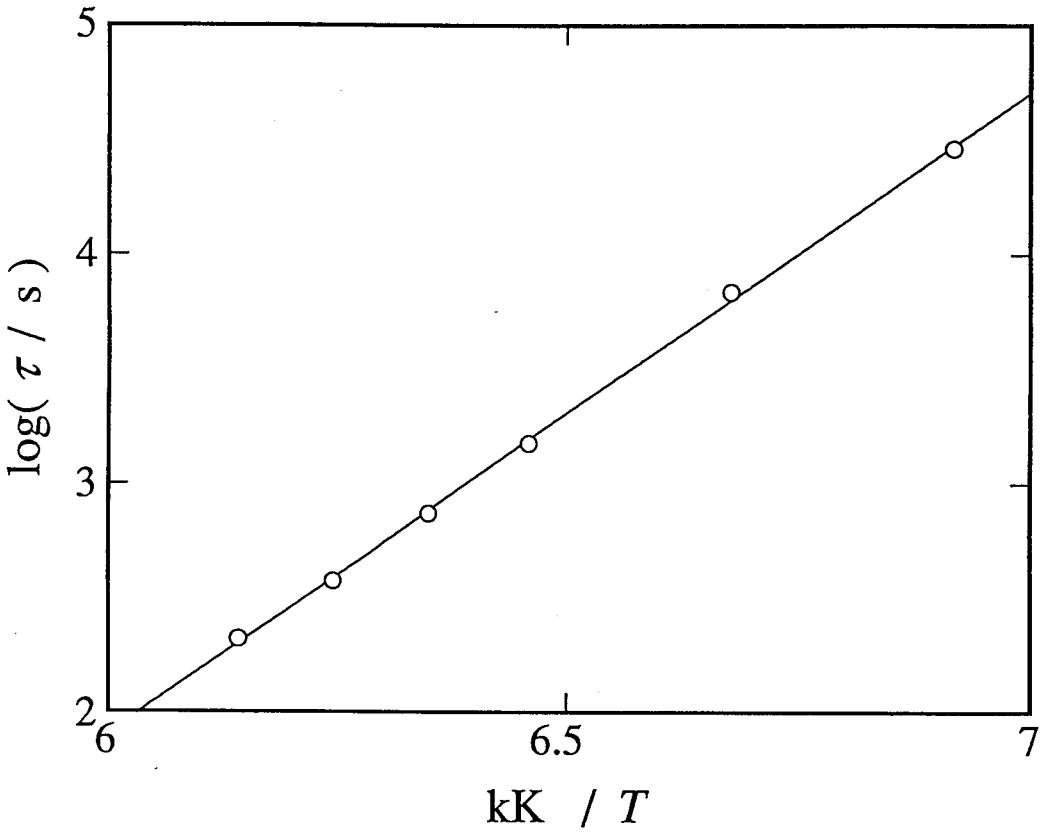

Fig. 5-9. Relaxation time of enthalpy around T_{g1}. Straight line in the figure was fitted to the data.

of the two quantities, the Kohlrausch-Williams-Watts (KWW) function was used to analyze the data.

$$F(t) = F(0) \exp[-(t/\tau)^{\beta}], \qquad (5\text{-}39)$$

where F is the relaxational quantity, τ an effective relaxation time and β a parameter representing departure from the simple exponential relaxation: for $\beta=1$ the function is the Debye type relaxation function. The parameter β takes a value between 0 and 1, and departure from the Debye type relaxation is larger for the smaller β.

For the actual fitting two additional terms, T_∞ and ct, were added to the relaxation function. T_∞ is the convergence temperature and c a correction term for heat leakage arising from incompleteness of the adiabatic condition. The magnitude of the relaxation of temperature is represented by A_T ($A_T > 0$ for exothermic, $A_T < 0$ for endothermic). The temperature data were thus represented by

$$T(t) = T - A(0) \exp[-(t/\tau_T)^{\beta T}] + ct, \qquad (5\text{-}40)$$

where the suffix T was used for the Kohlrausch-Williams-Watts parameters β and τ. In what follows, two suffixial quantities T and P are attached to observation of τ and β in order to differentiate the enthalpy (through the observation of temperature T) and polarization relaxations.

For the electric charge data two additional terms, Q_0 and jt, were added to the relaxation function. Q_0 is the initial value of

$Q(t)$ and j bias current arising from an instrumental origin. The magnitude of the relaxation of electric charge is represented by Q. The electric charge data were reproduced by

$$Q(t) = Q\{\exp[-(t/\tau_P)^{\beta_P}] - 1\} + Q_0 + jt . \qquad (5\text{-}41)$$

The optimal parameters β and τ for temperature and electric charge are listed in Table. 5-6. The Arrhenius plot of τ_T and τ_P thus determined is shown in Fig. 5-10. The non-exponential parameters β_T and β_P are plotted against temperature in Fig. 5-11. The relaxation time of enthalpy is roughly 20 times longer than that of polarization. The parameter β_T ranges from 0.7 to 0.8 and β_P from 0.4 to 0.5.

The non-exponential behavior at the glass transition can be accounted for as a superposition of exponential relaxation processes with distributed relaxation times[7]. The relaxation around T_{g2} was interpreted as follows. Isocyanocyclohexane relaxing at T_{g2} is a mixture of the axial and equatorial conformers. At this temperature the ratio of two conformers does not change anymore and behave as if they were distinct chemical species with different molecular shape and intermolecular interaction. Therefore the environment that each molecule feels is different from one site to the other because of the random occupation of the lattice sites by the two conformers. This gives rise to distribution of various relaxation times. In thiophene-benzene solid solution system[8], a KWW type function was applied successfully to the relaxation process, in contrast to a single exponential relaxation in pure thiophene for their glassy states. This was also attributed to

Table 5-6. Kohlrausch-Williams-Watts parameters of enthalpy and polarization relaxations in exothermic-depolarizing experiment around T_{g2}.

T / K	τ_H / ks	β_H	τ_P / ks	β_P
123.04	71	0.53	4.3	0.49
125.37	8.3	0.70	0.62	0.42
126.01	7.5	0.73	0.63	0.45
126.82	4.7	0.75	0.30	0.45
126.84	4.6	0.75	0.35	0.46
127.66	2.5	0.80	0.28	0.57

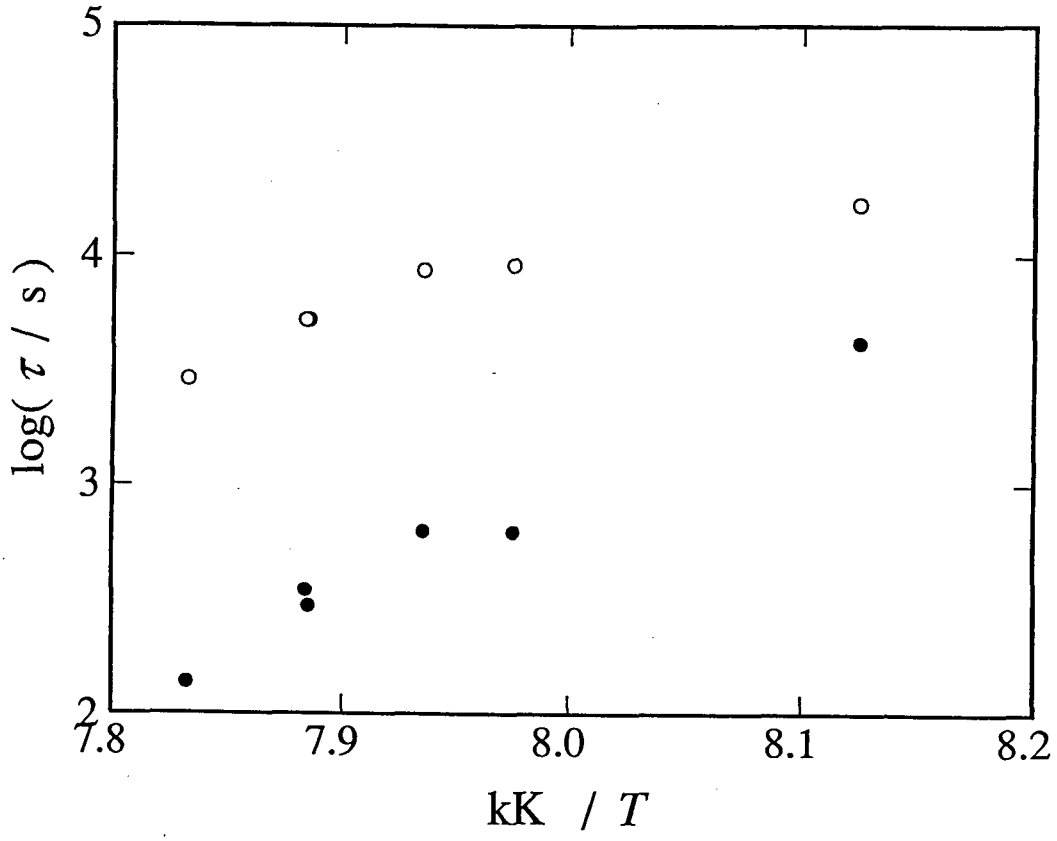

Fig. 5-10. KWW relaxation time of enthalpy (○) and polarization (●) *vs.* reciprocal of temperature in exothermic-depolarizing experiment around T_{g2}.

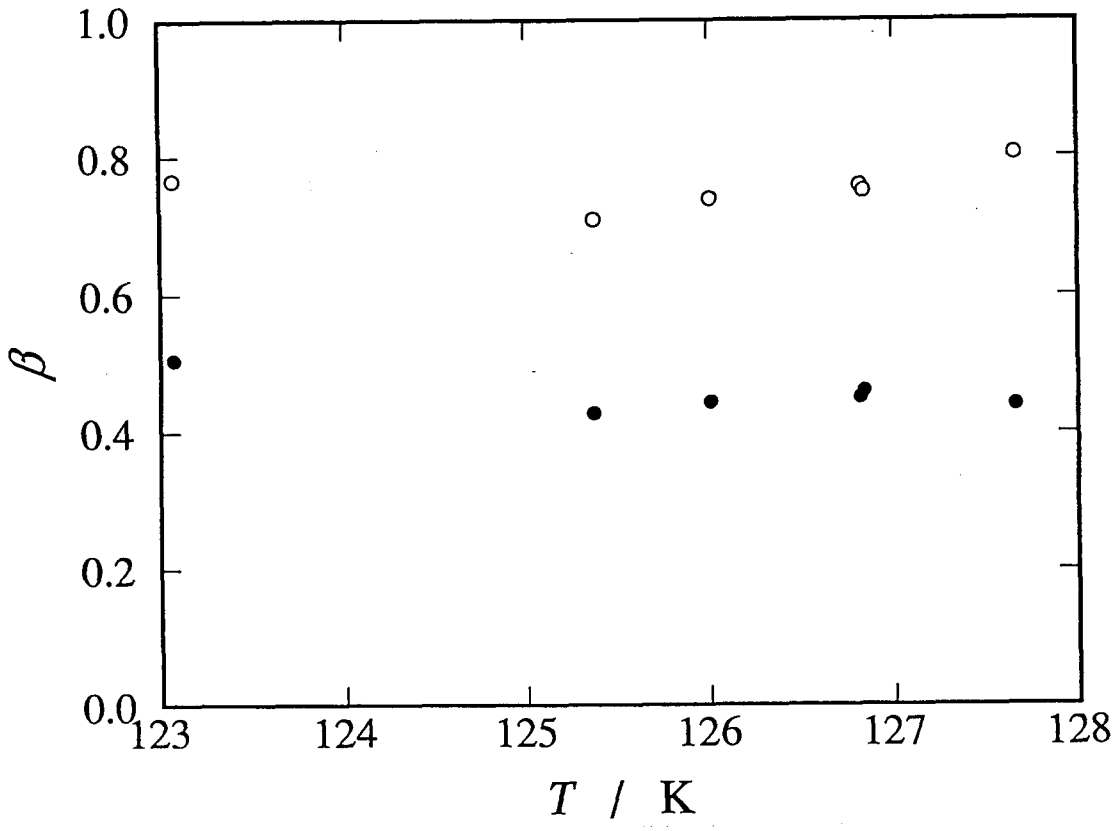

Fig. 5-11. KWW parameter β of polarization relaxation in exothermic-depolarizing experiment around T_{g2}. ○ :enthalpy, ● : polarization.

thiophene for their glassy states. This was also attributed to random distribution of the two components.

The relaxor of the longer relaxation time freezes at higher temperature. By a rough estimation using Eq. (5.11) the relaxation time τ_T for the actual cooling rate is several times longer than that of infinite cooling rate. The finite cooling rate also contributes to the difference of the relaxation times between enthalpy and polarization. At present, however, the difference between the enthalpy and polarization cannot be explained quantitatively.

Finally, it has to be pointed out that there was an experimental result which could not be understood by the distribution of relaxation times alone. The electric charge in the isothermal depolarization experiment (Fig. 4-17) was analyzed by Eq. (5-41). The parameters β_p and τ_p determined from the analysis are listed in Table. 5-7. The Arrhenius plot of the polarization relaxation time under isothermal condition is shown together with those derived from the exothermic-depolarizing experiment given in Fig. 5-12. β_p of the isothermal and exothermic experiments is plotted against temperature in Fig. 5-13. The isothermal polarization relaxation time differs from the exothermic polarization relaxation time. The difference increases as the temperature increased. This result cannot be interpreted by the distribution of relaxation times. It reflects the difference between the glassy state and equilibrium state. The excess configurational enthalpy at the beginning of exothermic relaxation is larger at the lower temperature.

Table 5-7. Kohlrausch-Williams-Watts parameters of polarization relaxation under isothermal condition around T_{g2}.

T / K	τ_P / ks	β_P
124.09	13.0	0.52
125.60	2.52	0.50
126.16	1.25	0.50
126.72	0.638	0.47
126.83	0.558	0.47
126.94	0.558	0.49
127.70	0.217	0.47
128.24	0.092	0.44

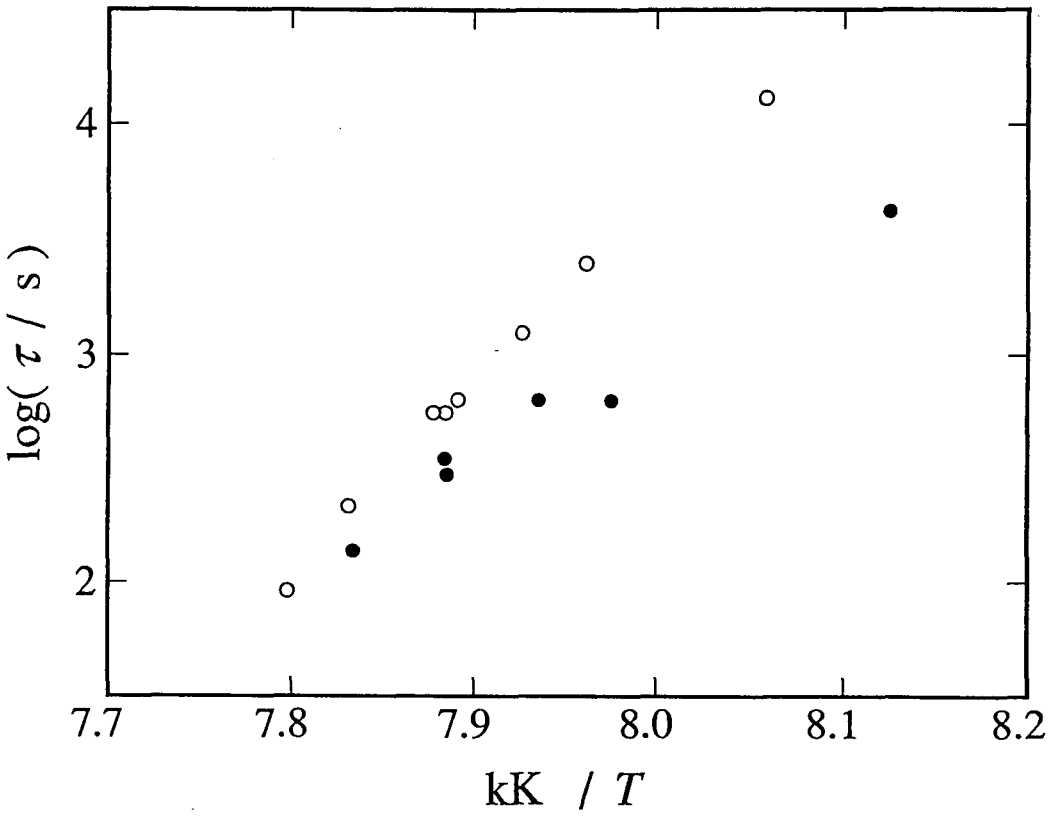

Fig. 5-12. KWW relaxation time of polarization in the exothermic-depolarizing experiment (●) and isothermal experiment (○) *vs.* reciprocal of temperature.

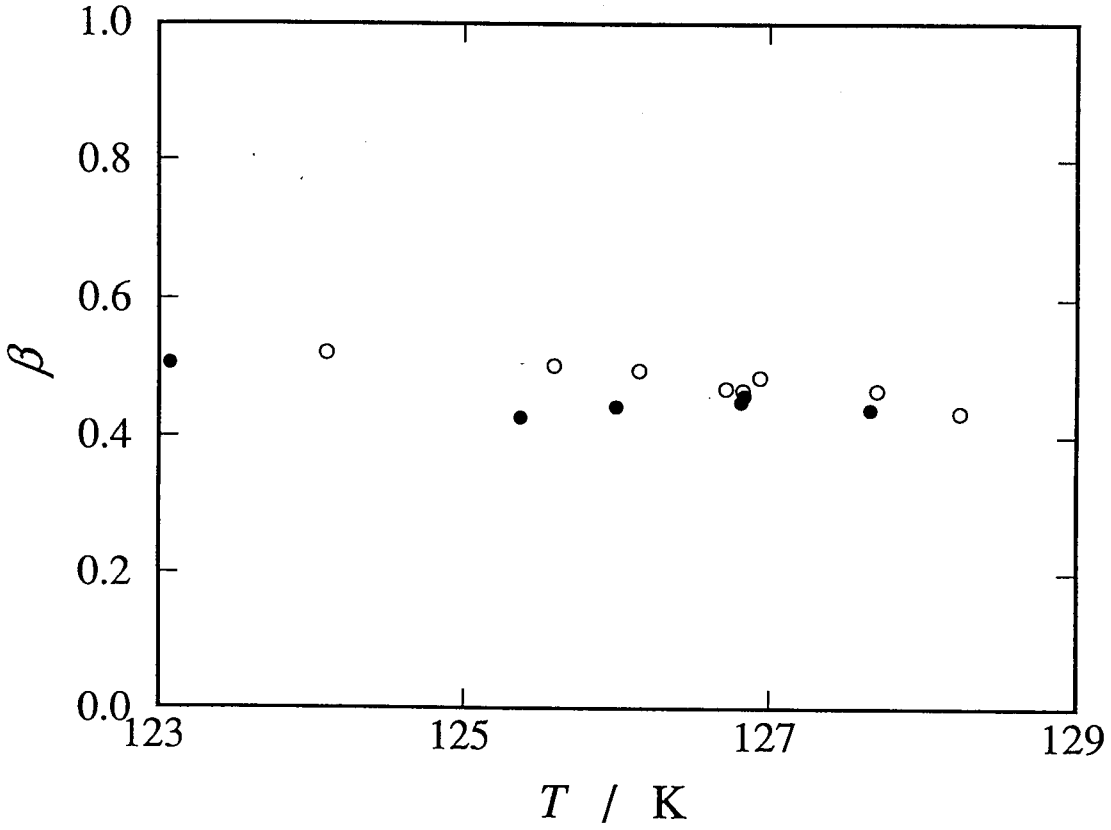

Fig. 5-13. KWW β of polarization in the exothermic-depolarizing experiment (●) and isothermal experiment (○) *vs.* temperature.

5-4 General Discussion

If there is no singularity in the distribution function $g(x)$ of the relaxation times for isocyanocyclohexane, the relaxation time τ_T should be equal to τ_H approximately. The enthalpy relaxation occurs even during the cooling process with a finite rate in the actual experiment. The observed τ_H is several times larger than the intrinsic enthalpy relaxation time that could be observed in an instantaneously-quenched ideal experiment. Actually, however, the enthalpy relaxation time τ_H is ten times larger than the polarization relaxation time τ_P. For 1-propanol the experimental correction term $C_{c,eq}/C_{vib}$ (see Eq. (5.30)) is smaller than 0.3. Then the values τ_{T1} and τ_{T2} determined in section 5-2 are regarded as the enthalpy relaxation times τ_{H1} and τ_{H2}, respectively.

Comparison between the relaxation times for the enthalpy and the polarization is summarized as follows.

For isocyanocyclohexane crystal,

$$\tau_P < \tau_H .$$

For the long-time relaxation component in 1-propanol liquid,

$$\tau_{P1} > \tau_{H1} .$$

For the short-time relaxation component in 1-propanol liquid,

$$\tau_{P2} \approx \tau_{H2} .$$

Apparently, there is no common relation between the enthalpy and polarization relaxation times for all of them. The origin of differ-

ence in the relaxation behavior for the enthalpy and polarization is interpreted as follows.

For the relaxation in isocyanocylohexane crystal, dipolar motion of single molecule is observed as the polarization relaxation. The polarization is proportional to the sum of molecular direction vectors.

$$\vec{P} \propto \sum_{i=1}^{n} \vec{r_i}, \tag{5.42}$$

where $\vec{r_i}$ is the direction vector of molecule i and n the number of molecules. While the configurational enthalpy in liquids is a function of molecular directions and positions, the configurational enthalpy in plastic crystals is a function of only molecular directions.

$$H_c = \Phi(\vec{r_1}, \vec{r_2}, \vec{r_3}, \ldots, \vec{r_n}). \tag{5.43}$$

Here Φ is composed of the molecular interactions such as dipole-dipole and van der Waals interactions. Isocyanocyclohexane molecule has a large dipole moment (≈ 4 D, see 1-3). The dipole-dipole interaction contributes significantly to the enthalpy of the system. To simplify the model, the interaction is restricted to the dipole-dipole interaction, and the dipole-dipole interaction is further restricted to the two-body interaction. The dipole-dipole interaction is written roughly by the following equation.

$$H_c \propto \Sigma \vec{r_i} \cdot \vec{r_j} / d_{ij}^3, \tag{5.44}$$

where d_{ij} is the distance between dipole i and j. If the polarization relaxation is represented by

$$P = P_0 \exp(-t/\tau), \tag{5.45}$$

the time autocorrelation function of the molecular direction is given by the following equation.

$$\langle \vec{r}(t) \cdot \vec{r}(0) \rangle = \exp(-t/\tau). \tag{5.46}$$

Using Eqs. (5.46) and (5.44), the relaxation of the configurational enthalpy is written by

$$\begin{aligned} H_C &\propto \exp(-t/\tau)\exp(-t/\tau) \\ &= \exp\{-t/(2\tau)\}. \end{aligned} \tag{5.47}$$

In this simplified model, the enthalpy relaxation time is twice longer than the polarization relaxation time. The actual interaction in isocyanocyclohexane crystal includes the van der Waals interaction and is not restricted to two-body interaction. Thus the actual interactions are much more complicated than that of the above model. However, the difference between the relaxation times for the enthalpy and polarization is explained by the model at least qualitatively.

This model can be applied generally to plastic crystals, in which the constituent molecules have three-dimensional periodicity with respect to their centers of mass but are disordered with respect to their orientations. It is expected that the enthalpy

relaxation time is longer than the polarization relaxation time.

Now the discussion is directed to the relaxation behavior of 1-propanol. For the long-time relaxation component, the polarization is due to not the single molecule but the cluster of molecules. The existence of the cluster in 1-propanol was suggested by Hirai and Eyring[9] and by Floriano and Angell[4]. But the configurational enthalpy composed of the van der Waals interactions, not the dipole-dipole interaction between the clusters. The elementary process for the reorientation of the cluster is observed as the enthalpy change. Hence the configurational enthalpy relaxes faster than the polarization.

On the other hand, the short-time relaxation component is believed to be due to the reorientation of the hydroxyl group in the molecule. Both relaxations for the polarization and enthalpy are dominated by this local motion. The relaxation times of the short time component for the polarization and enthalpy agree therefore each other. In this way, the difference in the relaxation behavior for the enthalpy and polarization observed simultaneously by the present polaro-calorimetric experiments will help to have better understanding of molecular motion in these substances.

References

1. D. W. Davidson and R. H. Cole, *J. Chem. Phys.*, 19(12), 1484 (1951).

2. R. H. Cole and D. W. Davidson, *J. Chem. Phys.*, 20(9), 1389 (1952).

3. T. Lyon and T. A. Litovitz, *J. Appl. Phys.*, 27(2), 179 (1956).

4. M. A. Floriano and C. A. Angell, *J. Chem. Phys.*, 91(4), 2537 (1989).

5. J.-J. Pinvidic, Ph. D. Thesis, Université de Paris Sud (1988).

6. A. Gonthier-Vassal and H. Szwarc, *Chem. Phys. Lett.*, 129(1), 5 (1986).

7. C. P. Lindsey and G. D. Patterson, *J. Chem. Phys.*, 73(7), 3348 (1980).

8. N. Okamoto, M. Oguni and H. Suga, *J. Chem. Phys.*, 50(12), 1285 (1989).

9. N. Hirai and H. Eyring, *J. Appl. Phys.*, 29(5), 810 (1958).

CHAPTER 6 CONCLUDING REMARKS

Glass transitions in 1-propanol liquid and isocyanocylohexane crystal were studied. The relaxational behavior of the configurational enthalpy and the electric polarization was observed using a polaro-calorimeter.

For 1-propanol, the glass transition was observed around 98 K by the heat capacity measurement. The results of the exothermic-depolarizing and endothermic-depolarizing experiments showed the non-exponential relaxations for the enthalpy and the polarization. The non-exponential relaxations in the enthalpy and the polarization were separated into two components which have different relaxational rates. The long-time component was described well by an exponential function. The long-time component for the polarization relaxation had a relaxation time 5–12 longer than that for the corresponding component of the enthalpy relaxation. Short-time component was described approximately as an exponential function. The relaxation times of the short-time relaxation were roughly the same for the enthalpy and the polarization. The long-time relaxation corresponds to the Debye type dispersion which has been found by previous dielectric measurement. The short-time relaxation corresponds to the non-Debye dispersion which has been observed in higher frequency region by the dielectric measurement.

Two glass transitions in isocyanocyclohexane crystal were

observed around 160 K (T_{g1}) and 130 K (T_{g2}). The enthalpy relaxation around T_{g1} was described as the Debye relaxation. This relaxation is associated with the interconversion between the axial and equatorial conformers of the internally flexible molecule. The temperature dependence of the relaxation time was well described by the Arrhenius law and the barrier height hindering conversion between the two conformers was determined to be 53.6 kJ mol^{-1}.

Non-exponential relaxation was observed around T_{g2} by the exothermic-depolarizing experiment. The relaxational behavior was described well by Kohlrausch-Williams-Watts (KWW) function. The relaxation time τ and the parameter β representing the departure from exponential function in the KWW function were determined for both enthalpy and polarization, respectively. The relaxation time for the enthalpy was longer than that for the polarization and β for the enthalpy was larger than that for the polarization. If the distribution of the relaxation times is significant, it contributes to the difference of KWW parameters: τ for the enthalpy can be several times longer than that for the polarization. However the actual difference could not be explained quantitatively by considering only the distribution of the relaxation times. A significant difference in the polarization relaxation behavior between the glassy state and equilibrium state was found by comparing the results of isothermal and exothermic experiments.

A phase transition between plastically crystalline and ordered low-temperature crystalline phases was found at 192.6 K. A glassy crystal was formed easily by supercooling the plastically

crystalline state. Thermodynamic quantities associated with the phase transition were determined. The residual entropy of glassy state was determined by a loop calculation to be 6.3 J $K^{-1}mol^{-1}$.

The relaxation times for the enthalpy and polarization differ to some extent depending on the cooperative nature for the reorientational motion of polar species. For the short-time component of 1-propanol, the difference is quite small. Each hydroxyl group is believed to reorient rather independently of each other, in spite of the fact that they form hydrogen-bond. For the other relaxations observed in 1-propanol and isocyanocyclohexane, the differences between the enthalpy and polarization relaxation times are large. The different relaxation rate may arise from the different nature whether the cooperativity contributes dominantly to the enthalpy or polarization of the system.

The present thesis described the first successful experiment of simultaneous observation for the enthalpy and polarization relaxations in two frozen-in disordered systems; one in orientationally disordered crystal of isocyanocyclohexane and the other in supercooled liquid of 1-propanol. It is highly desirable to accumulate this kind of information on relaxation rate of any physical quantity in order to get fuller understanding of the nature of glass transition and relaxation phenomena occurring widely in many disordered condensed systems. They are liquids, isotropically disordered crystals, anisotropically ordered liquids and other non-crystalline solids prepared by various techniques including vapor-condensation, chemical reaction and mechanical grinding of crystal.